

**IMPROVING THE THERAPEUTIC FUNCTIONALITY OF NEURAL
PROGENITOR CELLS BY ENCAPSULATION WITH
CHONDROITIN-4-SULFATE-A HYDROGEL**

A Dissertation
Presented to
The Academic Faculty

by

Myles Randolph McCrary

In Partial Fulfillment
of the Requirements for the Degree
Doctor of Philosophy in Biomedical Engineering in the
Georgia Institute of Technology and Emory University

Georgia Institute of Technology
Emory University
August 2019

COPYRIGHT © 2019 BY MYLES RANDOLPH MCCRARY

**IMPROVING THE THERAPEUTIC FUNCTIONALITY OF NEURAL
PROGENITOR CELLS BY ENCAPSULATION WITH
CHONDROITIN SULFATE-A HYDROGEL**

Approved by:

Dr. Ling Wei, Advisor
Department of Anesthesiology
Emory University

Dr. Michael E. Davis
Department of Biomedical Engineering
Georgia Institute of Technology

Dr. Shan Ping Yu,
Department of Anesthesiology
Emory University

Dr. Robert E. Gross,
Department of Neurosurgery
Emory University

Dr. Luke P. Brewster,
Department of Surgery
Emory University

Date Approved: 4/22/2019

ACKNOWLEDGEMENTS

I would like to especially thank Xiaohuan ‘Hannah’ Gu, Chao ‘Chelsea’ Qu, Dr. Qize ‘Michael’ Jiang, and Dr. James Zhang for their technical expertise, assistance, and friendship during my time in the Wei lab. I would also like to thank Kaleena Jesson and Stephan Tan who assisted greatly to the work presented in this thesis. Dr. Lohitash Karumbaiah and Meghan Logun provided critical expertise in the production and implementation of the hydrogels. I also thank the committee members Dr. Robert Gross, Dr. Michael Davis, and Dr. Luke Brewster for providing much needed guidance. I would like to recognize Dr. David Trac, Dr. Saumya Gurbani, Mariko Peterson, Matthew Stern, and Daniel Whittingslow for their encouragement throughout the MD/PhD curriculum. Finally, I thank my family for their continual support and affection.

TABLE OF CONTENTS

ACKNOWLEDGEMENTS	iii
LIST OF TABLES	vii
LIST OF FIGURES	viii
LIST OF SYMBOLS AND ABBREVIATIONS	xiii
SUMMARY	xv
CHAPTER 1. Introduction	1
CHAPTER 2. Specific Aims and Hypotheses	6
2.1 Aim 1: Determine the effects of CS-A on NPC survival and differentiation.	6
2.2 Aim 2: Determine the effects of treatment with CS-A encapsulated NPC on regeneration in the ischemic brain.	7
2.3 Aim 3: Determine the effects of treatment with CS-A encapsulated NPCs on local blood flow restoration and functional recovery after ischemic stroke.	7
CHAPTER 3. Literature Review	9
3.1 Stroke Epidemiological Trends	9
3.2 Stroke Types and Risk Factors	9
3.3 Cellular and Molecular Mechanisms in Ischemic Stroke	
Pathophysiology	12
3.3.1 Excitotoxicity, Calcium Dysregulation, and Ion Imbalance	13
3.3.2 Spreading Depolarization and Spreading Ischemia	14
3.3.3 Oxidative and Nitrosative Stress	15
3.3.4 The Inflammatory and Astrocytic Response to Cerebral Infarction	16
3.3.5 Cell Death after Cerebral Ischemia	20
3.4 Stroke Prevention and Treatment	23
3.5 The Role of Collateral Circulation in Ischemic Stroke	
Pathophysiology	24
3.5.1 Collateral Circulation Dynamics during Ischemic Stroke	25
3.5.2 Collateral Circulation and Stroke Severity	26
3.5.3 Collateral Circulation, Infarct Progression, and Tissue Fate after Reperfusion	27
3.6 Endogenous Repair and Regeneration in the Adult Brain after Ischemic Stroke	32
3.6.1 Post-stroke Neurogenesis	32
3.6.2 Vascular Regeneration and Remodeling after Ischemic Stroke	35
3.7 Mouse Ischemic Stroke Models	37
3.8 Stem Cell Therapy for Ischemic Stroke	39

3.8.1	Stem Cell Sources for Cellular Therapy	39
3.8.2	Neuronal Progenitor Cells and Neuronal Differentiation	42
3.8.3	Mechanisms of Cellular Therapy	43
3.8.4	Cell Transplantation Parameters and Strategies for Stroke	46
3.9	Biomaterials for Augmentation of Cellular Therapy for Ischemic Stroke	50
3.9.1	Hydrogels as cell carriers for transplantation in stroke	50
3.10	Chondroitin Sulfate Glycosaminoglycans and Brain Regeneration	53
CHAPTER 4.	Methodology	55
4.1	Experimental design	55
4.1.1	Aim 1: Determine the effects of CS-A on NPC survival and differentiation.	55
4.1.2	Aim 2: Determine the effects of treatment with CS-A encapsulated NPC on regeneration in the ischemic brain.	59
4.1.3	Aim 3: Determine the effects of treatment with CS-A encapsulated NPCs on local blood flow restoration and functional recovery after ischemic stroke.	62
4.2	Procedures	65
4.2.1	Mouse stroke model, laser Doppler flowmetry, and transplantations	65
4.2.2	Neural progenitor cell culture and CS-A hydrogel preparation	66
4.2.3	Cell retention imaging	68
4.2.4	Oxygen and glucose deprivation (OGD) conditions and lactate dehydrogenase (LDH) cytotoxicity assay	68
4.2.5	Immunohistochemistry and image analysis	69
4.2.6	Pial vessel imaging and analysis	70
4.2.7	Western blot analysis	71
4.2.8	Hydrogel haptotaxis assay	72
4.2.9	Primary stroke core macrophage isolation and culture	72
4.2.10	U-PLEX (Protein Multiplex)	72
4.2.11	Sensorimotor behaviour analysis	73
4.2.12	Statistics	74
4.2.13	Randomization and blinding	74
4.2.14	Chemicals and reagents	74
CHAPTER 5.	Results	75
5.1	Aim 1: Determine the effects of CS-A on NPC survival and differentiation.	75
5.1.1	CS-A encapsulation reduces cell death of transplanted NPCs	75
5.1.2	CS-A encapsulation improves NPC retention following transplantation	77
5.1.3	Characterization of NPC differentiation in vitro following CS-A encapsulation	78
5.1.4	Characterization of NPC differentiation in vivo following transplantation	81
5.2	Aim 2: Determine the effects of treatment with CS-A encapsulated NPC on regeneration in the ischemic brain.	86
5.2.1	Effect of CS-A encapsulation of NPCs on astrogliosis	86

5.2.2 Treatment with CS-A encapsulated NPCs promotes a pro-regenerative macrophage response	87
5.2.3 Neurogenesis and neuroblast recruitment are unaffected by treatment	101
5.2.4 Vascularity and angiogenesis are increased by CS-A+NPC treatment	105
5.3 Aim 3 Determine the effects of treatment with CS-A encapsulated NPCs on local blood flow restoration and functional recovery after ischemic stroke.	109
5.3.1 CS-A encapsulation of NPCs augments blood flow to the infarcted cortex	109
5.3.2 Pial collateral artery diameter and recruitment are increased with CS-A encapsulation of NPCs	111
5.3.3 CS-A encapsulation of NPCs fails to provide additional functional benefits in sensorimotor tests after ischemic stroke	114
5.3.4 Neutralization of bFGF abolishes CS-A + NPC-mediated improvements in vascular regeneration and blood flow recovery	119
CHAPTER 6. Conclusions	122
6.1 CS-A encapsulation of NPCs increases transplant retention, elicits a pro-regenerative inflammatory response, and augments vascular regeneration and blood flow after ischemic stroke	122
6.2 Pitfalls in CS-A + NPC therapy and transplantation directed to the infarct core region	128
6.2.1 Cellular therapy targeted to the infarct core failed to provide neuronal replacement after ischemic stroke	128
6.2.2 CS-A encapsulation of NPCs failed to improve functional outcomes	129
6.3 Opportunities for improvement of CS-A encapsulation of NPCs for the treatment of brain injuries	131
REFERENCES	135

LIST OF TABLES

Table 1	Comparison of important risk factors for hemorrhagic versus ischemic stroke. Overall relative risk (RR) noted in left column. Note: This list is not exhaustive. See [59, 60, 62-68] for comprehensive lists of risk factors.	10
Table 2	Published clinical trials on collateral enhancement therapy for the treatment of acute ischemic stroke.	30
Table 3	Rodent Stroke Models	38
Table 4	List of studies of hydrogel encapsulation for cellular therapy in stroke. Adapted and updated from [310].	51
Table 5	Cell differentiation markers.	80

LIST OF FIGURES

Figure 1	Overview of general experimental design. A) Treatment groups. B) Experimental timeline.	55
Figure 2	Encapsulation with CS-A reduces NPC cell death following 3 days after transplantation into the ischemic core.	76
Figure 3	LDH release following oxygen and glucose deprivation (OGD). Media was collected from NPCs exposed to hypoxic conditions (<i>Oxygen and glucose deprivation (OGD) conditions and lactate dehydrogenase (LDH) cytotoxicity assay</i>). A) Analysis of LDH release between treatment groups. B) Analysis of protein levels of cleaved caspase 3, BCL2, and HIF1 between treatment groups. n=3/group. * indicates p<0.05; One-way ANOVA with Bonferroni correction for A) and two-tailed T-test for B).	77
Figure 4	CS-A encapsulation improves NPC retention 14 days after transplantation. NPCs were transplanted intracranially with or without CS-A encapsulation and sacrificed 2 weeks later. A) Representative images of radiant efficiency heatmaps 2 weeks after transplantation of DiR-labelled cells (<i>Cell retention imaging</i>). B) Analysis of DiR fluorescence. n=4-5/group. C) Representative fluorescent images of transplanted GFP+ cells in the stroke core. D) Analysis of cell retention. n=6/group. E) Representative images of transplanted CS-A encapsulated cells at 10x (top) and 40x (bottom) 2 weeks after transplantation. * and ** indicates p<0.05 and p<0.005, respectively; two-tailed T-test.	78
Figure 5	Overview of in vitro differentiation experiments. Mouse iPSCs were induced into neurospheres using rotary culture then underwent the RA neural induction protocol (<i>Neural progenitor cell culture and CS-A hydrogel preparation</i>).	79
Figure 6	Neuronal differentiation of CS-A encapsulated NPCs. A. Representative Western blotting and analysis for NeuN, SNAP25, TUJ1, GAD67, and NMDAR1b. B. Representative image of MAP2 staining of differentiated NPC within CS-A. n=4/group. * p<0.05, two-tailed T-test.	80
Figure 7	Protein expression of non-differentiated and glial markers of CS-A encapsulated NPCs. A) Representative Western blotting	81

	of Nanog, Sox2, Nestin, and GFAP. B) Analysis of Western blotting. n=4/group. * p<0.05, two-tailed T-test.	
Figure 8	Neuronal differentiation of NPCs 14 days after transplantation. A) Representative images of NeuN+ and GFP+ colabeled cells in the infarct core 2 weeks after transplantation. B) Analysis of percentage and number of NeuN/GFP colabeled cells. n=6-8/group. * indicates p<0.05; two-tailed T-test.	82
Figure 9	Astrocytic and non-differentiation of NPCs 14 days after transplantation. A) Representative images of GFP, Sox2, and GFAP co-labelled cells in the infarct core 2 weeks after transplantation. B) Analysis of percentage of astrocytic and non-differentiated cells. n=6-8/group. * indicates p<0.05; two-tailed T-test.	84
Figure 10	Formation of axons within the stroke core region. A) Representative images of contralateral axonal expression patterns and axonal expression within the stroke core region 2 weeks after transplantation. B) Insets from panel A) illustrate axons travel parallel to the astrocytic barrier and do not traverse the astrocytic barrier.	85
Figure 12	CS-A + NPC treatment promotes alternatively activated microglia polarization 2 weeks after intracranial transplantation. A) Representative images of PPAR γ (an M2 marker) and IBA1 (a microglial marker) co-staining in the stroke area 2 weeks after transplantation. B) Analysis of number of PPAR γ /IBA1 co-staining. n=8-12. **indicates p<0.005; 1-way ANOVA	89
Figure 13	CS-A+NPC treatment significantly enhances IL-10 protein levels in the stroke core region 1 week after transplantation. n=4-8. *, **, and **** indicate p<0.05, p<0.005, and p<0.0001, respectively;	90
Figure 14	Expression of released immune factors within the stroke core region 1 week after transplantation. n=3-4. * indicates p<0.05;	92
Figure 15	Expression of released immune factors within the peri-infarct region 1 week after transplantation. * indicates p<0.05;	93
Figure 16	Comparison of immune factors in the stroke core versus peri-infarct region in CS-A+NPC treated mice 1 week after transplantation. **** indicates p<0.0001. Two-way ANOVA with Holm-Sidak correction.	94

Figure 17	Analysis of group relative expression of immune factors 2 weeks following intracranial transplantation. ***, and **** indicate $p<0.0005$ and $p<0.0001$, respectively. Two-way ANOVA with Holm-Sidak	95
Figure 18	Experimental design for <i>in vitro</i> macrophage culture.	95
Figure 19	CS-A encapsulation of stroke macrophages promotes a regenerative macrophage phenotype <i>in vitro</i> . A) Western blotting of VEGFR2, TIE2, PPAR, bFGF, and IL-10. B) Analysis of protein expression. $n=3-5$ <i>in vitro</i> replicates of macrophages pooled from 8 mice. * indicates $p<0.05$; two-tailed T-test.	96
Figure 23	CS-A + NPC treatment directed to the stroke core does not improve neurogenesis after stroke. A) Representative images of NeuN/BrdU and DCX staining at the peri-infarct region (top panel) and SVZ 2 weeks after intracranial transplantation. B) Analysis of neurogenesis, SVZ DCX staining intensity, and number of peri-infarct DCX+ neuroblasts. $n=8-12$. * indicates $p<0.05$; 1-way ANOVA	103
Figure 24	CS-A+NPC treatment increases BDNF expression in the stroke core region 1 week after transplantation. BDNF levels were increased in the CS-A+NPC group compared to all controls. NGF levels were not statistically different between groups. $n=4-8$. * indicates $p<0.05$; 1-way ANOVA	104
Figure 25	CS-A encapsulation of NPCs improves angiogenesis and stroke core vascularity. A) Glut1 and BrdU costaining. B) Analysis of angiogenesis (#Glut1/BrdU co-labelled endothelium). C) Analysis of vascularity. $n=8-12$. *, **, and *** indicate $p<0.05$, $p<0.005$, and $p<0.001$, respectively;	106
Figure 26	Representative image of a muscular artery (SMA/Glut/BrdU) formation within the hydrogel of mice treated with CS-A + NPC.	107
Figure 27	Increased expression of angiogenic proteins after treatment with CS-A+NPC. A) Western blotting of bFGF, p-STAT3, p-AKT, and VEGF. B) Analysis of angiogenic protein expression. *, **, and **** indicates $p<0.05$, $p<0.005$, and $p<0.0001$, respectively; 1-way ANOVA with Bonferonni correction.	107
Figure 28	CS-A promotes NPC-mediated endothelial haptotaxis (<i>Hydrogel haptotaxis assay</i>). $n=3$. ** indicates $p<0.005$;	108

Figure 29	CS-A may not affect endothelial replication <i>in vitro</i> . Western blotting analysis indicates CyclinD1, a cell cycle protein and marker for replication, was not different between groups. n=3; two-tailed T-test.	109
Figure 30	Diagram of cortical areas measured using laser Doppler flowmetry and representative pre-stroke and post-stroke flow heatmaps (<i>Mouse stroke model, laser Doppler flowmetry, and transplantations</i>).	110
Figure 31	CS-A encapsulation improves cortical blood flow after stroke. The top panel illustrates LCBF heatmaps at 2 weeks after transplantations (<i>Mouse stroke model, laser Doppler flowmetry, and transplantations</i>). n=8-12. * and **** indicates p<0.05 and p<0.0001, respectively; 2-way ANOVA	111
Figure 32	Treatment with CS-A+NPCs improves pial artery collateralization after stroke. A) Representative images of pial collaterals; red box indicates MCA-ACA anastomoses in similar locations between animals. B) Analysis of collateral vessel number. C) Analysis of average collateral vessel width. D) Analysis of pial collateral recruitment. n=8-12. * and ** indicates p<0.05 and p<0.005, respectively; 1-way ANOVA with Bonferroni correction; all groups significantly (****) greater than sham in C) and D).	113
Figure 33	Confirmation of outward remodeling in pial vessels following treatment with CS-A + NPC. A) Representative image of pial artery in the peri-infarct region with numerous SMA/BrdU colabelled cells. B) Representative image of pial artery in the stroke core region with multiple SMA/BrdU colabelled cells.	114
Figure 34	Corner and adhesive removal test performance after treatment. n=8-12. *, **, ***, and **** indicates p<0.05, p<0.005, p<0.0005, and p<0.0001, respectively; 2-way ANOVA	115
Figure 35	Rotarod test performance after transplantation. n=8-12. *, **, ***, and **** indicates p<0.05, p<0.005, p<0.0005, and p<0.0001, respectively; 2-way ANOVA with Bonferroni correction.	116
Figure 36	Isovolumetric pull test performance after treatment. n=3-4 *, **, ***, and **** indicates p<0.05, p<0.005, p<0.0005, and p<0.0001, respectively; 2-way ANOVA with Holm-Sidak correction.	117

Figure 37	Recovery of post-stroke neuropsychiatric deficits following treatment. n=8-12. * indicates $p<0.05$; 2-way ANOVA	118
Figure 38	Analysis of group relative sensorimotor test performance 2 weeks after ischemic stroke. Two-way ANOVA with Bonferroni correction. CS-A+NPC vs NPC $p=0.6722$; CS-A+NPC vs No treatment $p=0.0604$. NPC vs no treatment $p=0.2334$.	118
Figure 39	Experimental design for bFGF neutralization animal experiments.	120
Figure 40	Neutralization of bFGF abolishes vascular regeneration and blood flow in CS-A+NPC treated mice following ischemic stroke. A) Representative images of Glut1/BrdU costaining for angiogenesis, pial collateralization, and local cerebral blood flow in the stroke region 2 weeks after stroke. B) Analysis of angiogenesis, pial collateral recruitment, cortical blood flow, and corner test. n=4-5. *, **, and *** indicates $p<0.05$, ** $p<0.005$, *** $p<0.0005$ respectively; two-tailed T-test.	120

LIST OF SYMBOLS AND ABBREVIATIONS

ACA	Anterior cerebral artery
AD	Alzheimer's disease
AHA	American heart association
AIF	Apoptosis inducing factor
AIS	Acute ischemic stroke
AMPA	A-amino-3-hydroxy-5-methyl-4-isoxazole propionic acid
Ang1/2	Angiopoietin1/2
ANOVA	Analysis of variance
AP	Action potential
ATP	Adenosine-5'-triphosphate
BBB	Blood brain barrier
BDNF	Brain-derived neurotrophic factor
BMSC	Bone marrow-derived stem cells
Ca ²⁺	Calcium ion
CNS	Central nervous system
CS-A	Chondroitin-4-sulfate-A
DCX	Doublecortin
EB	Embryoid body
ECM	Extracellular matrix
ES	Embryonic stem
ESC	Embryonic stem cell
FDA	Food and Drug Administration
GABA	Gamma-aminobutyric acid
GAT	GABA transporter
GDNF	Glial cell-derived neurotrophic factor
GFAP	Glial fibrillary acidic protein
GFP	Green fluorescent protein
HA	Hyaluronan
hiPSC	Human iPSC
HP	Hypoxic preconditioning
IA	Intra-arterial
ICAM-1	Intercellular adhesion molecule 1
ICH	Intracranial hemorrhage
iPSC	Induced pluripotent stem cell
IV	Intravenous
IV	Intravenous

K ⁺	Potassium ion
LCBF	Local cerebral blood flow
LDH	Lactose dehydrogenase
MCA	Middle cerebral artery
MCAo	Middle cerebral artery occlusion
MI	Myocardial infarction
miPSC	Mouse ipsc
MMP	Matrix metalloproteases
MSC	Mesenchymal stem cells
MSC	Mesenchymal stem cells
Na ⁺	Sodium ion
NMDA	N-methyl-d-aspartate
NPC	Neural progenitor cell
PCA	Posterior cerebral artery
PD	Parkinson's disease
RA	Retinoic acid
ROS	Reactive oxygen species
SDF-1 α	Stromal cell-derived factor-1
SGZ	Subgranular zone
SMA	Smooth muscle actin
SVZ	Subventricular zone
TIA	Transient ischemic attack
Tie1/2	Tyrosine kinase with immunoglobulin-like and EGF-like domains
TNF- α	Tumor necrosis factor - α
tPA	Tissue plasminogen activator
TUNEL	Terminal deoxynucleotidyl transferase dutp nick end labeling
VEGF	Vascular endothelial growth factor
VEGF-R	Vascular endothelial growth factor receptor

SUMMARY

Stroke is a growing cause of morbidity and a significant cause of mortality in the United States. Currently, no therapies can promote recovery of neuronal networks lost to cerebral infarction. Tissue engineering strategies such as cellular therapy may be able to enhance functional regeneration of brain tissue. Neural progenitor cells (NPCs) are at the forefront of preclinical studies for regenerative stroke therapies. NPCs can differentiate into and replace neurons and promote endogenous recovery mechanisms. The stroke core region is the ideal location for replacement of neural tissue since it is *in situ*, and following degradation, develops into a potential space for targeting injections. However, the compromised cortical perfusion and degradation of the extracellular matrix following ischemia create an inhospitable environment resistant to cellular therapy. Overcoming these limitations are critical for clinical translation. In our studies, we test whether encapsulation of NPCs in a chondroitin-4-sulfate-A (CS-A) hydrogel enhances their ability to repair the injured brain following stroke in mice. We show that CS-A encapsulated NPCs improve vascular regeneration at multiple levels to increase cerebral blood flow. These outcomes are likely mediated by enhanced paracrine signaling effects and regenerative immunomodulation. Further research and additional strategies are necessary to overcome the shortcomings of CS-A encapsulated NPC treatment. In summary, extending the therapeutic potential of NPCs using angiogenic biomaterials such as CS-A may be a viable solution to overcoming limitations for regenerative cellular therapy in ischemic stroke.

INTRODUCTION

Ischemic stroke is one of the leading causes of mortality and morbidity worldwide, and the 5th leading cause of death in the US [1]. Nearly 800,000 people encounter new or recurrent stroke yearly in the US alone, and few successful treatments have been developed to treat this disease. Importantly, stroke is the leading cause of long-term disability, and there are millions of people with brain damage [2]. Current therapy guidelines involve reperfusion either by treatment with tissue plasminogen activator or by surgery, and in most cases, must be carried out within 6-24 hours after stroke onset. At the present time, there are no therapies that promote tissue recovery after this brief therapeutic window following cerebral infarction.

Cellular therapies made available using stem cell techniques hold promise for improving functional recovery after ischemia via mechanisms involving both trophic support and cell replacement [3-7]. Induced pluripotent stem cells (iPSCs) can be reprogrammed from autologous host cells to minimize immunogenicity and are at the forefront of pre-clinical studies for regenerative medicine [5, 8-13]. Transplanted iPSC derived neural progenitor cells (iPSC-NPCs) can differentiate into functional neurons that can integrate and replace host circuitry lost to stroke [14-20]. iPSC-NPCs also promote endogenous recovery mechanisms such as enhanced vascularization and host neuronal plasticity, immunosuppression, and recruitment endogenous progenitor cells [4, 6, 7, 21-25]. Released proteins such as growth factors and interleukins play an integral role in mediating these regenerative properties [4, 22, 26-28]. The current bottlenecks for iPSC-NPC

treatments include graft survival and retention following transplantation amidst the toxic stroke core, limited efficacy of improving homeostatic compensatory repair mechanisms, and restricted integration of differentiated cells into existing neural networks [10-12].

However, the specific pathophysiology of ischemic stroke makes infarcted brain tissue especially resistant to cellular therapy. Immediately following cessation of blood supply, cellular energy homeostasis is disrupted, and cell death develops within minutes [29]. Furthermore, the blood brain barrier is disrupted, leading to increased permeability of reactive oxygen species and inflammatory mediators, which can exacerbate the initial damage [30]. Following loss of blood flow, normal ionic gradients important for cellular membrane potential and neuronal signaling dilapidate and result in the release of toxic amounts of glutamate, which can reside in the tissue for days. Intracellular and extracellular proteases are activated which results both cellular damage and degradation of the extracellular matrix. Following this initial wave of cell death during the acute phase of stroke, inflammatory cells such as microglia/macrophages and monocytes infiltrate the hypoxic tissue [29]. Microglia/macrophages in the stroke region tend to exhibit a pro-inflammatory phenotype (M1/classically activated), which further antagonizes regenerative efforts. Days to weeks after focal brain ischemia, astrocytes congregate to create an interface between the core infarct region and the viable parenchyma to limit the spread of toxic inflammation. However, this astrocytic scar is thought to be inhibitory to axonal growth of both newly formed endogenous neurons and transplanted cells [29]. The adult brain's innate ability to recreate

damage neural tissue is extremely limited. After an ischemic insult, neural stem cells in the subventricular zone are recruited to the peri-infarct region where they can become newborn neurons. Unfortunately, the scale at which this occurs in humans without intervention is insufficient to generate meaningful recovery. Previous studies have attempted to overcome or bypass some of these difficulties by either increasing the resiliency and efficacy of the transplanted cells (for example, by hypoxic preconditioning [23, 24, 31] or genetic manipulation [32]), or by transplanting in the peri-infarct region where the microenvironment is less hostile. These efforts have proven useful but ultimately insufficient for clinical translation. Furthermore, directing injections to the peri-infarct region requires invasive placement in sensitive brain tissue, which can be damaged simply by delivery approach [33-35].

An alternative strategy is to create a microenvironment in the stroke core favorable for transplantation and regeneration via hydrogel encapsulation [3, 11, 12, 36-39]. Hydrogels are biocompatible carrier materials that can be used to promote survival, differentiation, trophic potency, and functional integration of transplanted cells [27, 37, 40-42]. Their ability to emulate the biophysical properties of soft neural tissue makes them ideal for engraftment into brain injuries [27, 43-48]. Previous studies have utilized hydrogels composed of extracellular matrix (ECM) such as hyaluronan (HA) to enhance transplant cell viability and direct differentiation of stem cells with varying success. Hyaluronan (HA) is a well-studied brain resident extracellular matrix (ECM) component that has previously been used as a hydrogel carrier for cellular therapy in stroke studies [33, 37, 41, 45]. HA can

improve cell survival after transplant, promote angiogenesis and anti-inflammatory signaling, and encourage neuronal differentiation of stem cells [27, 37, 41, 45]. Recently, a HA-based hydrogel was demonstrated to encourage vascular repair and neuronal migration to the stroke core in mice[49]. However, low molecular weight HA is pro-inflammatory, and transplanting HA into the degradatory stroke core would carry an unnecessary risk of exacerbating inflammation [37, 41, 50].

Unlike HA, chondroitin-4-sulfate (chondroitin sulfate-A/CS-A) possesses greater structural and functional elements to modulate trophic factor enrichment and promote autocrine/paracrine signaling [51, 52]. Endogenously, CS-A is an integral ECM constituent of the neural stem cell niche [47, 51-54]. ECM binding is a critical step of growth factor-mediated tissue repair [55]. Regenerative factors such as basic fibroblast growth factor (bFGF/FGF2) and brain-derived neurotrophic factor (BDNF), and the immunomodulatory protein interleukin 10 (IL-10) have high affinities for CS-A [53]. Our collaborators have recently shown that CS-A can improve growth factor and transplanted cell retention in a rat traumatic brain injury model, however, they are wholly unexplored as transplant mediums for the treatment of stroke [39, 53]. We hypothesize that these polymers can be used to create a depot in the stroke core for the growth factors necessary to synergize with and enable NPC-mediated tissue regeneration.

In the present study, we investigated the ability of CS-A to facilitate transplanted NPC survival, retention, and differentiation, the effects of CS-A encapsulation of NPCs on regenerative processes in the brain, and the extent to which CS-A could facilitate functional recovery of blood flow and behavioral

outcomes after ischemic stroke in mice.

SPECIFIC AIMS AND HYPOTHESES

The overarching goal of this project is to improve the therapeutic value of neural progenitor cells for the treatment of ischemic stroke. Transplantation of NPCs can help to repair damaged neural networks and enhance endogenous regeneration after stroke. However, several critical issues remain to be improved for the development of more effective and efficient stem cell treatment. Many transplanted cells die in the harsh stroke core and fail to differentiate into neurons or facilitate paracrine effects. We propose to encapsulate induced pluripotent stem cell derived NPCs in a neuro-regenerative and angiogenic chondroitin-4-sulfate-A hydrogel and hypothesize that this beneficial extracellular matrix scaffolding will provide an enriched environment for enhanced retention and trophic potential of transplanted NPCs. This central hypothesis was tested with the aims described below.

2.1 Aim 1: Determine the effects of CS-A on NPC survival and differentiation.

Transplanted NPCs may replace neurons lost to the ischemic brain damage. We hypothesize that CS-A encapsulation of NPCs will support neuronal differentiation *in vitro* and after transplantation into the ischemic brain. I hypothesize that CS-A encapsulation will enhance transplant cell survival and retention even in the ischemic core region. NPCs encapsulated CS-A will be transplanted into the ischemic core 7 days after cerebral ischemia targeting the right sensorimotor cortex in adult mice. Cell survival will be inspected after transplantation using terminal deoxynucleotidyl transferase dUTP nick end labeling (TUNEL) staining, and cell death/survival protein expression will be measured using Western blotting

and immunohistochemical (IHC) staining of brain sections. Cellular retention will be evaluated using IHC and tracking of DiI18(7); 1,1'-dioctadecyl-3,3',3'-tetramethylindotricarbocyanine iodide (DiR) labelled cells. The effect of CS-A encapsulation on iPSC-NPC differentiation will be interrogated at the molecular and cellular levels using Western blotting and immunohistochemistry.

2.2 Aim 2: Determine the effects of treatment with CS-A encapsulated NPC on regeneration in the ischemic brain.

Following successful engraftment, NPCs can improve endogenous angiogenesis, neurogenesis, and lessen inflammation [56-58]. Regenerative factor recruitment and retention are critical for this trophic support. We hypothesized that CS-A can augment NPC-mediated neuronal and vascular regeneration, and promote a pro-regenerative immune phenotype. Stroke mice will be treated with BrdU daily after treatment to label newly formed cells. The regenerative factor enriching effects of CS-A will be investigated using IHC and Western blotting. Microglia/macrophage polarization and astrocyte reactivity will be compared by IHC, Western blotting, and protein array assays. The potential specific effects of the CS-A hydrogel on stroke core microglia and brain endothelial will also be tested using *in vitro* methods. We will also employ a novel microfluidic hydrogel migration preference assay to test the effects of CS-A on recruitment of endothelial cells.

2.3 Aim 3: Determine the effects of treatment with CS-A encapsulated NPCs on local blood flow restoration and functional recovery after ischemic stroke.

Functional recovery is the ultimate goal for stroke treatment. Pial collateral artery recruitment and blood flow enhancement are essential to recovery. Mice with sensorimotor cortex stroke suffer from whisker and forearm sensorimotor deficits and gradually develop depression-like behaviors. I hypothesize that transplantation of CS-A encapsulated NPCs will promote additional collateral recruitment and regional blood flow recovery and will improve behavioral deficits following stroke. Arterial characteristics will be analyzed using fluorescent imaging of whole brains isolated from α SMA-GFP mice, and blood flow recovery will be measured using laser doppler scanning. Sensorimotor recovery will be evaluated using adhesive removal, cylinder, rotarod, volitional isometric pull strength, and corner tests. Recovery from post-stroke depressive-like behaviors will be evaluated by tail suspension, forced swim, open field, sucrose preference, and home cage monitoring tests.

The research proposed in these specific aims will provide insight into the potential benefits of CS-A encapsulation of NPCs for the treatment of ischemic stroke.

LITERATURE REVIEW

3.1 Stroke Epidemiological Trends

Stroke is one of the leading causes of death or long-term disability worldwide. According to the American Heart Association, stroke became the fifth leading cause of death in the United States in 2013 [2]. Nearly 1 in 20 people in the United States die due to stroke. Fortunately, population trends for stroke are improving. Over the last decade, the relative rate of death from stroke has decreased by nearly a third, and the number of stroke deaths fell by 18.2%. Overall, stroke mortality has declined across sex, race, and age. Stroke death rates have decreased among people aged ≥ 65 years. Many of these improvements are attributed to improved preventative, perioperative, and management guidelines, resulting in both reduced stroke incidence and lower stroke fatality rates [2, 59-61]. However, despite these promising epidemiological trends, nearly 800,000 people encounter new or recurrent stroke yearly in the US alone, and few successful treatments have been developed to treat this disease [2].

3.2 Stroke Types and Risk Factors

Most simply, stroke occurs when a portion of the blood flow to the brain is diminished or blocked, resulting in cell death, including both necrosis, apoptosis, and other mixed cell death phenotypes. There are two main types of stroke: hemorrhagic stroke, which results from blood vessel rupture, and ischemic stroke, which results from blood vessel occlusion. Hemorrhagic strokes account for about

15% of total strokes [62]. Blood from leaking vessels can enter the brain tissue (intracerebral hemorrhage, ICH), or the space below the arachnoid layer of the meninges (subarachnoid hemorrhage, SAH). ICH is more common than SAH. Over 80% of strokes are ischemic and can be categorized based on mechanism of blood vessel occlusion. The three primary ischemic stroke types are large artery atherosclerosis, cardiogenic embolism, and small vessel occlusion. The non-modifiable and potentially-modifiable risk factors for hemorrhagic and ischemic strokes are listed in (Table 1).

Table 1. Comparison of important risk factors for hemorrhagic versus ischemic stroke. Overall relative risk (RR) noted in left column. Note: This list is not exhaustive. See [59, 60, 62-68] for comprehensive lists of risk factors.

Risk Factors		Hemorrhagic Stroke	Ischemic Stroke
Non-modifiable	Sex (RR male 1.30-1.37)	Females during and immediately after pregnancy	Male
	Race/Ethnicity (RR 1.26-1.81 Black vs white)	Asian > African American > Hispanic > White	African American > Hispanic > White
Modifiable	Blood Pressure (RR 1.25-1.28)	Hypertension is a well-established risk factor for both types; strongest association with intracerebral hemorrhage	
	Diabetes (RR 1.10-1.68)	Association not well-established; may negatively affect outcomes	Strong association
	Smoking (RR 1.82-2.04)	Associated with subarachnoid but not intracerebral hemorrhage	Strong association

Table 1 continued			
Modifiable	Atrial fibrillation (RR 1.6-5.8)	Not directly associated, however, anti-thrombolytic (anticoagulation> antiplatelet) use is strongly associated	Strong association
	BMI/Waist-to-hip ratio (RR 1.75-2.37)	High BMI/Waist-to-hip ratio is associated with both stroke types	
	Diet (modified Alternate Healthy Eating Index) (RR	High mAHEI is negatively associated with both stroke types	
	Physical Activity (RR 0.69-0.82)	Regular physical activity is negatively associated with both stroke types	
	Alcohol Consumption (RR 1.04-1.17)	Heavy alcohol consumption is associated with both stroke types; light/moderate alcohol consumption is not associated with ischemic stroke, and may be protective [69]	

Numerous mechanisms regarding ischemic stroke pathophysiology have been elucidated. Understanding the contribution of each mechanism can inform research and the development of novel treatments. Brain tissue is highly dependent on oxidative phosphorylation to provide energy, and thus requires high amounts of oxygen and glucose. It is estimated that the brain utilizes about 20% of the body's resting metabolism, and about half of that is used to maintain ion gradients [70]. Impairment of cerebral blood flow cuts off the delivery of key nutrients and oxygen, compromising the energy consumption needed to maintain homeostasis. Many cells die as a direct result of ischemic stress. Ensuing biochemical and cellular events exacerbate brain damage after the initial hypoxic insult. Particularly, improper signaling due to ion imbalance after hypoxia plays a significant role in stroke progression. For the following sections, we will describe a series of temporal and spatial pathophysiological events that follow ischemic

stroke. We also will provide a detailed discussion of the mechanisms that contribute to stroke pathology at each stage.

3.3 Cellular and Molecular Mechanisms in Ischemic Stroke Pathophysiology

The ischemic stroke region is comprised of two parts. In the core area of the ischemic territory, the perfusion deficit results in low ATP. Cellular energy homeostasis is disrupted, and cell death develops within minutes. In the penumbra region, the area between unaffected and ischemic regions, partially preserved perfusion from non-occluded collateral blood vessels allows for milder but still significant damage to occur [71]. The core and penumbra regions are spatially and temporally dynamic. The penumbra comprises a large portion of the lesion volume during the initial stage of blood vessel occlusion [72]. However, if left untreated, the penumbra region may become infarcted and the core territory can expand over the course of hours and days. It is believed that the core region of the stroke is unsalvageable, while the ischemic penumbra is at risk, but still rescuable if perfusion is restored [73]. Recent literature has revealed that a select few cells can survive in the stroke core, suggesting that the core infarct region is not entirely unsalvageable [74]. However, the majority of research is targeted at enhancing the peri-infarct area with apparent therapeutic opportunity. A cascade of harmful events, including excitotoxicity, spreading depolarization, oxidative and nitrosative stress, inflammation, and cell death are central to stroke pathology. Understanding the mechanisms that underlie brain damage in the stroke core and the ischemic penumbra may direct research on future treatments.

3.3.1 Excitotoxicity, Calcium Dysregulation, and Ion Imbalance

Oxygen and glucose supply is impaired during the immediate perfusion deficit following stroke. This deficit compromises the energy supply required to maintain normal ionic gradients in neurons and glia. As a result, these cells can lose membrane potential resulting in depolarization events. Depolarization causes voltage-dependent calcium channel activation and excitatory amino acid (mainly glutamate) release into the extracellular space. Concurrently, presynaptic reuptake of glutamate is reduced due to the lack of energy needed to activate ion pumps, which further exacerbates the increased extracellular glutamate concentration. The excess glutamate binds AMPA (α -amino-3-hydroxy-5-methyl-4-isoxazole propionic acid) and NMDA (N-methyl-D-aspartate) receptors to increase the influx of water, sodium, and calcium into neurons, inducing a host of signaling events that cause cell swelling, activation of catabolic activity, and eventual cell death [75, 76]. Massive calcium influx initiates a series of cytoplasmic, nuclear, and mitochondrial events that directly contribute to the development of tissue damage, for example, via activation of proteases [77]. Uncontrolled activation of calcium-dependent enzymes leads to further ATP depletion and accelerates cell death. Acutely, calcium can activate phospholipase A2 to generate free radical species which cause membrane damage. Oxygen radicals can also contribute to inflammation and apoptosis, as will be discussed below. Calcium-induced activation of neuronal nitric-oxide synthase (nNOS) and other Ca^{2+} -dependent enzymes causes nitric oxide (NO) and superoxide production, which further promote cell death and tissue damage. Mitochondria, an important source of

reactive oxygen species (ROS), are also involved in acute cell toxicity [73, 78]. Aside from damaging cell membranes and proteins, free radicals also arrest energy production, further disrupting energy homeostasis. Calcium release from the dysfunctional mitochondria further exacerbates intracellular calcium signaling. Cell to cell interactions may also contribute to the spread of excitotoxicity as indicated by the apparent role of gap junctions in NMDA receptor mediated neuronal death [79]. While the glutamate toxicity hypothesis has been validated in laboratory settings, clinical trials targeting the NMDA and AMPA receptors have yielded negligible results [80]. It is likely that the cell death processes are far more complex than can be described by glutamate toxicity alone. The NMDA-AMPA pathway is only one player in the ion balance dysregulation following stroke. Indeed, many other ion channels have been implicated in calcium accumulation and toxicity. Sodium-calcium exchangers, gap junctions, volume-regulated anion channels, transient receptor potential channels, acid-sensing channels, and other non-selective cation channels contribute to ion imbalance [76, 81]. There is ample space for research on the influence of specific receptors to ion imbalance after acute infarction, and how targeting these receptors may provide therapeutic benefits.

3.3.2 Spreading Depolarization and Spreading Ischemia

As discussed above, ischemic neurons depolarize due to a lack of energy supply, and subsequently depolarize to release glutamate and potassium. Spreading depolarization describes a sustained depolarization of neurons, which is effectively a short circuit between neurons and the extracellular space [82]. This

depolarization is accompanied by cell swelling and dendritic spine distortion [83]. Direct gap junction mediated connections between neurons may facilitate spreading of depolarization [82]. Under pathological conditions such as stroke, the normal hemodynamic response to depolarization, namely vasodilation associated with neurovascular coupling, can become inverted. Thus, rather than dilating, arterioles may constrict to reduce blood flow, termed spreading ischemia [82]. Increases in extracellular cations (primarily potassium) and decreases in nitric oxide, augment vasoconstriction and reduces vasodilation. The ensuing spreading depolarization-induced ischemia creates a vicious cycle where supply of metabolic substrates is reduced and demand is simultaneously increased. Spreading depolarization is known to occur in the ischemic penumbra and may contribute to lesion progression [84, 85]. Each successive spreading depolarization can cause enlargement of the stroke area [85]. It has been suggested that targeting the inverse microvascular response to spreading repolarization may be a useful therapeutic intervention, since targeting depolarization has failed thus far [80, 82, 83, 86].

3.3.3 Oxidative and Nitrosative Stress

Oxidative and nitrosative stress also contribute to ischemic stroke pathology. Oxidative and nitrosative free radicals are byproducts of cellular metabolism and are normally removed by endogenous antioxidant enzymes and chemicals such as superoxide dismutase (SOD), glutathione peroxidase, catalase, ascorbic acid, and α -tocopherol [78]. In the injured brain, radical species are extremely harmful since endogenous antioxidant enzymes and vitamin concentrations are not high

enough to counteract excess radical formation [87]. The brunt of mitochondrial reactive oxygen species generation is believed to occur during reperfusion. Ischemia-induced post-translational modification of proteins in the oxidative phosphorylation pathway prime mitochondria for excessive activity upon the reintroduction of oxygen [88]. This hyperactive state could lead to a surge of ROS during reperfusion, overwhelming endogenous protective mechanisms. Excess ROS can directly damage proteins, nucleic acids, lipids, and carbohydrates to promote cell death. ROS can also be generated via NMDA receptor induced NADPH oxidase activation [89]. This pathway may be important acutely after ischemia during the excitotoxicity phase. Nitric oxide (NO) is a free radical and an important cellular signaling molecule involved in many physiological and pathological processes. However, excess NO can be directly and indirectly neurotoxic. Similar to ROS, reactive nitrogen species (RNS) are harmful to cellular components and can induce neuronal death [90]. NO can react rapidly with superoxide to generate the strong oxidant peroxynitrite, which is extremely cytotoxic [91]. NOS activity and NO production are increased in the ischemic brain, leading to increased peroxynitrite production and ensuing cellular damage. RNS are known to contribute to breakdown of the blood brain barrier (BBB) via activation of matrix metalloproteinases (MMPs) [91, 92]. Taken together, ROS and RNS are damaging neurotoxic agents that intensify ischemic damage after reperfusion. Targeting these reactive chemicals may be useful in reducing side effects after administration of tPA and the resulting reperfusion [91, 93].

3.3.4 The Inflammatory and Astrocytic Response to Cerebral Infarction

Inflammation plays an important role in the pathogenesis of ischemic stroke. After an ischemic insult, several key transcriptional factors, such as hypoxia inducible factor 1 (HIF-1), nuclear factor- κ B (NF- κ B), interferon regulatory factor 1 (IRF1), and signal transducer and activator of transcription (STAT3), are up-regulated via calcium-induced signaling pathways, increased oxygen free radicals, and hypoxia [94-96]. These transcriptional factors induce the expression of numerous pro-inflammatory genes, including tumor necrosis factor α (TNF α), interleukin 1 α (IL-1 α) and 1 β (IL-1 β), intercellular adhesion molecule 1 (ICAM-1), and selectins [75, 94, 97]. Circulating leukocytes interact with these adhesion molecules to adhere to brain endothelium, transmigrate through the vascular wall, and enter the brain parenchyma. Neutrophils are thought to be the first leukocytes to infiltrate after ischemic stroke, and can be found as early as 30 minutes after focal ischemia [98]. Peak infiltration is on the order of days (1-3 days), and may continue to remain in the ischemic area for weeks [99]. This initial infiltrate amplifies the inflammatory response by releasing cytokines and chemokines, activating matrix metalloproteinases, and producing ROS. These effects are primarily negative and can result in BBB disruption, edema, neuronal death, and hemorrhagic transformation [94, 96-98, 100]. However, at later stages, neutrophilic infiltration may promote recovery and regeneration, for example, via MMP-9 mediated neurovascular remodeling [94, 98, 100, 101].

Circulating macrophages and endogenous brain microglia also play dual roles in recovery by expressing anti- and pro-inflammatory mediators. Resident microglia respond initially (within hours following infarction), while blood-derived

macrophages infiltrate later, by 3 days [98, 101, 102]. They continue to accumulate over the course of weeks [98, 102]. A number of studies suggest that the majority of macrophages in the ischemic brain are derived from resident microglia, and that the relative contribution of circulating versus resident macrophages needs further evaluation [98]. Traditionally, microglia/macrophages have been thought to demonstrate two primary phenotypes: “classically activated” M1 (pro-inflammatory) and “alternatively activated” M2 (protective/trophic support) subtypes [102, 103]. There is likely a significant overlap between these subtypes and a growing body of research indicates microglia/macrophages have an incredibly diverse range of biological functions following brain damage which is outside the scope of this review [98, 100, 102-106]. The M2 phenotype is primarily restorative, and can promote processes such as neurogenesis, axon growth and remodeling, vessel growth and infiltration, and myelination processes [102]. Initially after stroke, they are responsible for clearing cellular debris and infiltrating neutrophils [98]. The M1 phenotype is primarily pro-inflammatory. For example, they can exert neurotoxic effects via the production and release of cytokines (i.e. IL-1 β , IL-6, TNF- α), ROS, and MMPs [102, 106, 107]. Initially, the injury site is dominated by M2 macrophages; however, M1 macrophages dominate after about 1 week [102]. This M2-to-M1 transition may create an unfavorable microenvironment for repair and can last for weeks after injury [102].

Astrocytes are the most abundant cell type in the brain. Similar to other players in neuroinflammation, astrocytes play a dichotomous role in both damage and regeneration after stroke. They are able to form barriers between the CNS

parenchyma and non-neural tissue, for example, along brain vasculature and the meninges [108]. After stroke, astrocytic scars, formed mainly of newly proliferated astrocytes, create an interface between viable CNS parenchyma and the core infarct region [108-111]. Within a couple days after ischemia, astrocytes become reactive, exhibiting stellate morphology and expression of glial fibrillary acidic protein (GFAP) [109, 110]. The glial scar acts as a protective functional barrier that prevents the spreading of toxic inflammation [108]. Early after stroke, astrocytes appear to play a primarily neuroprotective role [108, 111-113]. Disruption of scar formation after stroke allows for the spread of neuroinflammation and results in greater loss of neurons, increased lesion size, and decreased function [108-112]. However, during the recovery phase after ischemic insult, the astrocytic scar is thought to be inhibitory to axonal growth and is associated with reduced neural regeneration and functional recovery [111, 112, 114, 115]. Contrary to this binary dogma, a growing body of research suggests the astrocyte scar can play a role in axonal recovery [116]. Further research is needed to clarify the role of the glial scar in healing after stroke, and its relation to potential therapies.

The inflammatory mechanisms that occur in response to stroke are complex and exhibit dichotomies that can best be explained temporally. Detailed research is needed to tease apart the contributions of individual cell types across both time and space relative to infarction. Careful consideration of the cellular inflammatory responses must be accounted for in the development and evaluation of stroke treatments. Optimal treatment would attenuate the negative effects of neuroinflammation while preserving or accentuating the positive effects.

3.3.5 *Cell Death after Cerebral Ischemia*

Cell death pathways are at the heart of stroke pathophysiology. Multiple modes of cell death are evident in stroke. Traditionally, these mechanisms were separated into apoptosis, or controlled cell death, and necrosis, or unregulated cell death [117]. Apoptosis involves the organized dismantling of cells to minimize damage to neighboring cells, while necrosis leads to release of intracellular debris which can stimulate inflammatory responses and damage surrounding cells through various mechanisms, for example, by generating excess ROS [118, 119]. We now understand there is considerable overlap between these pathways, and that necrotic cell death can be regulated (termed necroptosis, programmed necrosis, or caspase-independent programmed cell death) [75, 118-124]. Autophagy, a lysosomal processes of cellular component recycling, is intimately associated with both cell death and survival mechanisms in ischemia [122, 123, 125-130]. In fact, apoptosis, autophagy, programmed necrosis, and necrosis all occur in stroke, and some cells even exhibit multiple mechanisms simultaneously [74, 124, 131]. Recent literature suggests that after about 1 day post-stroke in the core region, around 70% of cells show signs of necrosis while 30% appear apoptotic, and autophagy is also concurrently activated in both of these cell death pathways [74].

There are two primary pathways of apoptosis in cerebral ischemia: 1) the intrinsic pathway, which initiates via mitochondrial release of cytochrome-C and activation of caspase-9, and 2) the extrinsic pathway, which commences with the activation of cell surface death receptors and caspase-8 [117, 118, 121]. Both of these pathways eventually converge to activate the executioner proteases

caspase-3 and -7 which drive proteolysis [117, 118, 121]. Ultrastructural evidence indicates that during apoptosis, the nucleus and other cellular organelles are condensed and fragmented into smaller parts [117, 118]. DNA is also hydrolyzed into many fragments. Finally, phagocytes ingest apoptotic bodies with minimal release of inflammatory cytokines [117, 121, 122]. Necrosis is caused by overwhelming stress (i.e. acute hypoxia in stroke), resulting in unregulated cellular demise [75, 118, 121, 124, 132]. Nuclei appear swollen, ROS are generated, and cellular membranes begin to disintegrate to allow the release of inflammatory cellular contents into the extracellular space [118, 119, 124, 127]. Contrary to apoptosis and necrosis, programmed necrosis is highly regulated but occurs independently of caspase signaling, and is instead mediated via receptor-interacting protein1 (RIPK1) [120-122, 133]. Activation of death receptors by TNF α and FasL are also involved in programmed necrosis [119-121, 133]. In an evolutionary sense, programmed necrosis is believed to provide defense against intracellular pathogens that block apoptosis activation [121]. Necroptosis has been documented in stroke, but its significance needs further study [76, 78, 118, 134, 135].

A number of morphological studies have elucidated the roles of apoptosis and necrosis after ischemic injury. Wei et al used a series of chemical and immunohistological methods, including 2,3,5-triphenyltetrazolium chloride (TTC) staining, hematoxylin–eosin (H&E) staining, terminal deoxyribonucleotidyl transferase-mediated dUTP nick end labeling (TUNEL), and caspase-3 staining, and ultrastructural examination to study cell death mechanisms in the ischemic

cortex and non-ischemic thalamus after cortical focal ischemia [124]. They showed that the morphology of TUNEL+ cells in the ischemic core were primarily necrotic, whereas TUNEL+ cells in the thalamus and cortical penumbra exhibited both necrotic and apoptotic morphology [124]. Isin et al also examined cell death patterns after transient and permanent focal ischemia to show that apoptosis and necrosis, or a mixed/hybrid phenotype, can occur in the same cells [135]. They suggest that the ischemic neuronal cell death phenotype may be determined by the relative speed of apoptotic versus necrotic processes [135]. Jiang et al performed a detailed analysis of the stroke core to show that apoptosis is a significant mechanism of cell death in the ischemic core, with up to 30% of cells undergoing programmed cell death [74]. These findings need further clarification regarding the role of programmed necrosis in cellular demise.

Autophagy is a well-known player in cellular homeostasis. Superfluous or damaged proteins and organelles are packed into autophagosomes, which drain into lysosomes for degradation [122, 123, 134, 136]. The role of autophagy in cell death, particularly in ischemic cell death, is controversial and under intense study. The effects of autophagy are likely context dependent. Numerous studies have demonstrated that autophagy is activated following ischemic insult [123, 126-128, 136-138]. Whether autophagy is a driver of cell death in ischemia is still not clarified. Some experimental evidence suggests that reducing autophagy early after infarction can attenuate injury progression [136, 139-141]. Conversely, other studies indicate that promoting autophagy may induce cells to undergo apoptotic rather than necrotic cell death, leading to reduced lesion sizes [136, 142, 143].

Inadequate autophagy may also contribute to cell death in stroke [144]. It is conceivable that a moderate amount of cellular component recycling, particularly in the acutely hypoxic stages of stroke, may provide neurons with a larger physiologic reserve thereby allowing the cells to sustain ischemic damage. It is equally conceivable that digesting valuable cellular components in response to hypoxic insult, when the cell needs them the most, can lead to cell demise. This view is consistent with observations that apoptosis and autophagy appear to predominate in the penumbra, where cells may exhibit a physiologic reserve large enough to sustain the initial ischemic insult, and necrosis appears to predominate in the core region, where autophagy may be more associated with cell death [74, 123, 126, 127, 129, 134, 145]. Future research on autophagy and its role in ischemic cell death must place special consideration to location (i.e. infarct versus peri-infarct regions) and timing after stroke.

3.4 Stroke Prevention and Treatment

Primary prevention is the optimal method for reducing stroke burden since nearly 80% of strokes are first events. Modifiable risk factors such as those listed in Table 1 can be readily identified in stroke prone patients [60]. The AHA/ASA guidelines for primary prevention of stroke provide detailed recommendations with special weight towards modifiable risk factors. They provide evidence based recommendations on physical activity, dyslipidemia, hypertension, obesity, diabetes, cigarette smoking, and other cardiovascular conditions [60].

For those who have already suffered ischemic stroke, rapid administration of tissue plasminogen activator (tPA) within 4.5 hours of stroke onset is the mainstay of treatment [146]. tPA acts to dissolve the blood clot, directly improving blood flow to the perfusion-deficient area of the brain. There are benefits with earlier tPA administration [146, 147]. Beyond this narrow time window, treatment with tPA is not effective and its side effects, primarily bleeding, outweigh the marginal benefits [146, 147]. Mechanical thrombectomy within 6 hours of disease onset is another option for the treatment of acute ischemic stroke, and should be performed after treatment with tPA when indicated [146]. Recent clinical trials, including the DAWN and DEFUSE 3 trials, have indicated a clear benefit for an extended window of up to 24 hours for mechanical thrombectomy in certain patients with large vessel occlusion [148]. The results from these clinical trials are reflected in the 2019 Society of NeuroInterventional Surgery (SNIS) recommendations [149]. As with tPA, earlier surgical treatment is associated with greater benefits. Secondary prevention of patients who have already experienced stroke is another important method to reduce stroke burden [64]. Similar to primary prevention, secondary prevention focuses on control of risk factors, and special attention is paid to antiplatelet therapy [64].

3.5 The Role of Collateral Circulation in Ischemic Stroke Pathophysiology

The primary pathological feature of ischemic stroke is vessel blockage and loss of cerebral blood flow, resulting in tissue death. Collateral circulation, or the network of vascular channels that stabilize cerebral blood flow after a principal conduit fails, is a crucial determinant of ischemic stroke severity, progression, and recovery

[150]. The progression of brain tissue damage after artery occlusion is inversely correlated to the amount of residual blood flow. The cerebral vessel network is complex and consists of plexuses of cortical arteries, arterioles, penetrating arterioles, capillaries, venules, and veins. The connections at the Circle of Willis and anastomoses between terminals of major artery trees (for example, the leptomeningeal and pial anastomoses) ensure the penetrating arterioles can be sourced rapidly by blood flow from other regions when occlusions take place. While the hemodynamics of collaterals and their relationship to tissue perfusion has not been fully explored, the compensatory effect is evident for their significant role in stroke prognosis, infarct progression, and tissue fate after reperfusion in acute ischemic stroke (AIS) ascribed to large artery occlusion [151].

3.5.1 Collateral Circulation Dynamics during Ischemic Stroke

The leptomeningeal collateral channels are believed to be recruited immediately after AIS due to the formation of a pressure gradient caused by arterial occlusion. However, collateral flow can be highly variable in the hours, days, and weeks after stroke. A number of studies have highlighted changes in collateral circulation patterns and their relevance to outcomes in acute stroke patients. In a study including patients who did not undergo reperfusion 3-5 days after AIS, Campbell et al showed that deterioration in collateral quality is associated with infarct growth [152]. Using laser speckle imaging, Wang et al described three kinds of dynamic changes in leptomeningeal arteriole flow after middle cerebral artery occlusion: persistent LMAs, impermanent LMAs, and transient LMAs [153]. Persistent LMAs were patent observable over 3 hours, while impermanent LOs diminished after 90-

150 minutes, and transient LMAs that were no longer observable after 90 minutes. An early study in monkeys by Meyer et al found that after MCA occlusion, collateral flow can vary to meet the metabolic needs of the ischemic tissue; however the collateral flow is variable, and eventually stabilizes after ~2 weeks [154]. Importantly, these dynamic changes in collateral circulation were correlated to changes in regional blood flow. Some proposed mechanisms of collateral collapse include blood pressure reduction, dysfunction of auto-regulation, collateral vessel thrombosis, and venous steal. While collateral failure is known to be associated with infarct progression, it is unsure whether the effect is causative. These studies suggest that targeting collateral flow during the initial stages of AIS may be a viable therapeutic strategy.

3.5.2 Collateral Circulation and Stroke Severity

The amount of collateral circulation is related to functional outcomes in the natural history of anterior circulation large artery occlusion. In a prospective study of 126 untreated patients with anterior circulation large artery occlusion, Lima et al [155] found that the pattern of leptomeningeal collaterals assessed by conventional CT angiograms (CTA) were independent predictors of good clinical outcome on 6 months follow up. In another study, Seyman et al [156] found that the compensatory ability of collaterals in AIS patients (<12 h) is inversely correlated with final cortical infarct volume and long term modified Rankin Scale (mRS) score. A post-hoc analysis of data from the Warfarin-Aspirin Symptomatic Intracranial Disease (WASID) study also revealed increased risk of ischemic stroke in patients with poorer collaterals. However, the absolute relationship between collateral

grade, baseline severity, and infarction volume remains controversial. For instance, in one study involving AIS patients who underwent emergent endovascular treatment, there was no significant association between collateral grade and pretreatment infarct volume or National Institutes of Health Stroke Scale (NIHSS) score [157-159]. In another study which enrolled 60 patients with anterior circulation AIS (<12 h), there was no difference in the rate of good functional outcomes in patients with poor or good collaterals after reperfusion [160]. These conflicting studies suggest the significance of collateral grade on stroke severity may be time-dependent, or might rely on if and when reperfusion is achieved.

3.5.3 Collateral Circulation, Infarct Progression, and Tissue Fate after Reperfusion

The extent of viable collateral channels to the infarct region is an important factor in infarct development and response to reperfusion therapy. Cheripelli et al [161] examined the collateral state and penumbra volume of 144 AIS patients within 6 hours of stroke onset. The patients were grouped according to duration from stroke onset to brain imaging time. While there was little significant association between penumbra volume over time in patients with good collaterals, there was a trend towards reduction in penumbra proportion among those with poor collaterals [161]. This suggests that targeting the salvageable penumbra region may provide greater benefits for patients with poor collaterals. Collateral quality is strongly correlated with the rate of penumbra tissue loss during the early stages of stroke progression. Jung et al [159] collected data from 44 AIS patients with M1 or M2 occlusion and calculated the rate of penumbra tissue loss using sequent MRI images. In patients

who were successfully reperfused (without complication), there was a strong association between collateral quality and total penumbral tissue loss. Patients with poor collaterals (grade 0) lost 27% of their penumbral tissue, while patients with grade 1 lost only 11%, and patients with good collaterals actually saw an increase in their penumbra volume (-2% loss). Likewise, the rates of penumbral tissue loss were also associated with collateral quality. They concluded that rich collaterals can remarkably slow penumbra tissue loss and potentially extend the therapeutic window for reperfusion treatment [159]. This is supported by evidence linking residual blood flow and oxygen metabolism/extraction to the ability to salvage hypo-perfused brain tissue after infarction [162]. Using positron emission tomography studies in a swine model, Sakoh et al showed that animals subjected to only mild hypo-perfusion showed no oxygen-metabolism deficiencies within 6 hours, while moderately and severely ischemic tissues lost viability after only 3 and 1 hours, respectively [162].

Our understanding of the significance of cerebral collateral circulation has grown due to the increasing prevalence of reperfusion therapy following acute ischemic stroke. The benefits of reperfusion are magnified in patients with good collaterals. A meta-analysis of 2652 subjects who received endovascular reperfusion showed that patients with good collaterals had higher rates of favorable outcomes, reduced risks of peri-procedural symptomatic intracranial hemorrhage, and reduced 3 month mortality compared to patients with poor collaterals [163]. Another study showed that poor collateral circulation is a predictor of malignant infarction after reperfusion therapy [164]. In a study involving a cohort

of 207 AIS patients with M1 occlusion that received endovascular treatment within 8 hours, a shorter onset-to-reperfusion time was significantly associated with higher rate of favorable outcomes in those with poor collaterals, but the difference was not significant in the group with good collaterals [165]. Taken together, these studies suggest that patients with good collaterals appear to have a longer time window for reperfusion therapy, and those with poor collaterals were more likely to have dramatic reversion of functional outcome after prompt reperfusion [160]. Importantly, the beneficial effects of collateral blood flow are only prominent in patients who achieve reperfusion [166].

Recent updates to the AHA guidelines for the early management of AIS patients [148] reflect findings on the role of collateral flow in stroke. In short, secondary analyses from the MR CLEAN [167] and IMS III [158, 168] trials suggest it may be reasonable to incorporate collateral flow status into clinical decision making to determine whether or not mechanical thrombectomy should be pursued [148]. Furthermore, the DAWN and DEFUSE 3 trials showed that endovascular therapy is effective up to 16-24 hours in certain patients [148, 169]. Further clinical trials are needed to clarify how collateral status may be used to define treatment and extend therapeutic opportunities.

3.5.4 Therapeutic Strategies to Modulate Collateral Flow

The viability of cerebral collateral flow after acute proximal artery occlusion illustrates the possibility of enhancing collateral flow as a therapeutic strategy to preserve tissue before reperfusion. Such methods would effectively convert what

would be ischemic core tissue into salvageable penumbral tissue. Clinical trials for this strategy are listed in Table 2. As with other neuroprotective strategies that are struggling to move from bench to bedside, it is paramount to address the issues that prevent collateral enhancement therapy for AIS from translating to the clinic. One such effort was performed by Beretta et al [170]. In a preclinical rodent model, they investigated four different ‘collateral therapeutics’, including phenylephrine to induce hypertension, polygeline to increase intravascular volume load, acetazolamide to promote cerebral arteriolar vasodilation, and head down tilt (HDT) to encourage cerebral blood flow. They attributed the highest efficacy and safety profile to the HDT group. Despite these positive findings in rodent models, a recent clinical trial found no significant difference between treatment groups for AIS patients (Table 2) [171].

Table 2. Published clinical trials on collateral enhancement therapy for the treatment of acute ischemic stroke.

Trial Title	Intervention	Year	Inclusion criteria	Flow	Primary result
ENOS [172]	Glyceryl Trinitrate	2016	Randomized ischemic or hemorrhagic stroke patients within 48 hour after ictus	Perfusion not affected	Safe but not effective in improving functional outcomes
ALIAS [173]	25% albumin intravenous administration	2013	NIHSS>6; able to treat within 5 hours; i.v. tPA or other intra-arterial treatments were permitted	Not evaluated	No difference between groups; increased risk of intracranial hemorrhage and pulmonary edema

Table 2 continued					
SENTIS [174]	Partial aortic occlusion	2011	Symptomatic AIS patients; device could be implanted within 14 hours; patients who received i.v. tPA or other intra-arterial treatment were excluded	Not evaluated	Safe but not effective in improving functional outcomes
HeadPoST [171, 175]	Head position	2017	Clinical diagnosis of acute stroke, including intracerebral hemorrhage; excluded if head position could not be maintained	Not evaluated	Safe but not effective in improving functional outcomes

As a whole, preclinical studies suggest that augmenting collateral blood flow after acute ischemic stroke remains a promising therapeutic target to preserve the penumbra and alleviate ischemic reperfusion injury, particularly in the early stages of AIS management. More effort is needed clarify how these findings can be applied successfully to stroke patients.

Very few studies have interrogated collateral dynamics at later timepoints when the infarct zone has stabilized. Whether and how therapies may enhance collateral recruitment and remodeling during chronic stroke is not fully understood. Neovascularization is also very important to recovery after ischemic stroke. Post-stroke angiogenesis is a recognized phenomenon that occurs in effort to maintain long-term tissue remodeling and homeostasis [176]. In a rodent model of ischemic

stroke, Wei et al showed that establishment of collaterals after stroke was integral to functional recovery [177]. Arteriogenesis and angiogenesis in the penumbra region can facilitate later neurogenesis and likely plays a role in neuroplasticity [176, 178]. Methods and treatments to promote vascularization after stroke are being explored, and endogenous mechanisms of post-stroke neovascularization are discussed further in section 3.6.2.

3.6 Endogenous Repair and Regeneration in the Adult Brain after Ischemic Stroke

3.6.1 Post-stroke Neurogenesis

Neural stem cells (NCS-A) and neural progenitor cells (NPCs) in the adult brain are mainly located in two regenerative niches: the subventricular zone (SVZ) flanking the lateral ventricles and the subgranular zone (SGZ) of the dentate gyrus (DG) in the hippocampus [179-183]. In rodent models in healthy conditions, neurons originating from these two areas have distinct destinies: the neuroblasts derived from the SVZ migrate along the rostral migratory stream, become interneurons, and integrate with other cells in the olfactory bulb. The newborn neurons of the SGZ differentiate and assimilate into the local neural network of the hippocampus where they are involved in learning, memory, and mood regulation. Interestingly, human SVZ neurogenesis exhibits an evolutionary divergence which shows a remarkable difference from other vertebrates. In humans, it was shown that long-distance migration of SVZ-derived NPCs to the olfactory bulbs is virtually

nonexistent, while there is abundant neurogenesis from the SVZ into the adjacent striatum [184].

Neurogenic activities in the SVZ and SGZ are upregulated following stroke [185, 186]. Endogenous NPCs proliferate after ischemia and differentiate into neuroblasts and astrocytes, which subsequently migrate along the route from the SVZ to the infarct region[187, 188]. Neural progenitor cells from the SGZ do not migrate to the infarcted region [189, 190]. The rate of neurogenesis peaks at about 3-4 weeks after cerebral infarction in both the SVZ and the SGZ, and the migration of neural progenitors to the infarct region peaks at 4 weeks [189].

Accumulating evidence unveils that NPC functions are regulated by different signals, which should be taken into consideration when optimizing cell-based therapies [191-193]. Hypoxic-ischemic brain injury in neonates induces cell death in committed neural precursors but stimulates the proliferation and differentiation of immature neural progenitors for brain repair [194]. This suggests age may play an important role in the neurogenic potential of both endogenous neural progenitor cells and also transplanted cells following stroke. The activation of chemokine receptors can increase the number of migrating NPCs. The CXC chemokine receptor type 4 (CXCR4), which is the cognate receptor for stromal-derived factor 1 (SDF-1), crucial for coupling neurogenesis with angiogenesis after stroke and directing the migration of neuroblasts to the infarct region[195]. In addition, C-C chemokine receptor type 2 (CCR2), the cognate receptor for monocyte chemoattractant protein 1, is upregulated in migrating neuroblasts following ischemia and is critical for proper destination targeting [196].

Neurotrophic and growth factors also play important roles in the regulation of adult regeneration, including, but not limited to, granulocyte-colony-stimulating factor (G-CSF), insulin growth factor (IGF-1), glial cell-derived neurotrophic factor (GDNF), and brain-derived neurotrophic factor (BDNF) [196-199]. G-CSF and IGF-1 can reduce NPC death through altering key survival pathways (e.g., the phosphoinositide 3 kinase-Akt pathway). Several recent clinical trials demonstrated the ability of G-CSF to both mobilize endogenous bone marrow cells and exert its neuroprotective effects to promote stroke recovery [197]. In addition to growth factors, anti-inflammatory drugs such as indomethacin, noncoding RNA, and hormones can also increase endogenous NPC proliferation [200, 201]. Together, these studies corroborate the principle that factors which promote neurogenesis might contribute to better cell-based therapies for neurological disorders such as ischemic stroke.

However, the efficiency of endogenous neural regeneration is extremely limited, and is insufficient in itself for effective repair of damaged brain tissue [202]. For example, in a striatum stroke model, about 80% of newly formed neurons fail to survive, and endogenous neuronal regenerations replaces only ~0.2% of neurons lost to stroke [190]. Therefore, it is imperative to discover strategies which can augment neuronal replacement efficiency. Identification and modification of inhibitory factors and enhancement of contributory factors might help to augment the brain's adaptive endogenous regeneration to various neurological disorders and improve cellular therapy-mediated brain repair.

3.6.2 *Vascular Regeneration and Remodeling after Ischemic Stroke*

Neovascularization is a hallmark of tissue recovery after ischemic insult [203]. Angiogenesis is defined as the growth of new vessels from pre-existing vasculature, while vasculogenesis is the *de novo* formation of new blood vessels from vascular progenitor cells [204]. While both have been described in stroke, angiogenesis, and in particular endothelial sprouting, is thought to be the primary method of neovascularization following ischemic injury in adults [176, 195, 203, 204]. Angiogenesis is a key player in the regenerative process, and allows for increased blood flow and nutritional support to areas of hypoxia, and also facilitates restoration of the neurovascular network [176, 195, 203, 205]. Angiogenic mechanisms are induced by hypoxia [178, 203, 206]. The major angiogenic molecules, including vascular endothelial growth factors (VEGF), fibroblast growth factors (FGF), platelet-derived growth factors (PDGF), transforming growth factors (TGF), and also angiogenic chemokines stromal cell-derived factor 1 (CXCL12/SDF-1), as well as many of the cognate receptors for these molecules, are induced by hypoxia, and in many cases, directly or indirectly by hypoxia inducible factor (HIF-1) [178, 203, 206-210]. Angiogenesis following ischemic stroke occurs primarily in the peri-infarct region, although, some have reported angiogenesis in the stroke core region as well [74]. Peri-infarct angiogenesis persists for weeks after the initial ischemic insult [211].

A growing body of evidence supports the ‘vascular niche’ hypothesis that neural precursors in the adult brain are associated with an angiogenic environment [176, 195, 203]. Neuroblast migration relies heavily on the scaffolding provided by

blood vessels [13]. Capillaries in the infarct region release chemoattractant factors such as SDF-1 and Angiopoietin-1 which promote migration of neural progenitors from the SVZ [195]. Under healthy conditions, a large proportion of neuroblasts migrating along the rostral migratory stream are in close proximity to or in contact with the vasculature [212]. In line with the neurogenic 'vascular niche' hypothesis, some groups have shown that angiogenic therapies can promote neurogenesis and formation of new axons along newly generated blood vessels [49].

The remodeling of existing vasculature is also an important recovery mechanism following ischemia. Arteriogenesis, or the remodeling of pre-existing arteries to facilitate greater flow, plays a major role in stroke recovery. Fluid shear stress is the primary driver of arteriogenesis, and following cerebral infarction, shear stress is increased when flow is diverted away from the blocked vessel into collateral channels [205]. Positive outward remodeling of the vasculature is a major mechanism of arteriogenesis, and results in larger capacity for blood flow [176, 205, 206]. The mean diameter of both microvessels and large arteries increases in the peri-infarct region following stroke [153, 213].

The molecular and physical mechanisms of arteriogenesis involve 1) mechanical force via increased fluid shear stress and circumferential wall stress, 2) endothelial activation, 3) inflammation, and 4) structural remodeling [176]. Within these mechanisms of arteriogenesis, the stroke field most commonly focuses on the inflammatory response since it is most readily observable and therapeutically modifiable [176]. The monocyte chemoattractant protein-1 (MCP-1) is the major player for monocyte recruitment in arteriogenic inflammation [176,

205, 206]. These recruited arteriogenic macrophages (and brain-resident microglia) produce and release growth factors such as bFGF, TGF- β , and chemokines including MCP-1, CCL3, CCL4, and SDF-1. The infiltrated macrophages/microglia also remodel the extracellular matrix by production of matrix metalloproteinases [205, 207, 208]. These factors promote proliferation of endothelia and smooth muscle cells to facilitate vessel outward remodeling and expansion of collateral diameter [208, 214].

3.7 Mouse Ischemic Stroke Models

A number of rodent stroke models have been developed for preclinical studies. The table below, adapted from [13], summarizes the procedures and major benefits/drawbacks for each stroke model. Small ischemic strokes are the most common type of strokes seen in the clinic [148]. Therefore, increasing efforts have been made to study smaller strokes in animal models. Furthermore, the mini-stroke models are thought to be most useful for morphological examinations of structural repair in the mouse, and thus, are the most useful for assessing the effects of cellular therapy. The mini-stroke model often involves surgical occlusion of distal branches of the MCA. Other variations, including permanent ligation of the MCA coupled with bilateral CCA occlusions have also been described, and the infarcts produced are similar [13]. These branches feed the sensorimotor cortex, including the well-described barrel cortex, which is responsible for whisker function [177, 215, 216]. The whisker-thalamus-sensorimotor cortex neuronal pathways are prominent in rodents and a multitude of sensorimotor functional tests have been developed to interrogate the integrity of this pathway [217, 218]. Thus, the

sensorimotor cortex stroke models are ideal for examining the intracortical and thalamo-cortical neuronal morphological recovery, and importantly, the potential effects of treatment on sensorimotor recovery.

Table 3. Rodent Stroke Models

Model	Procedure	Benefits/Drawbacks	References
MCA Occlusion	Reversible occlusion of the proximal MCA with variable size suture	<ul style="list-style-type: none"> • Severe damage and large infarct volume useful for neuroprotective studies • Difficult to evaluate regeneration at structural and network levels due to stroke severity • Higher mortality rate 	[219-221]
Cortical strokes Mini-	Permanent ligation of 3-6 distal MCA branches with temporary common carotid occlusion	<ul style="list-style-type: none"> • Stroke limited to cortex (most often the sensorimotor cortex) • Large and well-defined penumbra region • Significant auto-recovery • Low mortality rate 	[74, 215, 222]
Photothrombosis	Intravascular photocoagulation and occlusion of irradiated vessels	<ul style="list-style-type: none"> • Non-invasive; wake animals • Local ischemic injury with minimal penumbra formation • Low mortality rate 	[13, 223]
Endothelin Stroke	Cortical application of vasoconstrictive protein endothelin-1	<ul style="list-style-type: none"> • Local ischemic injury with minimal penumbra formation • Produces atypical inflammatory response • Uncharacterized reperfusion • Low mortality rate 	[99, 224-226]

3.8 Stem Cell Therapy for Ischemic Stroke

3.8.1 Stem Cell Sources for Cellular Therapy

Stem cells are major sources of cell-based therapy. They can be classified as totipotent cells, naïve pluripotent stem cells, primed pluripotent cells, and tissue-specific multipotent stem cells. Totipotent cells, characteristic of the zygote and early blastomeres, can develop into all tissues, including extra-embryonic tissue. While both naïve and primed pluripotent cells can form teratomas, the two different pluripotent states have distinct molecular differences. Naïve stem cells are in a ground state, harboring the prerequisite potential to differentiate into all embryonic lineages and develop into chimeric blastocysts. They possess high clonogenicity and do not carry specification markers [227]. Primed pluripotent cells, which do not produce chimeras, express FGF-5 specification marker and have low clonogenicity. For pluripotency markers, naïve stem cells display greater levels of pluripotency marker proteins, including OCT-4, NANOG, SOX-2, KLF-2, and KLF-4, while primed cells lose KLF-2 and KLF-4 expression. Aside from the naïve and primed pluripotent states, a study discovered an intermediate pluripotent stage between the two states [228]. The tissue-specific multipotent stem cell has the least differentiating potency among all stem cell types, with the ability to form tissue-specific cell types [229, 230].

The success in generation and culture of ESCs from mice, primates, and human embryos has been considered a milestone of stem cell research. ESCs are a useful tool for exploring early embryonic development, modeling pathological

processes of diseases, and developing therapeutics through drug discovery and potential cell replacement [231]. Human ESCs (hESCs) now hold a great promise for regenerative medical treatments as the cells can generate any cell type of the body. Human ESCs are mainly defined as primed pluripotent cells, which are different from and show less plasticity than the murine ESCs. It remains unclear whether human-naïve pluripotent stem cells, obtained either by continued transgene expression or through specific chemical manipulation of the culturing microenvironment, are analogous to mouse counterparts [232-234]. Nevertheless, it is worthwhile to validate the findings from these reports using naïve human ESCs generated from different strains and laboratories in future studies.

Differentiation of ESCs *in vitro* has been achieved at very high efficiencies into various transplantable progenitors/precursors and terminally differentiated neuronal and glial cell types, which include cortical glutamatergic, striatal GABAergic, forebrain cholinergic, midbrain dopaminergic, serotonergic, and spinal motor neurons, as well as astrocytes and oligodendrocytes [235-241]. These differentiated cells, including neurons, astrocytes, and oligodendrocytes, have been exogenously transplanted and evaluated in animal models. Translation into the clinic is ongoing for various neurological disorders, including: (1) PD, in which nigro-striatal neurons are lost before other neurons, (2) HD, in which MSNs are lost, resulting in striatal atrophy, and (3) glial and myelin disorders [242-244]. Other disorders, including AD and Lewy body disease, which involve a multitude of neuronal cell types, and amyotrophic lateral sclerosis (ALS) and spinal muscular

atrophy, which are multicentric and diffuse neurodegenerative disorders, remain poor targets for stem cell-based therapies.

Induced pluripotent stem cells (iPSCs) are pluripotent cells that are artificially de-differentiated from adult somatic cells by several transcription factors or small-molecule compounds and have ignited the field of lineage reprogramming [245, 246]. There are epigenetic differences between iPSCs and ESCs, which include expressions of unique genetic signatures, teratoma formation capacity, and the differentiation potency and flexibility (e.g., dissimilar differentiation potential into various transplantable neural cells [247, 248]). Furthermore, compared to ESCs, iPSCs can be more amenable as donor cells for cell replacement therapy, in vitro disease models, and drug screening [247, 249]. First, iPSCs are derived from adult somatic cells, which can be easily obtained from patients, and then banked and stored. Second, cultures of hiPSCs and hESCs are technically similar, but the generation of iPSCs harbors much less ethical concern and opposition. Third, given the somatic cell source and the autologous nature of iPSCs, cell therapy using iPSCs should have no immune rejection in theory, or at least minimize the risk of immune system rejection. However, a recent report suggests that some unusual gene expressions in transplanted cells derived from the iPSCs may trigger an immune response [250].

Mesenchymal stem cells (MSCs) derived from the bone marrow, umbilical cord blood, and adipose tissue can exert immunomodulatory and anti-inflammatory effects in CNS disease models such as stroke and MS [251, 252]. Overexpression of some neurogenic/angiogenic factors such as VEGF in the

transplanted MSC cells might help improve memory and induce neovascularization/neurogenesis within the adult brains [252]. Clinical trials demonstrated safety and feasibility of MSC transplantation in acute and chronic stroke with no tumorigenicity reported following cellular transplantation [251]. However, despite the ability of MSCs to exhibit significant plasticity reflecting a stem-like phenotype *in vitro*, some studies suggest that MSCs do not behave as tissue-specific progenitors *in vivo*, and rather, may take on a pericyte-like phenotype following transplantation or even endogenously [253, 254].

Fetal NPCs, which can differentiate into functional neurons and multiple types of neuroglia, are an ideal platform to bridge the gap between traditional model systems and human biology [255-257]. The differentiation of fetal NPCs *in vitro* could be used to experimentally recapitulate brain development. Recent efforts intending to measure the transcriptome from the fetal human brain provide an unbiased *in vivo* standard using single-cell approaches and genome-wide transcriptome analyses [258, 259]. These studies suggest that fetal NPCs have a stronger genomic overlap with the *in vivo* cortex compared to iPSCs, allowing for the identification of specific neurodevelopmental processes related to pathophysiology of developmental disorders.

3.8.2 Neuronal Progenitor Cells and Neuronal Differentiation

Neuronal progenitor cells (NPCs) are at the forefront of preclinical studies for cellular therapy for brain disease [260-262]. There are a number of sources of neural precursors, including conditionally immortalized cell lines derived from fetal

tissue, neuronal stem cells derived from carcinomas, fetal neuronal stem cells, neuronal precursors isolated from the cortex after cerebral infarction, and precursors derived from embryonic or induced pluripotent stem cells [13, 57, 262-271]. Most commonly, undifferentiated stem cells are treated with a neural induction protocol prior to transplantation to acquire lineage specificity and also to reduce the risk of tumorigenesis [13, 266, 272-274]. The retinoic acid (RA) differentiation protocol is the most frequently used for neuronal differentiation of mouse iPS or ES cells. Retinoic acid is a vitamin A derivative which plays a role in the specifying anterior-posterior development broadly across mammals. Anteriorly, RA promotes expression of master regulators such as the Hox genes which dictates developmental paradigms within the central nervous system [275]. RA interacts with cellular RA-binding proteins (CRABP), which then bind nuclear RA receptors to facilitate neuroectodermal differentiation [276]. Neural-specific transcription factors are expressed in iPSCs and ESCs following RA exposure [277]. Multiple cell types are produced using the RA differentiation method. Importantly, a small percentage of cells differentiate into glia [277]. The vast majority of cells derived from this method become mature neurons. Following the RA induction process, neurons express mature neuronal markers such as neuronal nuclei (NeuN), neurofilament, and type 3 tubulin, and are able to produce sodium, potassium, and calcium currents, and elicit spontaneous action potentials [278]. Both GABAergic and glutamatergic neurons are produced [277].

3.8.3 Mechanisms of Cellular Therapy

Broadly speaking, the mechanisms of cellular therapy can be grouped into either cellular replacement or trophic support. However, it is difficult to separate these mechanisms in practice since many of the outcomes from either theoretical mechanism are often similar or the same. For example, transplanted NPCs may differentiate into functional neurons and replace those lost to stroke, and concurrently, also release factors which improve the synaptic plasticity of endogenous neurons in the vicinity to facilitate network recovery.

Cellular replacement is an important mechanistic target for treatment of stroke and other focal brain lesions. In the case of NPC transplantation, neuronal replacement requires neuronal differentiation of NPCs and integration into the host neural circuitry. The former requisite, neuronal differentiation, is relatively easily achieved with the appropriate differentiation protocols [262, 279]. Some groups have carefully studied neural differentiation of transplanted cells. In one study, transplanted ESC-derived neural precursors differentiated into multiple neuronal subtypes, with the dominate subtype being GABAergic neurons (>50%), however, the proportion of glutamatergic neurons was not reported [280]. Following 3 months after transplantation, only 25% of the remaining cells were NeuN+, while 8% were positive for the astrocyte marker glial fibrillary acidic protein (GFAP), suggesting that both overall retention of cells is low, and that a significant proportion become astrocytes. Furthermore, continued proliferation after transplantation was also detected, but no tumor formation was noted at 1 and 3 months after transplantation. In a separate study involving transplantation into the striatum following striatal stroke, 30% of transplanted cells were retained at 1

month, and the majority expressed neuronal markers [281, 282]. Very few expressed astrocyte or oligodendrocyte markers, and they did not report any proliferation following transplantation.

The latter requisite for cellular replacement in stroke, integration into the host neural circuitry, is thought to be a major limitation of cellular replacement. Functional integration been reported by only a few groups. Neural progenitors have a greater ability to integrate if they differentiate into the appropriate phenotype [57]. Recently, a group described functional integration of transplanted NPCs using fluorometric calcium imaging and nerve tracing in a traumatic brain injury mouse model [56]. Other groups have described integration using immunohistochemistry techniques in various models, including in both healthy brains, PD, TBI, stroke, and others [18, 283-285]. More research is required to understand the extent of neuronal integration of NPCs following transplantation, and how it may be manipulated for network recovery.

Trophic support is another major mechanism of cellular therapy. Transplanted cells can improve the survival, repair, and regeneration of surrounding tissue by providing factors which facilitate these recovery processes. Transplanted cells may act as vehicles for the sustained delivery of factors to promote regeneration [286]. Transplanted NPCs and other cell types release factors which can promote repair of the injured parenchyma following stroke [287-289]. These trophic effects are both paracrine and autocrine [290-293]. A wide variety of released factors has been reported, including neurotrophins such as BDNF, GDNF, and NGF, vasculogenic proteins including VEGF, bFGF, and

immunomodulatory proteins such as the interleukins IL-10, IL-1, and CSF-1 [6, 32, 292-296]. The secreted factors are thought to promote recovery via reduction of harmful inflammation and promotion of endogenous regenerative and reparative processes, including neurogenesis and angiogenesis [13, 260, 279, 297-301]. For some cellular therapies and in particular for BMSCs, trophic support is likely the major therapeutic mechanism. This is supported by experiments using BMSC conditioned media to treat the post-stroke brain, which led to similar levels of functional recovery compared to cellular treatments [292, 302].

3.8.4 Cell Transplantation Parameters and Strategies for Stroke

A major goal of preclinical cell transplantation studies is to optimize the transplantation parameters to maximize their therapeutic efficacy. In terms of cellular therapy for ischemic stroke, the major parameters include administration route and timing of delivery; the optimal conditions likely depend on the cell type and animal model of cerebral infarction. The Stem Cell Therapy as an Emerging Paradigm for Stroke (STEPS) committee has determined guidelines for preclinical studies which should be accomplished prior to translating cellular therapy for human stroke patients [274]. The committee emphasized the need for a well-characterized cell population, dose-response studies, and functional tests in at least two different models in two animal species [274].

The specific pathophysiology of ischemic stroke creates challenges for directing cellular therapy to ischemic brain tissue. Following the cessation or reduction of blood supply to the brain parenchyma, cell death develops within

minutes (Chapter 3.3.5). The ionic gradients important for cellular membrane potential and neuronal signaling dissipate and result in the release of toxic amounts of glutamate, which can reside in the tissue for days, and can interfere with transplanted cell survival and retention. Intracellular and released proteases are activated which accentuate cell death of native and transplanted cells, and also degrade the extracellular matrix, creating an environment inhospitable for cellular therapy. Inflammatory cells such as microglia/macrophages and monocytes infiltrate the hypoxic tissue and tend to exhibit a pro-inflammatory phenotype, which further antagonizes regenerative efforts (Chapter 3.3.4). The astrocytic barrier, which develops days to weeks after focal brain ischemia, may be inhibitory to axonal growth of both newly formed endogenous neurons and transplanted cells [29]. Strategies to overcome these limitations are necessary to advance preclinical efforts into therapeutics viable in human populations.

Timing of cell transplantation is an essential parameter to be considered and can be optimized to overcome potential barriers to clinical translation. Transplantation timing has been performed at widely varying times after infarction (<1hr to months) but has rarely been compared directly. Early transplantation (hours-days) has shown some neuroprotective effects [281, 285, 303, 304], however, early time points are often avoided due to the widespread belief that the ongoing stroke pathology will interfere with transplant cell survival, and ultimately, transplant cell therapeutic efficacy. Our group and others perform transplantations around 7 days after stroke. At this point, the extracellular glutamate and edema have subsided, and regenerative activities are ramping up [305]. Transplantation

at this delayed timepoint may also be optimal since it allows for the augmentation of endogenous regeneration, which is thought to be the major therapeutic mechanism of transplanted cells for ischemic stroke. Treatment at a later timepoint may miss this window. It is also possible that repeated delivery may offer additional benefits, but this has also rarely been studied [296].

Transplantation location is also a major consideration for cellular therapy for stroke. The most common and theoretically appealing strategy for cellular replacement for ischemic stroke is intracerebral transplantation. Many hypothesize that replacement of tissue *in situ* will facilitate greater recovery compared to treatment targeted elsewhere, however, this has very rarely been directly tested. Following degradation, the stroke core develops into a potential space where injections may be targeted with minimal compression of healthy brain tissue. However, transplantation into the cytotoxic stroke core results in massive cell death of transplanted cells, particularly in the setting of acute stroke [268, 289, 306]. Previous studies have attempted to overcome or bypass some of these difficulties by either increasing the resiliency and efficacy of the transplanted cells (for example, by hypoxic preconditioning [23, 24, 31] or genetic manipulation [32]), or by transplanting in the peri-infarct region where the microenvironment is less hostile. Interestingly, one study tested the possibility of transplanting into the hemisphere contralateral to the stroke lesion, and not surprisingly, found greater transplant cell survival compared to injection into the lesion or intraventricular injection [271]. However, directing injections to healthy or peri-infarct regions requires invasive placement in sensitive brain tissue, which can be damaged

simply by delivery approach [33-35]. However, the extent of neuronal damage due to transplantation of cells or biomaterials is not well studied. Others have also tested intravascular and intranasal administration routes for cellular therapy with varying success [13]. Interestingly, many of these studies reported improvements in recovery despite low numbers of cells homing to the injury region, suggesting the therapeutic effects may be facilitated by released factors rather than cellular replacement [13]. Further research is needed to clarify the optimal time points and location targets for particular cellular therapies after stroke.

The optimal number of cells needed to achieve therapeutic efficacy is also unknown. Previous studies have shown that intracranial transplantation of greater numbers of neural stem cells did not result in greater survival or neuronal differentiation [13, 281]. However, in a study that utilized an intravenous method of delivery, the improvements in behavioral deficits and infarct volume were dose-dependent [303]. These discrepancies are not well understood, however, it is possible that first-pass circulation via the lungs and liver reduced the effective dose which reached the brain in the latter study [303]. Together, these studies suggest there is an upper limit in terms of therapeutic benefit. In our lab and others, we have demonstrated that transplantation of 200,000 cells into the peri-infarct region is safe and effective for the treatment of mini-strokes in mice [13, 268, 306, 307]. Future preclinical and clinical studies are necessary to determine the quantity of cells as a function of cell type, stroke size, and stroke location.

3.9 Biomaterials for Augmentation of Cellular Therapy for Ischemic Stroke

3.9.1 Hydrogels as cell carriers for transplantation in stroke

An alternative strategy to enhance cellular viability and effectiveness is to create a microenvironment in the stroke core favorable for transplantation and regeneration via hydrogel encapsulation [3, 11, 12, 36-39]. Hydrogels are biocompatible carrier materials that can be used to promote survival, differentiation, trophic potency, and functional integration of transplanted cells [11, 12, 27, 37, 39, 41]. Their ability to emulate the biophysical properties of soft neural tissue makes them ideal for engraftment into brain injuries [44-47]. Formulating hydrogels from extracellular matrix (ECM) components allows for reduced immunogenicity, preserves bio-inductive properties, and allows for degradation by native mechanisms [308, 309]. Many tissue engineering studies in the stroke field have centered on hyaluronan (HA), which when used as a carrier for cellular therapy, can improve cell survival after transplant, promote angiogenesis and anti-inflammatory signaling, and encourage neuronal differentiation of stem cells [27, 33, 37, 41, 45]. However, low molecular weight HA is pro-inflammatory, and transplanting HA into the degradatory stroke core would carry an unnecessary risk of exacerbating inflammation [45]. Recently, a HA-based hydrogel was demonstrated to encourage vascular repair and neuronal migration to the stroke core in mice [49]. Released proteins such as growth factors play an integral role in regeneration, and ECM binding is a critical step of NPC mediated trophic support [4, 22, 27, 28, 53]. However, HA is an un-sulfated glycosaminoglycan which lacks the functional components necessary to enhance trophic factor retention and signaling. Other

brain ECM glycosaminoglycans may provide structural elements and functional microdomains that allow for sustained and endogenously regulated trophic signaling, which may improve regenerative potential.

A number of studies have investigated hydrogels as potential scaffolding for cellular therapy for the treatment of ischemic stroke. The hydrogel used, cell types implanted, stroke model studied, and main findings are summarized in Table 4.

Table 4. List of studies of hydrogel encapsulation for cellular therapy in stroke. Adapted and updated from [310].

Reference	Hydrogel	Cell Types	Stroke Model	Main findings
[311]	HA + PLGA+ VEGF + Ang1 HA	Endothelial cells and NPC	Mouse MCAo	<ul style="list-style-type: none"> • Controlled VEGF/Ang1 were released • Cells survived and adhered to gel in vitro • Reduced inflammation and gliosis • Induction of angiogenesis • Functional behavior recovery
[312]	HA	Adipose stem cells	Mouse FeCl ₃ thrombosis model	<ul style="list-style-type: none"> • Reduced glial scar formation • Reduced regenerative activities

Table 4 continued				
[37]	HA and heparin sulfate	ESC-NPCs	Mouse MCAo	<ul style="list-style-type: none"> • HA promotes transplant cell survival • Reduced microglial inflammation within grafted area
[33]	HA	iPSC-NPCs	Mouse photothrombotic stroke	<ul style="list-style-type: none"> • Increased expression of multiple growth factors • Improved neuronal differentiation • Improved transplant cell survival
[38]	Collagen Type I	Primary rat NSCs	Rat MCAo	<ul style="list-style-type: none"> • Collagen did not influence cell division after transplantation • Monitored collagen degradation over 1 month • Improved neurologic scores • Improved neuronal differentiation of transplanted cells
[313]	VEGF-PLGA microparticles	Human NSCs	Rat MCAo	Improved angiogenesis
[314]	Xenogenic (brain ECM) bioscaffold	Human NSCs	Rat MCAo	Formation of <i>de novo</i> tissue

3.10 Chondroitin Sulfate Glycosaminoglycans and Brain Regeneration

Unlike HA, chondroitin-4-sulfate A (CS-A) possesses greater structural and functional elements to modulate trophic factor enrichment and promote autocrine/paracrine signaling [51, 52]. Endogenously, CS-A is an integral ECM constituent of the neural stem cell niche [47, 51-54]. ECM binding is a critical step of growth factor-mediated tissue repair [55]. CS is a multifunctional sulfated glycosaminoglycan implicated in regeneration and the response to brain injury. The sulfated elements of the CS disaccharide chains attached to native brain CS proteoglycans facilitate growth factor binding, retention, and presentation [47, 51, 52]. The various roles of CS can be attributed to their sulfation patterns and pathobiological context. CS-A is involved in endogenous neural stem cell differentiation and migration, neurite/axon growth, and angiogenesis [315-321]. Other CS moieties such as CS-E and CS-C play a role in neuroprotection as part of the glial scar limits the spread of inflammation and necrotic debris following cerebral infarction [108, 322, 323]. The homeostatic deposition of these glycosaminoglycans in the peri-infarct region may also assist in regeneration [116, 322, 323]. Previous studies have demonstrated that CS-A can support neural stem cells *in vitro* and transplanted cells *in vivo* following traumatic brain injury [53, 324]. Regenerative factors such as basic fibroblast growth factor (bFGF) and brain derived neurotrophic factor (BDNF), and the immunomodulatory protein interleukin 10 (IL-10) have higher affinities for CS-A compared to HA [53, 325]. The secreted mitogen bFGF in particular plays an important role in brain repair after injury by promoting proliferation, migration, and survival of endothelial cells [326].

Furthermore, bFGF also stimulates production of vascular endothelial growth factor (VEGF) which acts in conjunction with bFGF to promote angiogenesis [320, 326]. Arteriogenesis and pial collateral vascular remodeling are also carried out by bFGF signaling after cerebral ischemia [176, 327, 328]. Our collaborators have recently shown that CS-A can improve growth factor and transplanted cell retention in a rat traumatic brain injury model, however, they are wholly unexplored as transplant mediums for the treatment of stroke [39, 53]. We hypothesize that these natural polymers can be used to create a depot in the stroke core for the growth factors necessary to synergize with and enable NPC-mediated tissue regeneration.

METHODOLOGY

4.1 Experimental design

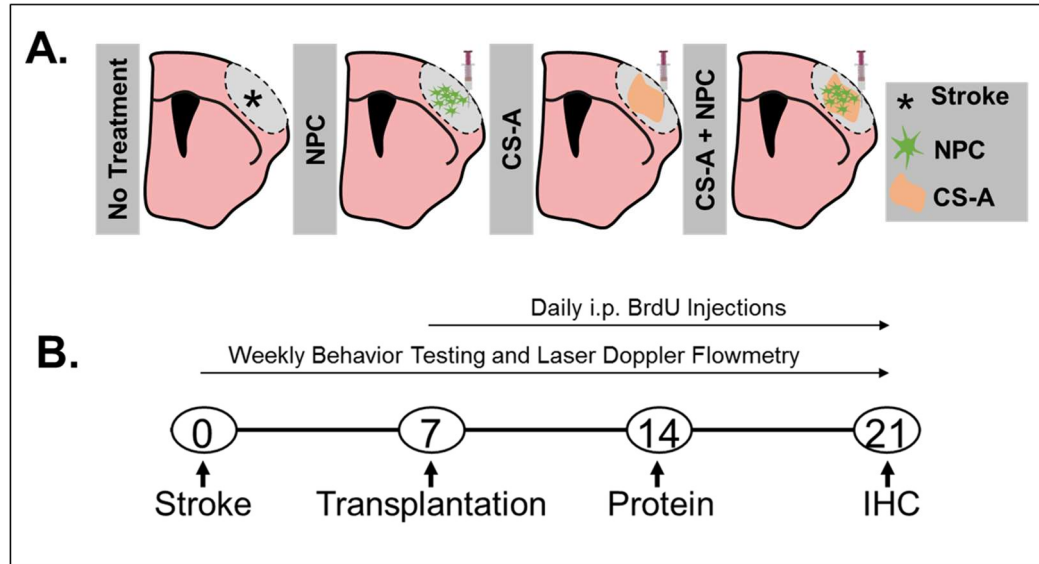


Figure 1. Overview of general experimental design. A) Treatment groups. B) Experimental timeline.

4.1.1 Aim 1: Determine the effects of CS-A on NPC survival and differentiation.

The limited survivability of transplanted cells in the ischemic brain is a significant barrier to clinical translation [3, 4, 37]. Sustained retention of transplanted cells is also necessary to effectuate recovery. Ensuring cell survival and creating a hospitable environment for prolonged retention will facilitate regeneration after transplantation and is a primary endpoint for CS-A encapsulation. Neuronal differentiation is desirable to achieve cellular replacement of neurons lost to stroke [9, 15, 284]. NPCs can differentiate become functional neurons that can integrate with host circuitry [16-20]. Previous studies have indicated that CS-A can promote

NPC proliferation and stemness, however, none have tested whether CS-A is amenable to neuronal differentiation for cellular therapy purposes [53]. Other groups have shown that CS with other sulfation patterns such as CS-E, may actually inhibit axonal growth in certain contexts such as spinal cord injury [47]. The ability of NPCs to differentiate into neurons with proper axon formation within CS-A *in vitro* and following transplantation into the stroke region is unknown. We hypothesized that CS-A encapsulation of NPCs will improve cellular retention and permit neuronal differentiation *in vitro* and *in vivo* following transplantation into the ischemic stroke core in mice.

The effect of CS-A on NPC cell death and retention following transplantation was investigated using immunohistochemical (IHC) methods and *ex vivo* IVIS Spectrum imaging (Perkin Elmer, Waltham, MA) of brains transplanted with DiR (Thermo Fisher Scientific Life Sciences, Waltham, MA)-labelled cells following experimental endpoints. To test for acute transplant cell death, animals were sacrificed 3 days following transplantation of iPSC-derived NPCs with stable expression of GFP, and brains were isolated and sectioned. Transferase-mediated dUTP nick end labeling (TUNEL) and GFP co-staining were used to measure the number of dying transplanted cells. To measure cell retention, DiR-labeled NPCs were transplanted into the stroke core, and brains were isolated and imaged with the IVIS Spectrum imager. Cell retention was estimated using radiant efficiency. The total number of retained GFP-expressing transplanted cells were also counted 2 weeks after transplantation into the stroke core. To determine whether CS-A can protect NPCs from low oxygen and glucose conditions, we performed oxygen and

glucose deprivation test using 0.1% oxygen for 3 hours in OGD media [186]. Media was collected and the lactose dehydrogenase (LDH) release assay was performed as a proxy for cell death. Protein was also collected, and the levels of the cell death and survival proteins cleaved caspase 3, BCL2, and HIF1 were measured and compared using Western blotting.

In vitro and *in vivo* neural progenitor cell differentiation was studied using IHC and Western blotting techniques. For *in vitro* iPSC-NPC culture experiments, following completion of neurosphere induction, cells were either plated on a polystyrene culture dish coated with PDL-laminin, or loaded into the CS-A hydrogel, and maintained until the completion of the retinoic acid neural induction protocol (4 days without followed by 4 days with retinoic acid). The neuronal markers NeuN, SNAP25, TUJ1, GAD67, and NMDAR1b were measured and normalized to the housekeeping marker tubulin. Other markers, including non-differentiated markers Nanog, SOX2, and Nestin, and the astrocyte marker GFAP, were also measured and compared. For *in vivo* differentiation experiments, the numbers and percentages of NeuN, GFAP, or SOX2 cells colabeled with GFP were counted in sections from brains isolated from animals 2 weeks after transplantation. Axon formation within the stroke core was determined using MAP2 as an axonal marker, and GFAP as a marker for the glial scar, which demarcates the stroke core.

Experimental design limitations: We initially chose 3 days post-transplantation to test the potential protective effects of CS-A for transplantation of NPCs into the ischemic core region based on previous studies of ischemic cell death [78, 120,

121, 132, 135]. However, it is possible that a small fraction of dead/dying cells may be cleared prior to this timepoint. Furthermore, the specific types of cell death were not studied. Transferase-mediated dUTP nick end labeling (TUNEL) staining can be used to count the number of cells with fragmented DNA, which canonically is implicated in apoptotic cell death. However, many cell death pathways are activated concurrently in ischemia, and it is possible that TUNEL staining does not cover a small proportion [131]. We chose to measure cell retention 2 weeks after transplantation since this time point matches our other experimental endpoints. Chronic (months) retention of transplanted cells was not tested and is a future point of study. Using DiR is beneficial in that it does not affect cell function, however, it is possible that it may not remain completed within the transplanted NPCs. Following cell death and phagocytosis, some DiR may be transferred to other cells. Furthermore, this technique does not have the spatial resolution to track individual cells or their intracranial distribution.

While our lab and others have shown that iPSC-NPC derived neurons can produce spontaneous and evoked action potentials, we were unable to determine whether neurons differentiated in the CS-A hydrogel can as well [6]. Technical difficulties, in particular the failure of multiple experts to patch cells within the 3D hydrogel *in vitro*, was a major limitation to determine neuronal activity *in vitro*. For *in vivo* differentiation, we used immunohistochemical methods to determine transplanted cell differentiation phenotypes and axonal formation. However, this is insufficient to determine the possible neuronal function of transplanted cells, and whether they form viable connections with the host neural network. Finally,

transplantation into the stroke core may limit axonal formation, since they must first bypass the inhibitory astrocytic barrier.

4.1.2 Aim 2: Determine the effects of treatment with CS-A encapsulated NPC on regeneration in the ischemic brain.

The immune response plays a major role in the natural history of stroke pathophysiology and the response to transplanted materials [11, 27, 329, 330]. Microglia/macrophages are the major immune cells involved in stroke [103]. It is desirable for the hydrogel to either reduce harmful inflammation, remain immune-inert, or promote a regenerative immune phenotype [41, 45]. The anti-inflammatory M2-type macrophage population is associated with neurogenesis, angiogenesis, and stroke recovery, while the M1 response is inhibitory to recovery and associated with infarct progression [103, 331]. Transplanted NPCs can dampen the immune response to facilitate recovery [7]. CS-A may augment this effect since it can enrich the anti-inflammatory factor IL-10 [53]. The astrocytic response is also important to nervous system repair [110, 323]. Following infarction, palisading astrocytes form a barrier separating the stroke core from healthy tissue to limit infarct extension, and likely limits the potential of cellular therapy directed to this region [323]. CS-A has been shown to reduce the astrocytic scar following traumatic brain injury, which may enhance cellular therapy [39].

We performed IHC analysis to test the astrocytic response to transplantation. Glial scar width and the intensity of GFAP staining in the peri-infarct region 2 weeks after treatment. To study the immune response to CS-A

encapsulation, we performed immunohistochemical and protein assays, including protein multiplex (Meso Scale Diagnostics, Rockville, MD) assays and Western blotting analysis from both *in vivo* tissue samples and primary stroke core macrophage cultures *in vitro*. IHC was used to detect the number of PPAR expressing macrophage/microglia. PPAR γ is a marker for the M2 subset of macrophages, which express pro-regenerative molecules to facilitate tissue repair [102, 103, 107, 206, 330]. The protein expression levels of IBA1 and IL10 were also measured using Western blotting. A protein array was used to quantitatively measure the levels of inflammatory related proteins monocyte chemoattractant protein 1 (MCP-1), macrophage inflammatory protein 1a and 1b (MIP-1a, MIP-1b), tumor necrosis factor (TNF), and interleukins 4 and 6 (IL-4, IL-6) using tissue isolated from both the stroke core and peri-infarct regions across treatment groups. To study the potential effects of CS-A on macrophage phenotype, stroke core macrophages were isolated from mice 3 days after infarction, dissociated, and plated onto 6 well polystyrene culture dishes or into CS-A hydrogel. Following 3 days of *in vitro* culture, the markers VEGFR2, TIE2, PPAR, bFGF, and IL10 were measured using Western blotting. In some experiments, neutralizing IL10 antibody was added to the culture media to determine the significance of IL10 on CS-A-mediated macrophage polarization.

The innate capability of the adult brain to create new neurons is inadequate to facilitate meaningful recovery after stroke. Formation of new neurovascular units is paramount to reestablishment of neuronal circuitry lost to infarction [332]. Intracranially transplanted NPCs provide trophic support to the surrounding tissue

via the production and release of regenerative factors [6, 7, 9]. Neovascularization in the hypoxic stroke region is necessary for the survival and success of both endogenously formed newborn neurons and transplanted NPCs and is also prognostic of recovery [176]. The interaction of released growth factors with surrounding ECM is a critical step of trophic support and growth factor mediated regenerative activities [28, 55, 333]. Following ischemic damage, the ECM is extensively degraded and is unable to fully support trophic enrichment offered by transplanted NPCs [37, 41, 57, 334]. CS-A is an ECM component of the endogenous neural stem cell niche and can bind, partition, and orchestrate signaling of BDNF, bFGF, IL10, and other released factors important for healing [39, 53]. These factors can promote endogenous neurogenesis and angiogenesis/arteriogenesis to facilitate recovery [5, 6, 9, 22, 36, 335]. We hypothesized that the combination of CS-A and NPCs may synergize to enhance the formation of new neurovascular units.

To measure neurogenesis and angiogenesis following transplantation of CS-A encapsulated NPCs, animals were injected with BrdU daily after treatment, which labels newly formed cells. Glut1 and NeuN co-labeling with BrdU was used to measure the formation of newly formed endothelial and neuronal cells, respectively. DCX staining was used to label migrating neuroblasts, a fraction of which contribute to neurogenesis after stroke [111, 180, 186, 305, 336]. The number of Glut1+ microvessels in the stroke core region was also counted. Angiogenic signaling was detected in the stroke core region using Western blotting for bFGF, p-STAT3, p-AKT, and VEGF. Endothelial migration also contributes to

the formation of new vasculature [178, 206, 208, 337]. Endothelial haptotaxis was tested using a hydrogel preference microfluidic device designed by our collaborators [338]. NPC-conditioned medium was used to promote haptotaxis towards a well, and brain endothelial cells (B.end3) migrated through either hyaluronan or CS-A hydrogel towards the well. The number of cells in each type of hydrogel was counted after 24 hours. The effects of endothelial division were also tested using Western blotting for the cell division marker Cyclin D1.

Experimental design limitations: Neurologic recovery can occur via multiple mechanisms. Neurogenesis is among the most hopeful since it can reproduce neuronal tissue lost to infarction. However, the rates of native endogenous, even after they are amplified in response to ischemic insult, are very low and are insufficient for functional recovery [111, 180, 335, 339, 340]. Post-stroke neurogenesis peaks at 3-4 weeks after stroke [187, 305, 341]. It is possible that the time point selected for monitoring DCX migration and formation of newborn neurons (2 weeks post-treatment, 3 weeks post-stroke) may not capture peak neurogenic activities potentially affected by treatment. Other recovery mechanisms, such as altered synaptic plasticity and cortical remapping may also be affected by treatment, however, they cannot be easily measured using IHC methodology [342]. Future studies may take these alternate mechanisms into account.

4.1.3 Aim 3: Determine the effects of treatment with CS-A encapsulated NPCs on local blood flow restoration and functional recovery after ischemic stroke.

Blood flow recovery is essential to functional recovery after stroke and for sustained support of transplanted cells [22]. Pial collaterals are a primary regulator of blood flow to the ischemic area and their recruitment is prognostic of recovery [176]. Restoring function is the ultimate goal of treatment. Stroke directed to the sensorimotor barrel cortex in mice results in loss of whisker and forelimb sensation and deficits in both general and forelimb motor function [215, 343, 344]. Furthermore, post-stroke neuropsychiatric deficits have also been reported in rodents. Mice suffering from cortical stroke develop behavioral abnormalities such as apathy, anhedonia, and anxiety-like behaviors [345]. We hypothesized that treatment with CS-A encapsulated NPCs would improve their ability to promote blood flow and behavioral recovery. Furthermore, given that CS-A is known to enrich bFGF *in vitro* and *in vivo* following transplantation into the post-TBI brain, we hypothesized that bFGF may facilitate vascular regeneration and blood flow recovery [39, 47, 53].

To test blood flow recovery, we utilized laser Doppler flowmetry to estimate cortical perfusion of the ischemic hemisphere [186]. Cortical blood flow was measured before and weekly after stroke. To measure collateralization, we used genetically modified mice expressing alpha smooth muscle actin tagged with GFP (SMA-GFP) to visualize muscular vessel dynamics in the pial layer of the meninges. Following the conclusion of the experiment, SMA-GFP mouse brains were imaged, and the numbers and widths of the pial collateral arteries were measured. Immunohistochemistry was used to verify alterations in pial vessel diameter were due to outward remodeling.

The stroke model used in the Wei lab is targeted to the right sensorimotor cortex which results in left whisker and left forepaw sensory and motor deficits [124, 215]. Sensorimotor behavioral recovery was tested using the rotarod, adhesive removal, corner, and pull tests [186, 262, 264, 306, 346]. The rotarod test assesses general motor coordination and balance. The adhesive removal test assesses the ability of the mouse to sense and remove a sticker from their affected (left) forepaw. The corner test assesses the whisker function of mice after they enter a corner in a behavior arena. The isometric volitional pull test assesses paw and forelimb strength. To screen for post-stroke neuropsychiatric deficits, we used the open field test and the tail suspension test. The open field test assesses anxiety as a function of the time spent in the center 25% of the arena. An added benefit of the open field test is that sensorimotor-related data, such as travel distance and velocity, can also be gleaned from the analysis as secondary outcomes. The tail suspension test assesses apathy to the stress of being suspended by the tail upside down.

Experimental design limitations: Mice suffering from mini-strokes to the sensorimotor cortex incur well-defined deficits that can be readily tested using the behavior tests described above. However, the auto-recovery rate is high due to the relatively small size of the infarction, and also due to the resiliency and plasticity of the mouse brain. In our model, a large proportion animals exhibit behavior that is similar to pre-stroke (uninjured) levels by 3-4 weeks after surgically-induced infarction. This can be reduced by removing animals that showed weak behavioral phenotypes prior to randomization and treatment, however, it is possible that the

experimental design is underpowered to test differences between treatment groups at delayed timepoints (i.e. 3 weeks after stroke). Future studies using more severe infarct models or increased numbers may be necessary to elucidate potential differences at delayed timepoints after treatment.

4.2 Procedures

4.2.1 Mouse stroke model, laser Doppler flowmetry, and transplantations

All animal procedures were approved by the Institutional Animal Care and Use Committee (IACUC) at Emory University and are in accordance with the NIH and Animal Research: Reporting of In Vivo Experiments (ARRIVE) guidelines. The mouse stroke model was performed as previously described using C57BL/6 mice (8-12 weeks) from Jackson Laboratories [347]. Briefly, under anesthesia, the right middle cerebral artery was permanently ligated using a 10-0 suture (Surgical Specialties Co., Reading, PA), accompanied by bilateral common carotid artery ligation for 7 min. Laser Doppler flowmetry was performed as previously described [186]. Briefly, incisions were made under anesthesia to expose the skull above the right MCA territory, and the Periscan Laser Doppler perfusion imaging (LDPI) system was used to scan a 3x3 mm square area with a center point of medial-lateral (ML) +4.1 mm, and six edges of the infarct area: ML +2.9 mm, ML +5.3 mm, anterior-posterior (AP) -1.5 mm, and AP +2.0 mm, respectively. The LDPI software (Perimed, Stockholm, Sweden) was used to analyze perfusion. Seven days after stroke surgery, mice skulls were thinned over the visible region of the stroke core, and 200,000 cells suspended in 2 μ l SATO or 200,000 cells loaded into 2 μ l CS-A

hydrogel, or 2 μ l CS-A hydrogel with medium only were loaded into a Hamilton syringe (Hamilton, Reno, NV, USA) and injected at a depth of 1mm from the skull. This number and volume of cells was shown to be safe and effective in our published studies. Effort was taken to avoid damaging arteries and veins during transplantations; animals with detectable vascular damage were excluded from the study.

This mouse sensorimotor cortex mini-stroke model was selected for its defined and highly reproducible cortical infarct and significant generation of a regenerative peri-infarct region. The survival rate for this surgery compared to the MCAo is very high (>95%). Male mice were selected to reduce the potential neuroprotective effects of estrogen, which may also affect regenerative capacity after stroke. Adult mice were selected to reduce potential confounding effects of brain maturation in neonatal mice, and also to avoid the high mortality rates in aged mice after cerebral infarction surgeries. The stroke core was targeted as the transplantation site since it is a potential space for injections and is preferable to damaging the viable regenerative penumbra.

4.2.2 Neural progenitor cell culture and CS-A hydrogel preparation

Mouse induced pluripotent stem cell–derived neural progenitor cells (iPSC-NPCs) were differentiated from iPSCs originally generated from mouse embryonic fibroblasts (Stemgent Inc., Cambridge, MA) as previously described [32]. This line of iPSC-NPCs expresses GFP to permit tracking following transplantation. iPSCs were cultured in the N2B27 serum free medium at 20% O₂, 5% CO₂, at 37° C.

The medium was prepared with 45% Dulbecco's modified eagle medium: nutrient mixture F-12 (DMEM/F12; Sigma Aldrich, St Louis, MO), 45% Neurobasal (Thermo Fisher Scientific,), 0.5% N2 supplement (Thermo Fisher Scientific), 1% B27 supplement (Thermo Fisher Scientific), 1% GlutaMAX, 1% nonessential amino acids (Sigma Aldrich), 0.1 mM β -mercaptoethanol (β -ME; Sigma Aldrich), 100 U/mL penicillin/streptomycin (Sigma Aldrich), 5% knockout serum replacement (KSR; Thermo Fisher Scientific). The small molecules were recombinant leukemia inhibitory factor (LIF; 10 ng/mL; Millipore, Billerica, MA), CHIR 99021 (3 μ M; Tocris), (S)-(+)-Dimethindene maleate (2 μ M; Tocris) and minocycline hydrochloride (2 μ M; Santa Cruz Biotechnology, Santa Cruz, CA)³⁷. Before differentiation, the iPSCs were cultured in DMEM (Sigma Aldrich), 10% ES-FBS (Thermo Fisher Scientific), GlutaMAX, nonessential amino acids, nucleoside mix, LIF, β -ME (Sigma Aldrich), LIF, b-ME, and penicillin/streptomycin. All cells used in this study were harvested and ready for transplantation after an established '4-/4+' retinoic acid (RA, 1 μ M; Sigma Aldrich) neural differentiation protocol. Chondroitin sulfate hydrogel was prepared as previously described [53]. Lyophilized chondroitin sulfate glycosaminoglycan hydrogel (5% w/v) was reconstituted with SATO medium or cell suspension (100,000 cells/uL), then loaded into the Hamilton syringe for injection. For bFGF-neutralizing antibody experiments, 2.5ug/mL antibody (Millipore, Billerica, MA) was added to the cell suspension prior to reconstitution of the lyophilized hydrogel. For *in vitro* iPSC-NPC culture experiments, following completion of the RA differentiation protocol, cells were

either plated on a polystyrene culture dish coated with PDL-laminin, or loaded into the CS-A hydrogel, and maintained for 7 days.

4.2.3 Cell retention imaging

Cells were labeled with DiR (1,1'-Diocadecyl-3,3,3',3'-Tetramethylindotricarbocyanine Iodide) (Thermo Fisher Scientific Life Sciences, Waltham, MA) per manufacturer's protocol immediately prior to transplantation. Following conclusion of the *in vivo* experiments, brains were isolated and imaged with the IVIS Spectrum imager (Perkin Elmer, Waltham, MA). Cell retention was estimated using radiant efficiency.

4.2.4 Oxygen and glucose deprivation (OGD) conditions and lactate dehydrogenase (LDH) cytotoxicity assay

Cells were maintained in a neurobasal media with B-27 serum-free culture supplement and L-glutamine (Invitrogen, Carlsbad, CA) until time of experimentation. Media was exchanged for a physiological buffer solution lacking glucose (120 mM NaCl, 25 mM Tris-HCl, 5.4 mM KCl, 1.8 mM CaCl₂, pH to 7.4 with NaOH). Cells were then incubated in a calibrated hypoxia chamber perfused with 5% CO₂ and balanced nitrogen for a final ambient oxygen level of 0.2% for 3 hours. Oxygen level was established, maintained, and monitored by the ProOx 360 sensor (Biospherix, NY). After 3 hours, cells were returned to the normal incubator and the existing OGD media was completely changed out into normal

oxygenated complete neuronal culture media for 24 hours. At 24 hours after OGD, media was collected for the lactate dehydrogenase (LDH) cytotoxicity colorimetric assay (Sigma). The LDH assay was performed according to the manufacturer's protocols.

4.2.5 Immunohistochemistry and image analysis

Animals were sacrificed by decapitation and brains were immediately removed and immersion fixed in 10% buffered formalin for 72 hours, then dehydrated in 30% sucrose, then mounted and sliced using a cryostat into 10 μ m thick coronal sections (Leica Microsystems, Buffalo Grove, IL). Stereology was carried out as previously described. For systematic random sampling in design-based stereological counting, every 10th (90 μ m apart) brain section across the entire region of interest were counted. For multi-stage random sampling, six fields per brain section were randomly chosen under 10, 20 \times , or 40 \times magnification of an epifluorescent microscope or in confocal images. The sections were air dried and fixed with 10% buffered formalin (Fisher Scientific, Pittsburgh, PA, USA). Brain sections were then submerged in an ethanol/acetic acid solution (2:1) for 10 min, washed 3 times with 1x PBS solution, and incubated with 0.2% Triton X-100 for 45 min. Slides were then blocked with 1 % fish gelatin (diluted in PBS; MilliporeSigma) for 1 hr at room temperature. Slides were incubated with, rabbit anti-Glut-1 (1:400) and goat anti-SMA (1:400, Santa Cruz Biotechnology, Dallas, TX, USA), chicken-anti-GFP (1:300, Abcam) and mouse anti-NeuN (1:400, MilliporeSigma), or mouse anti-MAP2 (1:200, MilliporeSigma) primary antibodies diluted in PBS at 4°C overnight. For double-staining of slides with BrdU, brain sections were post-fixed

with formalin in 10% buffered formalin and washed in PBS. Slides were then treated with methanol (-20°C) and allowed to air dry. After rewetting in PBS, sections were treated with 0.1 mL borate buffer (pH 8.4). Slides were then incubated with rat anti-BrdU (1:400; ABD Serotec, Raleigh, NC) overnight at 4°C. Primary antibodies were washed with PBS and replaced with secondary antibodies Alexa Fluor488 goat anti-mouse (1:300; Life Technologies, Grand Island, NY), and Cy3-conjugated donkey anti-rat (1:300; Jackson ImmunoResearch Laboratories, West Grove, PA) for 1 hr at room temperature before rinsing with PBS. After a final PBS wash, slides were mounted with Vectashield fluorescent mounting medium (Vector Laboratory, Burlingame, CA), and cover-slipped for microscopy and image analysis. Blinded stereological counting was performed on 6 randomly chosen microscope images of the stroke core region per section, and 6-8 sections were analyzed per animal. The number of microvessels (Glut1) within the stroke core, and the number of Glut1/BrdU colabeled endothelial cells within the core and the peri-infarct area were counted. The number of GFP and NeuN co-labelled cells were counted.

4.2.6 Pial vessel imaging and analysis

Two weeks after transplantation experiments, smooth muscle actin-GFP animals from Jackson Laboratories were sacrificed by decapitation and brains were immediately removed and imaged (1.25x and 4x) using an Olympus BX61 upright epifluorescent microscope (Olympus, Center Valley, PA, USA). Whole hemisphere images were reconstructed using Adobe Photoshop CS6 (Adobe Inc., San Jose, CA, USA). For each MCA pial collateral artery, diameters were measured using

ImageJ (NIH) at 6-10 locations along the anastomoses and then averaged. A recruited collateral was defined as having a diameter greater than 25% than the average collateral in the non-injured (sham surgery) mouse. Only anastomoses with explicit and discernable origins were measured.

4.2.7 Western blot analysis

The infarct core region was homogenized using Mammalian Protein Extraction Reagent (M-PER) Lysis buffer with phosphatase and proteinase inhibitors (Pierce, Rockford, IL). Tissue samples were centrifuged and the supernatant was isolated. Protein concentration was determined using the Bicinchoninic Acid Assay (Sigma Aldrich, St. Louis, MO). Protein samples were loaded into 12% polyacrylamide gels and separated via sodium dodecyl sulfate polyacrylamide gel electrophoresis (SDS-PAGE) in a Hoefer Mini-Gel system (Amersham Bioscience, Piscataway, NJ). Protein was then transferred onto a polyvinylidene fluoride (PVDF) membrane (BioRad, Hercules, CA). Membranes were blocked using 5% BSA diluted with TBS and 0.05% Tween 20 (TBST) at room temperature for 1 hour, then incubated overnight with primary antibodies for bFGF (1:500, Cell Signaling, Danvers, MA, USA), p-STAT3 (1:1000, Cell Signaling, Danvers, MA, USA), p-AKT (1:1000, Cell Signaling, Danvers, MA, USA), VEGF (1:1000, Cell Signaling, Danvers, MA, USA), and the loading control Tubulin (1:5000, Sigma-Aldrich, St. Louis, MO). After washing with TBST, membranes were incubated with AP-conjugated secondary antibodies (GE Healthcare, Piscataway, NJ) for 1 hour, then washed with TBST, and exposed to bromochloroidolylphosphate/nitroblue tetrazolium. Signal intensity was quantified using ImageJ (NIH) and normalized to tubulin intensity.

4.2.8 Hydrogel haptotaxis assay

Microfluidic devices were fabricated as previously described [338]. Briefly, side channels composed of CS-A or HA hydrogel surrounding a central channel where 10,000 mouse brain endothelial cells (bEnd.3, ATCC, Manassas, VA, USA) pre-labelled with Hoechst were loaded with either SATO medium or NPC conditioned medium. Following 24 hours, devices were imaged and the number of cells within each hydrogel were counted. The experiment was repeated in triplicate.

4.2.9 Primary stroke core macrophage isolation and culture

Mice were subjected to stroke surgeries as discussed in 4.2.1: Mouse stroke model, laser Doppler flowmetry, and transplantations. 3 days and 7 days after stroke, the visible infarct core regions from the mice were carefully dissected, pooled, and then dissociated in trypsin + EDTA. The pooled tissue suspension was centrifuged, washed with PBS, and resuspended with DMEM + 10% FBS and plated on polystyrene tissue culture plates or into CS-A hydrogel. Following culture overnight, non-adherent cells and stroke core debris were removed, and the media was replaced. For the IL-10 neutralization experiments, 1ug/uL anti-IL-10 antibody (R&D Systems, MAB417) was added to the cell culture media.

4.2.10 U-PLEX (Protein Multiplex)

The U-PLEX Assay platform was purchased from Meso Scale Diagnostics (MSD, Rockville, MD, USA) and used according to the manufacturer's protocol. Sample

preparations and measurements were performed by the Emory Multiplexed Immunoassay Core (EMIC).

4.2.11 Sensorimotor behaviour analysis

For all behavior tests, mice were tested prior to stroke surgeries, 1 week after stroke, and 1-2 weeks after treatment. The corner and adhesive removal tests were carried out as previously described [186]. The corner test gauges rodent whisker function. For the corner test, mice were placed in a star-shaped chamber with each corner forming a 30° angle and allowed to roam freely for 15 minutes. Animal activity was recorded with an overhead camera, and at a later timepoint, a blinded investigator observed and counted instances where the mouse entered the corner, reared up, and turned either right or left. The adhesive removal test is used to monitor mouse motor and sensation of the forelimb. For the adhesive removal test, a small adhesive was placed on the mouse forepaw and the time for the animal to remove the adhesive was recorded. Animals were trained for 3 days prior to stroke surgery and all tests were carried out by a blinded investigator. The pull test was used to monitor mouse forelimb strength. The automated isometric volitional pull test was performed and analyzed using MotoTrak software (Vulintus, Dallas, TX, USA) as previously described [348]. Briefly, mice were trained over 2 weeks to pull a lever of their own volition. Following training, a force threshold of 30g was set; a 'hit' was defined as >30g of pull force. The mice were placed in the

pull test chamber for 1 hour and pull force and number of pull attempts were recorded by the MotoTrak software. Hit rate is defined as the fraction of successful pulls (>30g), and mean attempt force is defined as the average force used for each attempt.

4.2.12 Statistics

Data were expressed as the means \pm SEM. GraphPad Prism 6 (GraphPad Software, San Diego, CA) was used for statistical analysis and graphic presentation. Calculated power analysis based on the variance and effect size in preliminary blood flow studies were used estimate a sample size of $n=9$ for 95% power in a 1-way ANOVA; to account for potential unforeseen increases in variation we extended the group size to $n=12$.

4.2.13 Randomization and blinding

All animals were assigned a number and box label and randomly assigned to treatment groups evenly. All researchers performing stroke surgeries, injections, blood flow measurements, *in vivo* imaging, microscopy, histological analysis, and data analysis were blinded to the treatment groups until collection and analyses were completed.

4.2.14 Chemicals and reagents

Unless otherwise explicitly stated, all chemicals and reagents were purchased from Sigma-Aldrich (Darmstadt, Germany).

RESULTS

5.1 Aim 1: Determine the effects of CS-A on NPC survival and differentiation.

5.1.1 CS-A encapsulation reduces cell death of transplanted NPCs

Mouse induced pluripotent stem cells underwent the 4-/4+ retinoic acid differentiation protocol which produces neuronal lineage committed NPCs. NPCs were transplanted into the ischemic stroke core in mice 7 days after infarction either encapsulated with CS-A (CS-A + NPC) or directly without encapsulation (NPC). 200,000 NPCs tagged with GFP in 2ul were transplanted. Following 3 days, mice were sacrificed, their brains were isolated and sectioned, and stained for GFP and TUNEL, a marker of cell death (Figure 2 A). The proportion of TUNEL+/GFP+ cells in the stroke core region was compared. The percentage of transplanted NPC cell death was found to be significantly reduced in the CS-A encapsulated group.

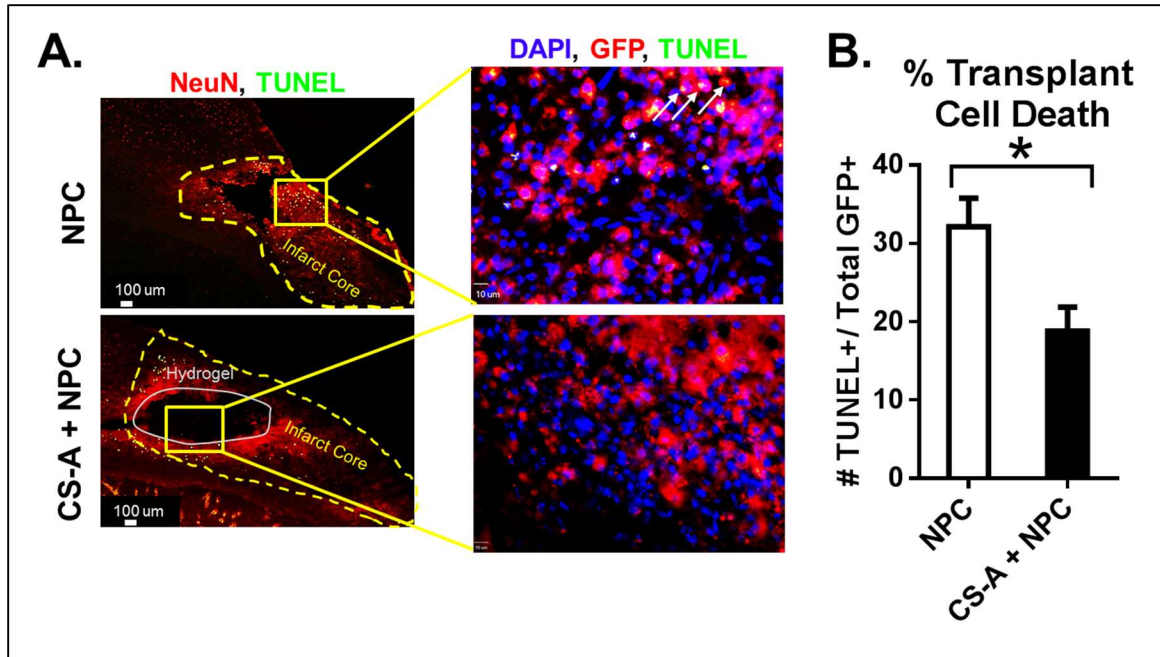


Figure 2. Encapsulation with CS-A reduces NPC cell death following 3 days after transplantation into the ischemic core. NPCs were transplanted with or without CS-A encapsulation into the ischemic stroke core 3 days after surgically induced infarction. A) Representative images of TUNEL staining. Arrows indicate TUNEL/GFP co-stained cells. B) Analysis of transplant cell death. $n=4$ and 6 /group. * indicates $p < 0.05$; two-tailed T-test.

We next tested whether CS-A may provide neuroprotection in an *in vitro* oxygen and glucose deprivation (OGD) experiment. Neuronal lineage committed NPCs were either encapsulated in CS-A or non-encapsulated, then exposed to OGD conditions (0.1% oxygen, 5% CO₂) for 6 hours. Following exposure to OGD, cells were 'reperfused' with fresh media for 24 hours. After this, media was collected for lactose dehydrogenase (LDH) assay, which reflects the extracellular release of lactose dehydrogenase which is an intracellular enzyme. Increased LDH activity reflects increased cell death [121-123, 129, 130, 185]. We also tested whether bFGF may play a neuroprotective role to OGD insult by co-administering a neutralizing antibody to bFGF during OGD and reperfusion. We found that LDH

release correlated to ~50% cytotoxicity in all groups compared to the full kill positive control (Figure 3 A). There was no difference between treatment groups or those exposed to neutralizing bFGF antibodies. Cells were isolated for protein collection, and levels of cleaved caspase 3, BCL2, and HIF1 were compared (Figure 3 B). Correspondingly to the LDH release results, we found no differences between these protein levels.

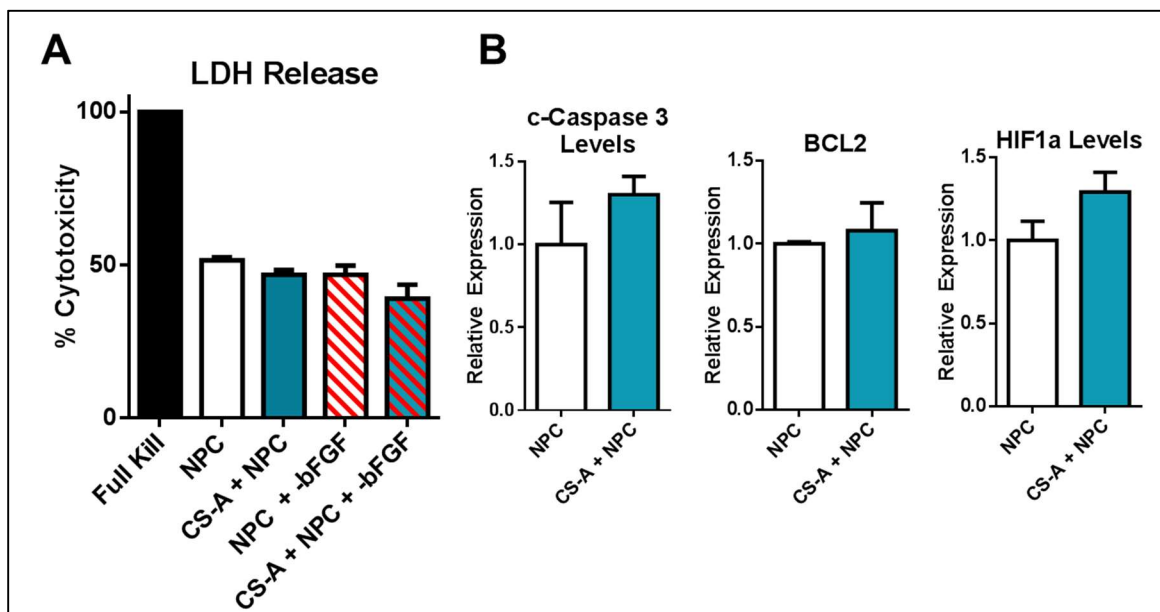


Figure 3. LDH release following oxygen and glucose deprivation (OGD). Media was collected from NPCs exposed to hypoxic conditions (*Oxygen and glucose deprivation (OGD) conditions and lactate dehydrogenase (LDH) cytotoxicity assay*). A) Analysis of LDH release between treatment groups. B) Analysis of protein levels of cleaved caspase 3, BCL2, and HIF1 between treatment groups. n=3/group. * indicates $p < 0.05$; One-way ANOVA with Bonferroni correction for A) and two-tailed T-test for B).

5.1.2 CS-A encapsulation improves NPC retention following transplantation

We next tested the capabilities of CS-A to promote transplanted cellular retention. Intracranial transplantations (2 μ L, 100k cells/ μ L) were performed into the stroke

core region 7d after stroke and animals were sacrificed 14d after transplantation. Significantly more transplanted cells were detectable 2 weeks after transplantation in the CS-A encapsulation group as detected by *ex vivo* fluorescent imaging and also immunohistochemical cell tracking (Figure 4).

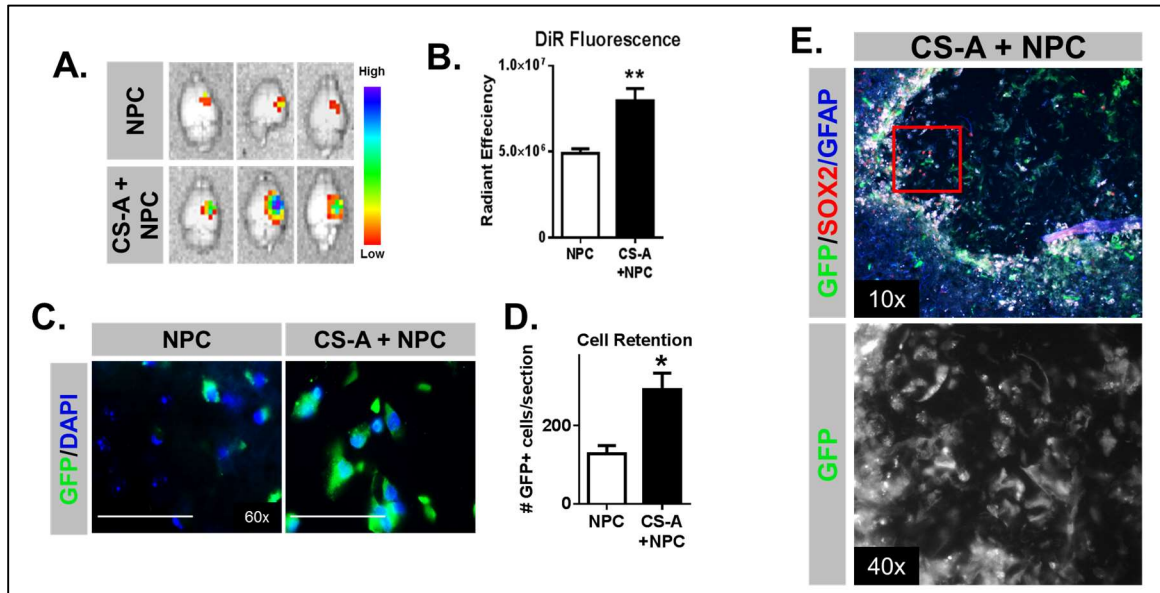


Figure 4. CS-A encapsulation improves NPC retention 14 days after transplantation. NPCs were transplanted intracranially with or without CS-A encapsulation and sacrificed 2 weeks later. **A)** Representative images of radiant efficiency heatmaps 2 weeks after transplantation of DiR-labelled cells (*Cell retention imaging*). **B)** Analysis of DiR fluorescence. $n=4-5/\text{group}$. **C)** Representative fluorescent images of transplanted GFP+ cells in the stroke core. **D)** Analysis of cell retention. $n=6/\text{group}$. **E)** Representative images of transplanted CS-A encapsulated cells at 10x (top) and 40x (bottom) 2 weeks after transplantation. * and ** indicates $p<0.05$ and $p<0.005$, respectively; two-tailed T-test.

5.1.3 Characterization of NPC differentiation *in vitro* following CS-A encapsulation

Whether and to what degree CS-A can facilitate neuronal differentiation of NPCs under the retinoic acid (RA) differentiation protocol is unknown. To test the

possibility of neuronal differentiation, we encapsulated iPSC-derived neurospheres into CS-A and exposed them to the RA 4-/4+ neural lineage commitment protocol as previously described (Figure 5) [6].

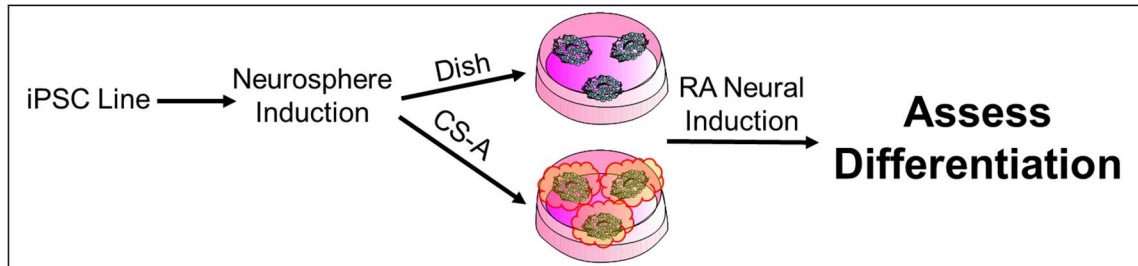


Figure 5. Overview of in vitro differentiation experiments. Mouse iPSCs were induced into neurospheres using rotary culture then underwent the RA neural induction protocol (*Neural progenitor cell culture and CS-A hydrogel preparation*).

NPCs grown *in vitro* in the CS-A hydrogel expressed the same levels of neuronal markers, including the mature neuron marker NeuN, the pre-synaptic marker SNAP25, and the axonal/dendrite markers MAP2 and TUJ1 as NPCs grown on traditional PDL-laminin coated polystyrene plates. Furthermore, we also found similar levels of expression of GAD67, a GABAergic neuron marker, and NMDAR, a glutamatergic marker in the CS-A group compared to the non-encapsulated group. The cells within the hydrogel also appeared to have neuronal morphology following MAP2 immunostaining. This suggests NPCs grown with CS-A can differentiate into multiple neuronal types and show similar growth of axons and synapses compared to non-encapsulated differentiation on PDL-laminin coated polystyrene plates. Together, these results suggest that CS-A does not affect neuronal differentiation.

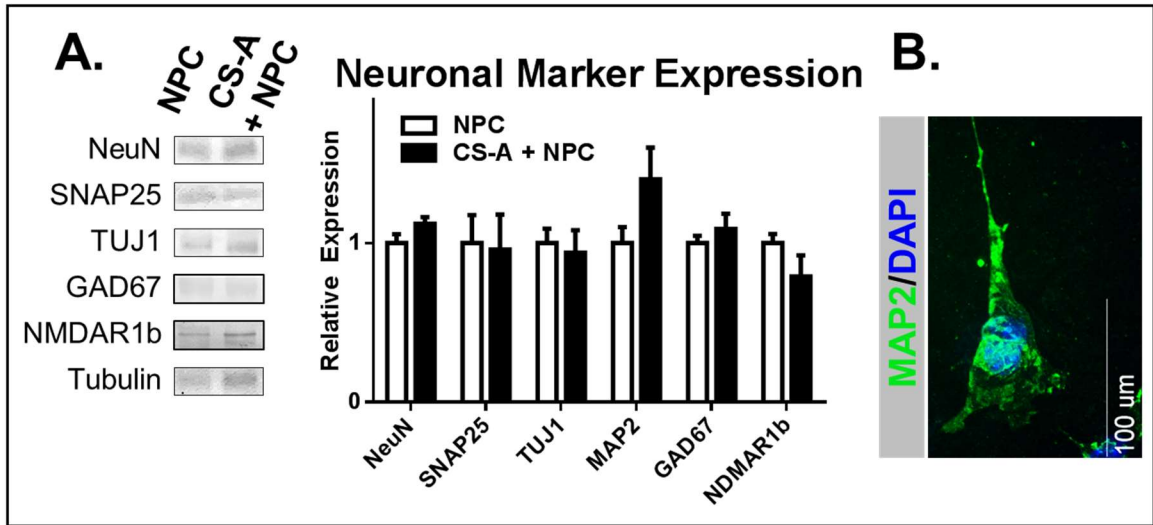


Figure 6. Neuronal differentiation of CS-A encapsulated NPCs. A. Representative Western blotting and analysis for NeuN, SNAP25, TUJ1, GAD67, and NMDAR1b. B. Representative image of MAP2 staining of differentiated NPC within CS-A. n=4/group. * $p < 0.05$, two-tailed T-test.

Next, we tested whether CS-A encapsulation may affect differentiation into non-neuronal cell types, including astrocytic differentiation or non-differentiation. Markers including Nanog, Sox2, Nestin, and GFAP were used to distinguish astrocytic and non-differentiated cells (Table 5).

Table 5. Cell differentiation markers.

	iPSCs	NPCs	Astrocytes	Neurons
Nanog	High	Low	None	None
Sox2	High	High	Low	None
Nestin	Low	High	Low	Low
GFAP	None	Low	High	None
NeuN	None	Low	None	High

Using Western blotting, we found that Nanog and Sox2 levels were both expressed at very low levels in either culture condition. However, Nanog was significantly reduced by CS-A encapsulation. This indicates that CS-A may reduce the proportion of iPS cells which fail to differentiate following the RA differentiation protocol *in vitro*. The levels of Nestin and GFAP were similar, suggesting that non-differentiated NPCs and astrocytic differentiation was not affected by CS-A encapsulation. Taken together, these results suggest that *in vitro* differentiation of NPCs is largely unaffected by CS-A encapsulation.

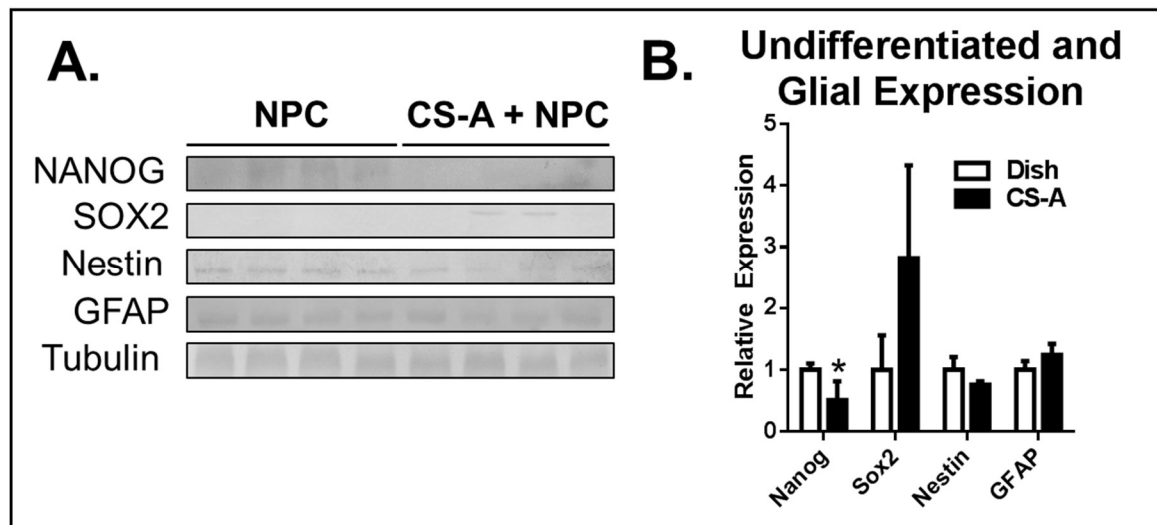


Figure 7. Protein expression of non-differentiated and glial markers of CS-A encapsulated NPCs. A) Representative Western blotting of Nanog, Sox2, Nestin, and GFAP. B) Analysis of Western blotting. n=4/group. * p<0.05, two-tailed T-test.

5.1.4 Characterization of NPC differentiation *in vivo* following transplantation

Following tests for differentiation *in vitro*, we next studied differentiation of cells transplanted into the infarct core region 7 days after infarction. Neuronal differentiation of transplanted cells allows for the possibility of replacing neurons

lost to cerebral ischemia. Two weeks after transplantation, the number of NeuN and GFP colabeled cells were compared between CS-A encapsulated and non-encapsulated treatment groups using IHC. In line with the *in vitro* differentiation studies, CS-A did not alter the proportion of neuronal differentiation (Figure 8 A-B). Approximately 60-65% of transplanted cells were NeuN+, indicating a large proportion of neuronal differentiation. However, the total number of differentiated neurons was nearly 3 times in the CS-A encapsulation group compared to the non-encapsulated NPC treatment group (Figure 8 B). This is likely due to the increased cellular retention.

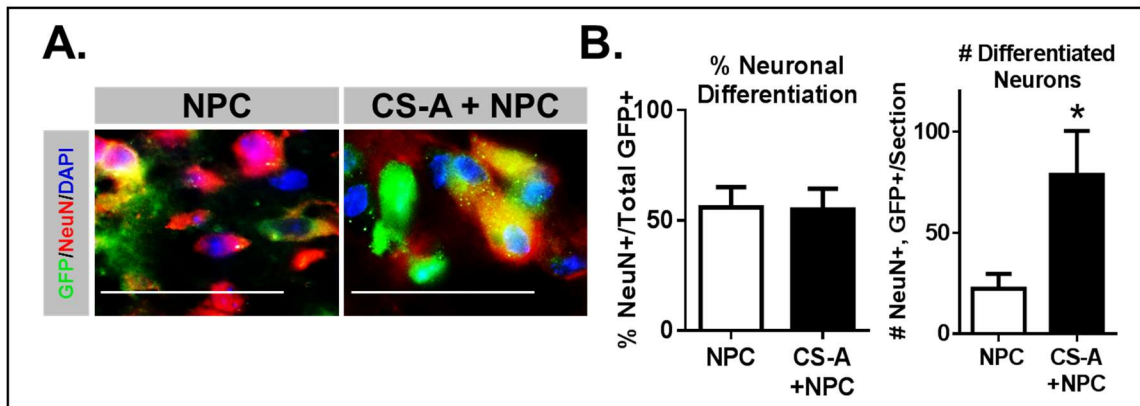


Figure 8. Neuronal differentiation of NPCs 14 days after transplantation. A) Representative images of NeuN+ and GFP+ colabeled cells in the infarct core 2 weeks after transplantation. B) Analysis of percentage and number of NeuN/GFP colabeled cells. n=6-8/group. * indicates p<0.05; two-tailed T-test.

The proportion of non- and astrocytic differentiation were also measured using IHC methods. Glial differentiation was determined using GFAP/GFP co-labelling, and non-differentiation was determined with Sox2/GFP co-labelling (Figure 9 A). Following 14 days after transplantation, the proportion of astrocytic differentiation of NPCs was significantly reduced by CS-A encapsulation (Figure 9 B).

Interestingly, we also noted that many of the non-encapsulated cells which transplanted into GFAP+ astrocytes appeared to integrate into the astrocytic barrier. While very low, the proportion of non-differentiation of NPCs was significantly increased by CS-A encapsulation (Figure 9 B). This is contrary to the *in vitro* finding that CS-A reduces expression of Nanog, a marker of non-differentiation (Figure 7). Together, these results suggest that CS-A encapsulation permits similar neuronal differentiation of NPCs, reduces astrocytic differentiation of transplanted cells, and increased the proportion of non-differentiated cells. Furthermore, CS-A increases cellular retention of transplanted cells, leading to an increased number (but not percentage) of differentiated neurons. This allows for the possibility of neuronal replacement.

The finding that CS-A may promote stemness of NPCs following transplantation is supported by similar work by our collaborators [39]. In their treatment scheme, neural stem cells are isolated from SVZ are encapsulated in CS-A and transplanted without any type of differentiation intervention. This suggests that CS-A may promote stemness in the absence of factors which promote differentiation, i.e. the retinoic acid differentiation protocol we employ to encourage neuronal differentiation prior to transplantation. Therefore, one possible explanation for the increased proportion of non-differentiated cells in this work may be that following transplantation, the pro-neural differentiation factors such as RA are lost or reduced, allowing the CS-A hydrogel to instead promote NPC stemness and non-differentiation.

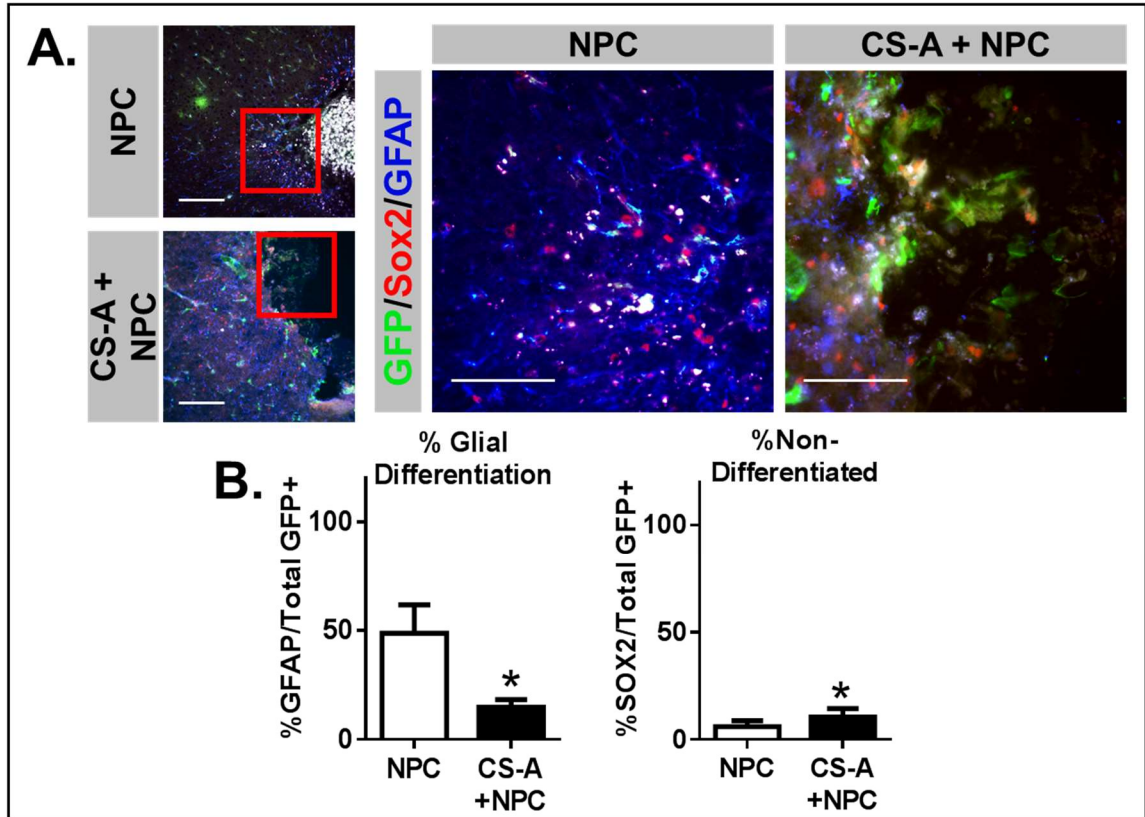


Figure 9. Astrocytic and non-differentiation of NPCs 14 days after transplantation. A) Representative images of GFP, Sox2, and GFAP co-labelled cells in the infarct core 2 weeks after transplantation. B) Analysis of percentage of astrocytic and non-differentiated cells. n=6-8/group. * indicates $p<0.05$; two-tailed T-test.

Following our analysis of neuronal, glial, and non-differentiation after transplantation, we next sought to determine whether our cellular treatments may bypass the inhibitory glial scar to participate in neuronal replacement within the stroke core. We performed MAP2 and GFAP immunostaining to ascertain whether axons could pass through the glial scar. We found numerous cells expressing the axonal marker MAP2 within the stroke core region (Figure 10. However, the axons appeared to be strictly limited to within the stroke core region and ran parallel to the glial scar. We were unable to find any evidence that suggested Map2+ axons

traversed the astrocytic barrier. These findings suggest that while CS-A may permit neuronal differentiation of NPCs *in vitro* and *in vivo*, the strategy of targeting transplantation to the infarct core region may not be conducive to replacing the axonal connections lost to stroke.

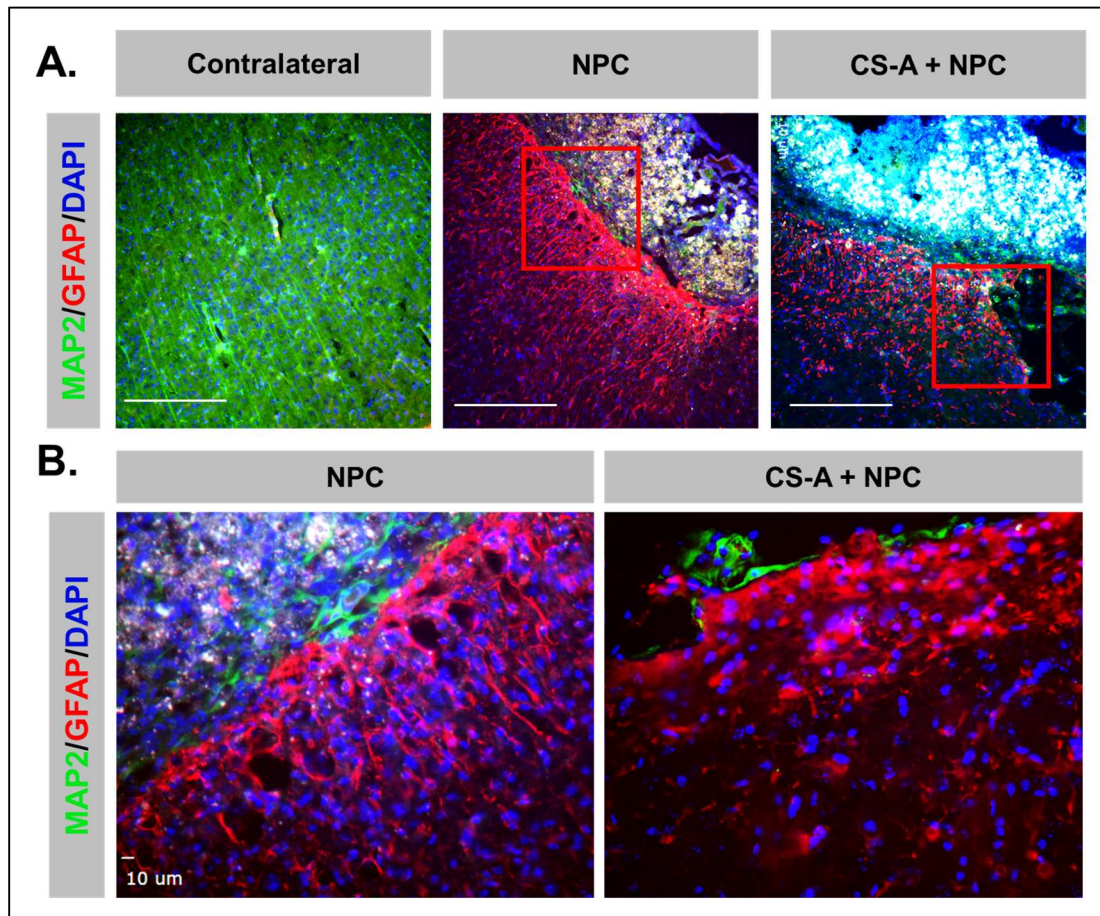


Figure 10. Formation of axons within the stroke core region. A) Representative images of contralateral axonal expression patterns and axonal expression within the stroke core region 2 weeks after transplantation. **B)** Insets from panel A) illustrate axons travel parallel to the astrocytic barrier and do not traverse the astrocytic barrier.

5.2 Aim 2: Determine the effects of treatment with CS-A encapsulated NPC on regeneration in the ischemic brain.

5.2.1 Effect of CS-A encapsulation of NPCs on astrogliosis

Astrogliosis entails reactive astrocytosis and the formation of the glial scar surrounding the infarcted tissue. These processes involve both the migration of activated astrocytes to the infarct region, and also the production of new astrocytes locally. The extent of the glial scar formation is thought to reflect the extent of damage and inflammation within the stroke core. Similarly, reactive astrocytosis, which includes the upregulation of GFAP in astrocytes and a transition from an ameboid to a stellate morphology, may signify the inflammatory state of the brain parenchyma [108, 114, 322, 323, 349]. Whether the hydrogel encapsulated neural progenitors may affect the astrocyte response to the infarcted cortex was unknown. We measured glial scar width and intensity of GFAP staining 2 weeks after transplantation using ImageJ. The average glial scar width was not significantly different between treatment groups, however, the intensity of GFAP staining in the peri-infarct region was significantly reduced in the CS-A + NPC treatment group compared to the cellular therapy and stroke controls (Figure 11). This suggests that treatment with CS-A encapsulated neural progenitor cells may abrogate the astrocytic response following transplantation.

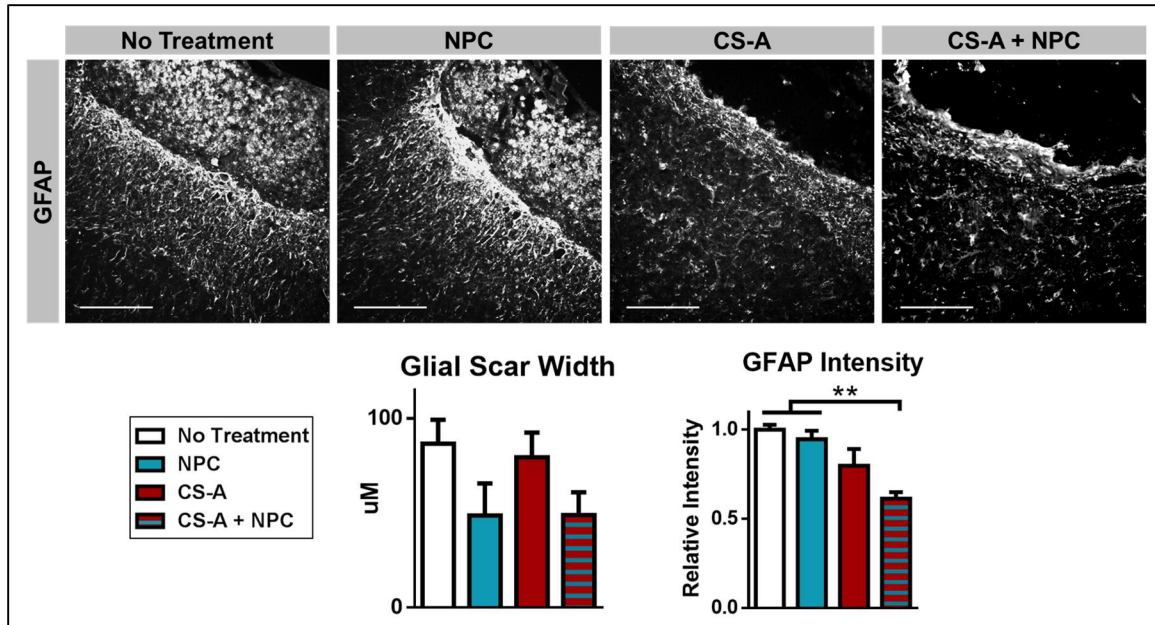


Figure 11. CS-A encapsulation reduces peri-infarct GFAP staining intensity. Representative images of GFAP staining of the infarct and peri-infarct region and analysis of glial scar width and GFAP staining intensity were measured using ImageJ at 2 weeks after transplantation. n=8-12. ** indicates $p < 0.005$; 1-way ANOVA with Bonferonni correction.

5.2.2 Treatment with CS-A encapsulated NPCs promotes a pro-regenerative macrophage response

Microglial infiltration and production and release of immune factors is the major inflammatory response associated with cerebral infarction [100, 102, 107]. Certain microglial phenotypes, in particular the alternatively activated ‘M2’ phenotype, is associated with neural regeneration, angiogenesis and arteriogenesis, and functional recovery [102, 103, 331]. Cellular therapy and also implantation of hydrogels such as hyaluronan can affect microglial polarization and even promote local immunosuppression [34, 307, 350, 351]. Previous studies in our lab have shown that transplantation of NPCs is broadly immunosuppressive, and reduces

multiple harmful inflammatory mediators and the number of infiltrating microglia [6]. Similarly, transplantation of BMSCs also drastically reduces inflammation [307]. The microglial/macrophage response to CS-A and CS-A encapsulated NPCs is uncharacterized.

To test the effects of treatment with CS-A + NPCs, we used immunohistochemical and protein expression analysis to probe microglial-related inflammatory markers. Following 2 weeks after transplantation, the number of M2 type macrophages/microglia is significantly increased by CS-A + NPC treatment as determined by counting of PPAR γ (an M2 marker) and IBA1 (a microglial marker) co-staining in the stroke area compared to the stroke and cellular treatment control. This suggests that transplantation of CS-A encapsulated neural progenitor cells markedly increases the amount of pro-regenerative microglia in the stroke area.

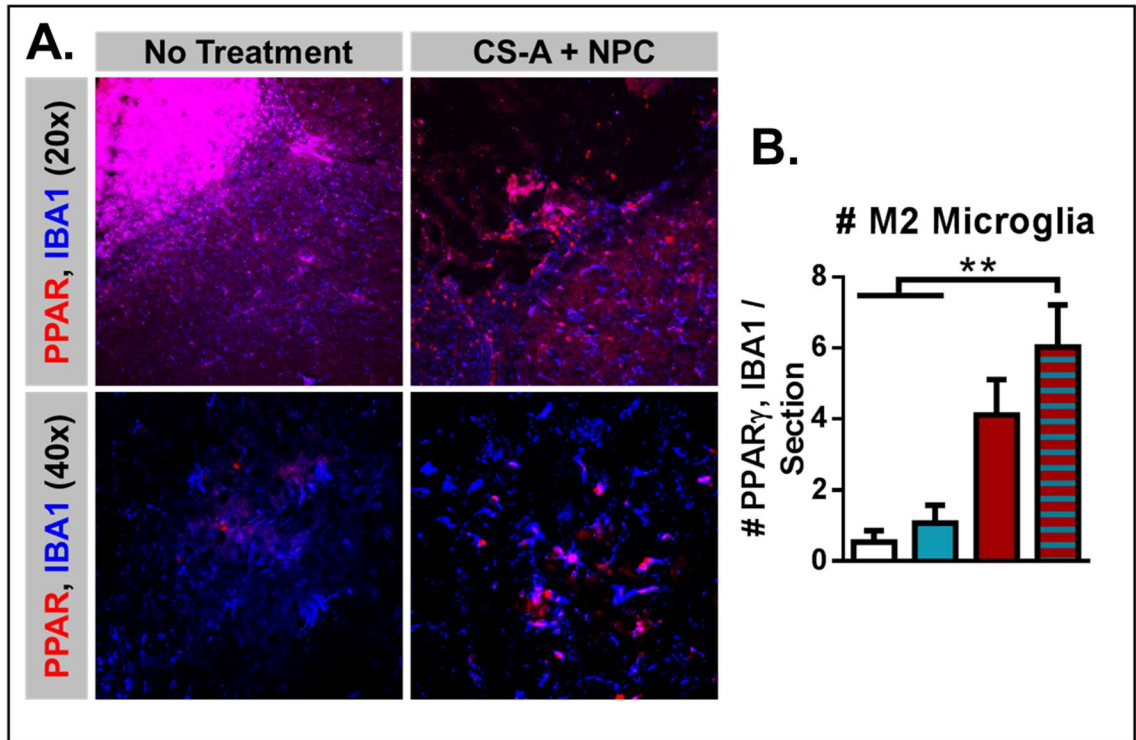


Figure 12. CS-A + NPC treatment promotes alternatively activated microglia polarization 2 weeks after intracranial transplantation. A) Representative images of PPAR γ (an M2 marker) and IBA1 (a microglial marker) co-staining in the stroke area 2 weeks after transplantation. B) Analysis of number of PPAR γ /IBA1 co-staining. n=8-12. **indicates p<0.005; 1-way ANOVA with Bonferroni correction.

Next, we used Western blotting to probe the amount of IL-10 accumulated in the stroke area. IL-10 is produced primarily by microglia/macrophages and is thought to be a primary mediator in inducing an alternatively activated microglial phenotype. [100, 102-104, 107, 307, 331]. We have also shown that iPSC-derived NPCs and BMSCs can produce and release IL-10 [6, 296]. Furthermore, CS-A has a high affinity for IL-10, and in *in vitro* experiments, was shown to enrich IL-10 following neural stem cell encapsulation [53, 324]. We also measured the amount of IBA1 expression in the infarct core region (Figure 13). We found that the interleukin 10 (IL-10) levels were significantly increased in the CS-A + NPC

treatment group compared to all controls (Figure 13). The macrophage marker was significantly reduced in the NPC treatment group compared to the stroke control and the combined CS-A + NPC treatment group, which is consistent with previous findings that transplanted NPCs can suppress the inflammatory response.

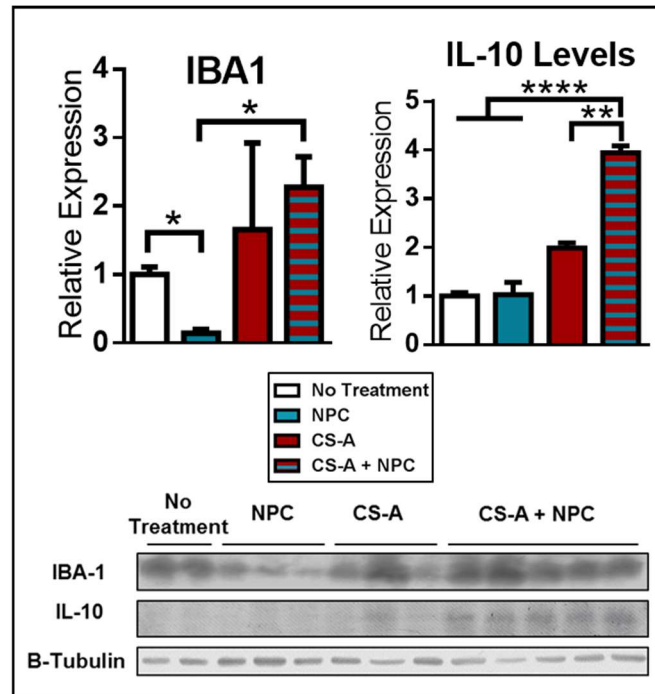


Figure 13. CS-A+NPC treatment significantly enhances IL-10 protein levels in the stroke core region 1 week after transplantation. n=4-8. *, **, and ** indicate $p < 0.05$, $p < 0.005$, and $p < 0.0001$, respectively; 1-way ANOVA with Bonferonni correction.**

To further probe the expression of immune mediators within the stroke region after treatment with CS-A encapsulated NPCs, we measured the expression of a variety of released factors, including monocyte chemoattractant protein 1 (MCP-1), macrophage inflammatory protein 1a and 1b (MIP-1a, MIP-1b), tumor necrosis factor (TNF), and interleukins 4 and 6 (IL-4, IL-6). Expression of these factors were interrogated at both the infarct core and the peri-infarct regions.

We found that at the stroke core region, MCP-1 was significantly increased by CS-A encapsulation of NPCs compared to all other treatments (Figure 14). MCP-1 is a released factor involved in the recruitment of microglia/macrophages. Following ischemic injury and in various treatment paradigms, MCP-1 has been shown to recruit specific subsets of macrophages that participate in regeneration, including angiogenesis, arteriogenesis, and even neurogenesis [176, 196, 206, 214, 328]. MIP-1a and MIP-1b also participate in the recruitment of microglia/macrophages, however, they are more associated with the classically activated M1 macrophage phenotype, which is involved in neurotoxicity and infarct progression during the early phases of stroke pathophysiology [100, 106]. MIP-1a and MIP1b levels were significantly reduced by NPC transplantation compared to the stroke control and also the CS-A encapsulated NPC group Figure 14. There was no significant increase in MIP-1a/b expression in the CS-A encapsulated NPC group compared to the stroke and hydrogel controls. These findings are consistent with our work and others showing that transplanted NPCs are broadly immunosuppressive and can reduce microglial infiltration and activity. Similarly, IL-4 levels were also significantly reduced by NPC treatment compared to the stroke control and the CS-A + NPC groups (Figure 14). In the context of microglial inflammation, IL-4 is a released protein which inhibits the M1 polarization of microglia/macrophages, thereby promoting M2 polarization [102-104, 106, 200]. IL-4 is also neuroprotective and can promote neurogenesis after brain ischemia [102-104, 106, 200].

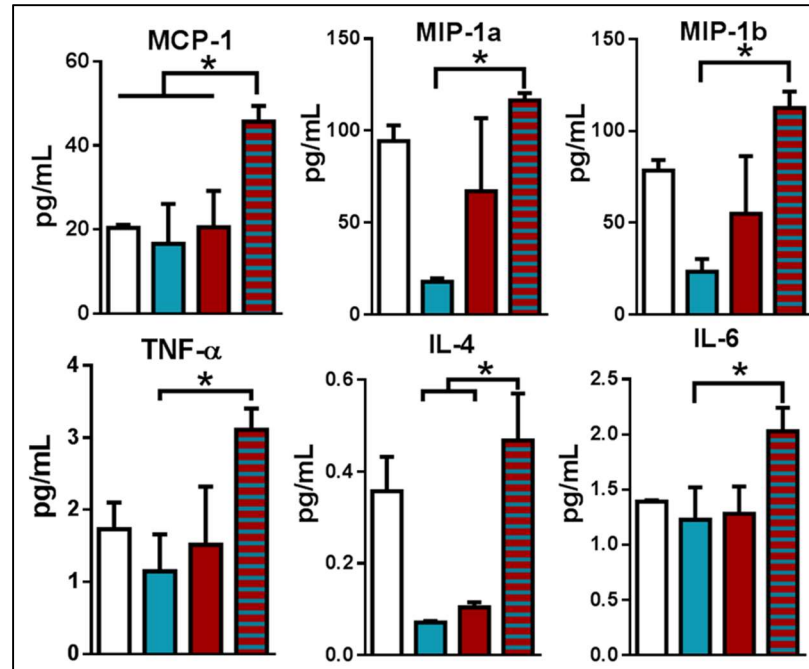


Figure 14. Expression of released immune factors within the stroke core region 1 week after transplantation. n=3-4. * indicates $p < 0.05$; 2-way ANOVA with Holm-Sidak correction.

Together, these released immune factor expression findings suggest that CS-A encapsulation of NPCs may promote recruitment of regenerative macrophages via increase of MCP-1. Furthermore, these findings verify that treatment with NPCs can reduce both harmful and beneficial microglial inflammation, and that encapsulation with CS-A may allow expression recovery of some of these proteins. The extent to which CS-A can facilitate beneficial versus harmful microglial inflammation is not easily discernable. However, it should be noted that in all cases except for MCP-1, the expression levels in the CS-A + NPC treatment group were not statistically significantly different than the stroke controls. These samples were isolated from stroke tissue weeks after infarction, which is long after the initial wave of neurotoxic inflammation during the acute phases of

ischemic stroke [100, 106, 331]. This suggests encapsulation with CS-A does not worsen the inflammatory response compared to the natural history of inflammation in stroke pathology.

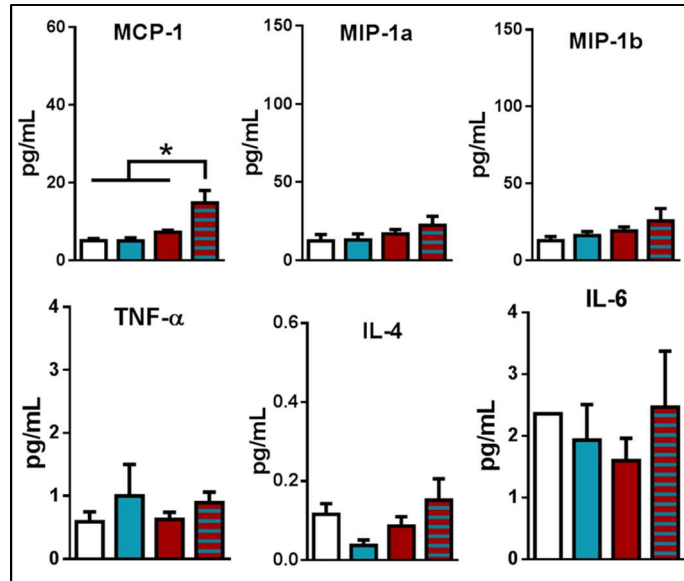


Figure 15. Expression of released immune factors within the peri-infarct region 1 week after transplantation. * indicates $p < 0.05$; 2-way ANOVA with Holm-Sidak correction.

The expression of the same proteins was also measured in the peri-infarct region (Figure 15). We found that MCP-1 was also significantly upregulated in the peri-infarct region of mice treated with CS-A encapsulated NPCs, suggesting that the recruitment of pro-regenerative microglial, in particular the recruitment of arteriogenic macrophages, extends outside of the stroke core region and into the peri-infarct zone. There was no significant difference in expression of other factors in the peri-infarct region. We also compared the total expression patterns of the immune factors in the stroke core region versus the peri-infarct region in mice

treated with CS-A encapsulated NPCs (Figure 16). The group expression was significantly reduced in the peri-infarct region compared to the stroke core region.

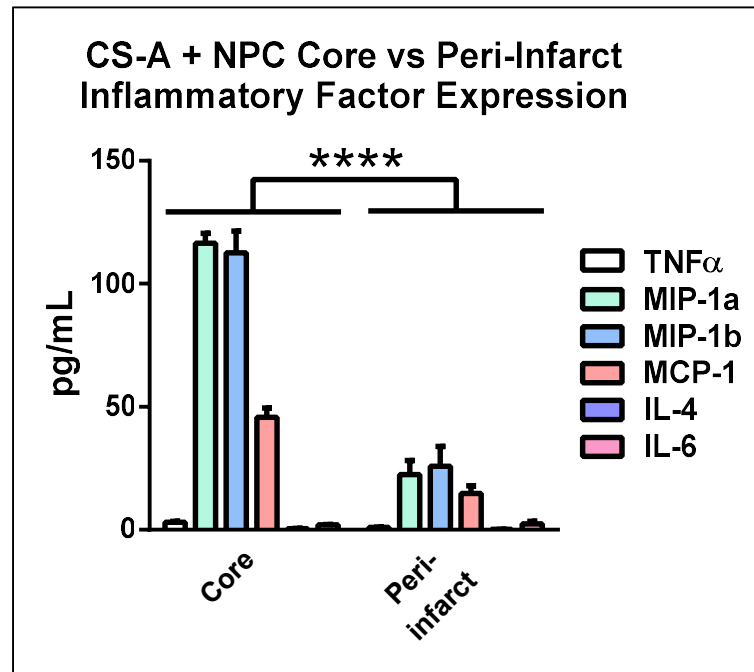


Figure 16. Comparison of immune factors in the stroke core versus peri-infarct region in CS-A+NPC treated mice 1 week after transplantation. ** indicates p<0.0001. Two-way ANOVA with Holm-Sidak correction.**

We compared the overall relative expression of these factors by treatment group to ascertain whether or not the group expression profiles as a whole were significantly different from each other. We found that the CS-A + NPC group expression of immune factors was significantly increased compared to all controls (Figure 17). Furthermore, the NPC treatment group was significantly reduced compared to the stroke control. These findings are in line with previous findings that intracranially transplanted NPCs are broadly immunosuppressive. Interestingly, the combination of the NPCs with the CS-A hydrogel seems to promote rather than inhibit the expression of the inflammatory factors in the stroke

core region. This may due to the increased recruitment of M2 type macrophages observed in previous experiments (Figure 12).

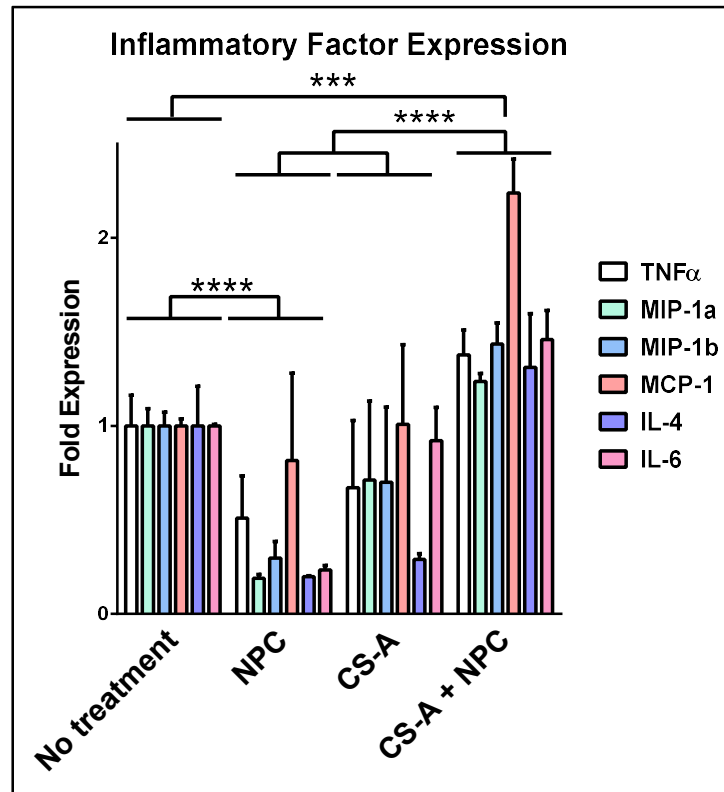


Figure 17. Analysis of group relative expression of immune factors 2 weeks following intracranial transplantation. ***, and **** indicate $p < 0.0005$ and $p < 0.0001$, respectively. Two-way ANOVA with Holm-Sidak correction.

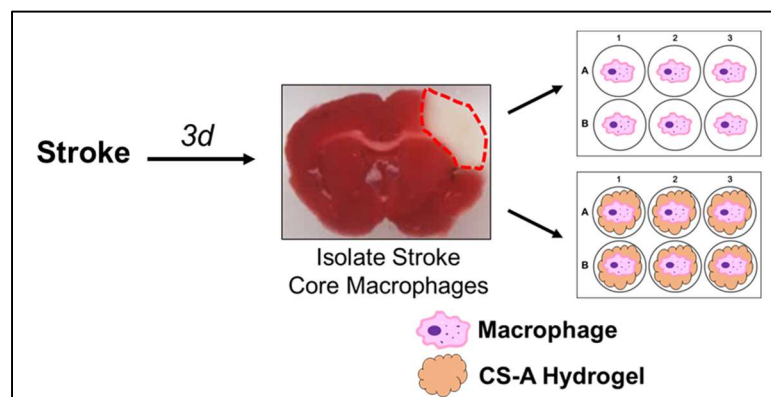


Figure 18. Experimental design for *in vitro* macrophage culture.

Next, we tested whether the CS-A hydrogel may have direct effects on microglia/macrophages. Microglia were isolated from the stroke core region at 3 days after infarction and either directly encapsulated in CS-A or plated on tissue culture polystyrene (Figure 18). We initially chose to isolate macrophages at 3 days after stroke since the infiltration peaks at this timepoint, allowing for collection of sufficient numbers for *in vitro* applications. Furthermore, microglia are more active at this timepoint [100, 103, 104, 331].

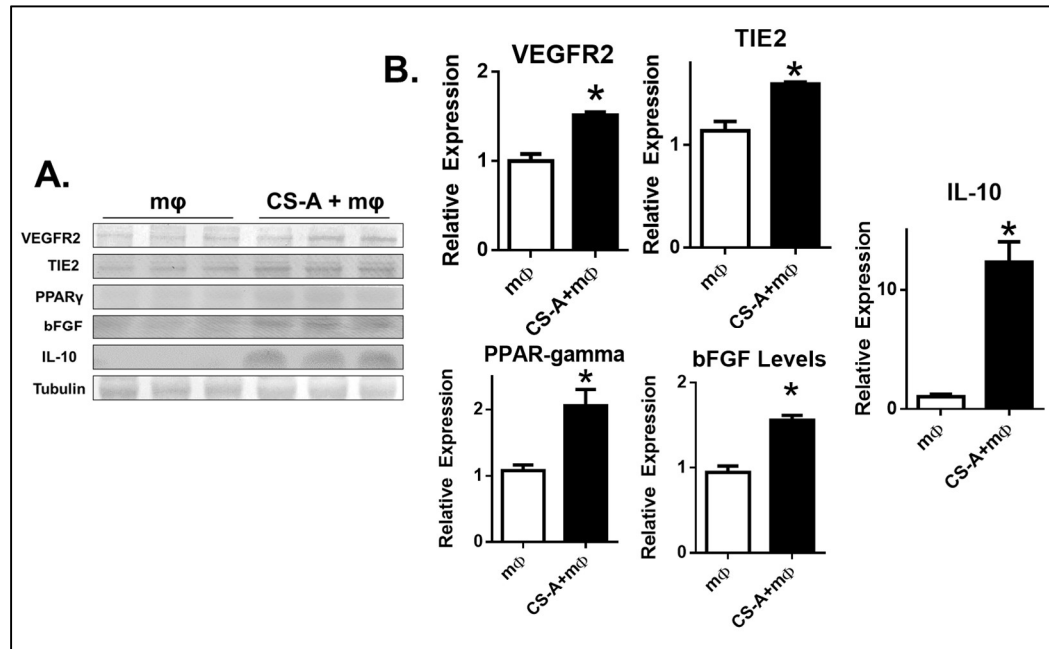


Figure 19. CS-A encapsulation of stroke macrophages promotes a regenerative macrophage phenotype *in vitro*. A) Western blotting of VEGFR2, TIE2, PPAR γ , bFGF, and IL-10. B) Analysis of protein expression. n=3-5 *in vitro* replicates of macrophages pooled from 8 mice. * indicates p<0.05; two-tailed T-test.

After 3 days *in vitro*, we found that microglia grown in the CS-A hydrogel expressed higher levels of VEGFR2, TIE2, PPAR γ , bFGF, and IL-10 as determined by Western blotting (Figure 19). On macrophages, VEGFR2 and TIE2

expression, which correspond to the angiogenic/arteriogenic receptors for VEGF and Ang respectively, are involved in promoting vascular regeneration. Similarly, macrophages can produce bFGF, which can promote both angiogenesis and arteriogenesis. The enhanced expression of VEGFR2, TIE2, and bFGF suggests that CS-A encapsulation may promote macrophages to assist in vascular regeneration. The M2 associated proteins PPAR γ and IL-10 were also significantly increased, suggesting that CS-A may play a role in promoting M2 macrophage polarization.

CS-A can regulate IL-10 binding, partitioning, and presentation [47, 53, 324]. Thus, we tested whether IL-10 may play a role in promoting the macrophage phenotype seen *in vitro* by neutralizing released IL-10 by addition of an anti-IL-10 neutralizing antibody to the cell culture media (Figure 20). Microglia for this experiment were isolated at 7 days after infarction. This timepoint was chosen since it was believed the macrophages at this timepoint may better reflect those present at the stroke core during transplantation. We found that following 3 days in culture, all CS-A encapsulated groups showed increased TIE2 expression compared to the non-encapsulated macrophages. TIE2 expression was independent to addition of IL-10 neutralization antibody in either group. The levels of bFGF and PPAR γ were reduced by addition of anti-IL-10 in the non-encapsulated microglia, but not in the encapsulated group. This may suggest that IL-10 does not play a major role in determining CS-A mediated macrophage polarization. However, the levels of bFGF and PPAR γ were similar in the CS-A encapsulated group versus the non-encapsulated group, which is contrary to the

results found in the previous experiment Figure 19. This suggests that the timing of macrophage isolation from the stroke core tissue is important in determining their response to the CS-A hydrogel. We hypothesize that the macrophages isolated at 7 days following infarction may be more senescent and less responsive to alterations in their physical environment or to IL-10 signaling, and thus, are not ideal for the study of the role of IL-10 in CS-A mediated macrophage polarization [100].

For these reasons, the experiment was repeated with stroke core macrophages isolated from tissue 3 days (rather than 7 days) after stroke. The experimental conditions were nearly identical except for the timepoint at which the macrophages/microglia were dissected from the stroke core region. We found that the protein levels of TIE2 and bFGF were significantly increased by CS-A encapsulation, which is consistent with previous *in vitro* and *in vivo* findings. Furthermore, IL-10 neutralization resulted in reduction in TIE2 and bFGF in both the CS-A encapsulated and non-encapsulated treatment groups. This suggests that IL-10 plays a role in promoting macrophage arteriogenic phenotype irrespective of encapsulation.

An important limitation of these *in vitro* studies is that the macrophages isolated from the stroke core and subsequently cultured *in vitro* may not reflect their phenotype *in vivo*. Furthermore, for this experiment, the macrophage/microglial interaction with the transplanted NPCs was not evaluated, which appears to be a major influence on immune factor expression *in vivo* (Figure 17). Another important limitation is that the dissection and culturing of the stroke

core tissue following dissociation does not yield a pure population of microglia/macrophages. Other cell types contaminants from the stroke core such as surviving endothelium or neurons may be present, however, they are very few and likely do not provide a significant contribution to the protein isolated for these experiments [74]. Also, the use of a neutralizing antibody may not completely reduce the levels of IL-10; alternate strategies such as genetic knockdown or knockout may provide more definitive reductions in bioavailability of IL-10. Finally, as discussed above, the timing of isolation of the stroke core tissue appears to be of critical importance. Macrophages isolated at early time points (3 days) may be primed to respond to the ischemic injury and may exhibit more plasticity in their response to CS-A encapsulation and IL-10 neutralization [100]. This may explain the discrepancy in response to IL-10 neutralization and overall expression of pro-arteriogenic markers in the macrophages isolated at early versus later timepoints.

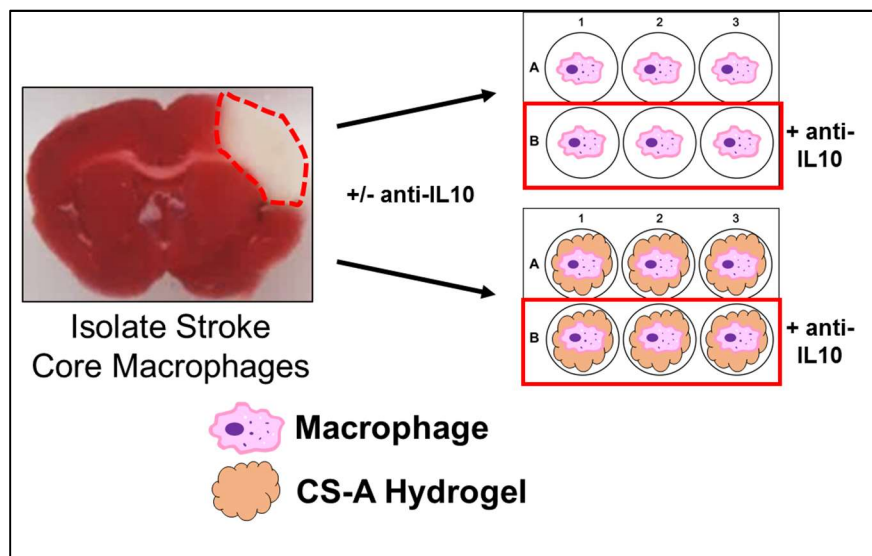


Figure 20. Experimental design for testing the role of IL-10 on CS-A mediated macrophage polarization *in vitro*. Stroke core macrophages were dissected

at either 7 (Figure 21) or 3 days (Figure 22) after surgical induction of cortical ischemia (*Primary stroke core macrophage isolation and culture*).

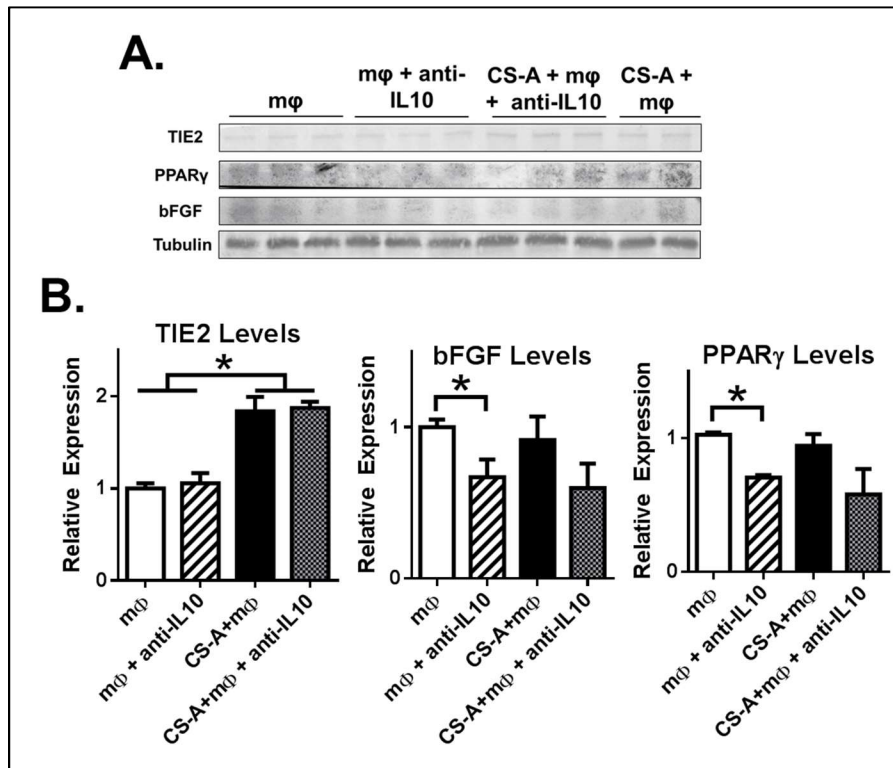


Figure 21. IL-10 neutralization may abolish the regenerative capability of stroke core microglia/macrophages collected 7 days after stroke. A) Western blotting of TIE2, PPAR, and bFGF. B) Analysis of protein expression. n=3-6 *in vitro* replicates of pooled macrophages from 10 mice. * indicates $p < 0.05$; 1-way ANOVA with Bonferroni correction.

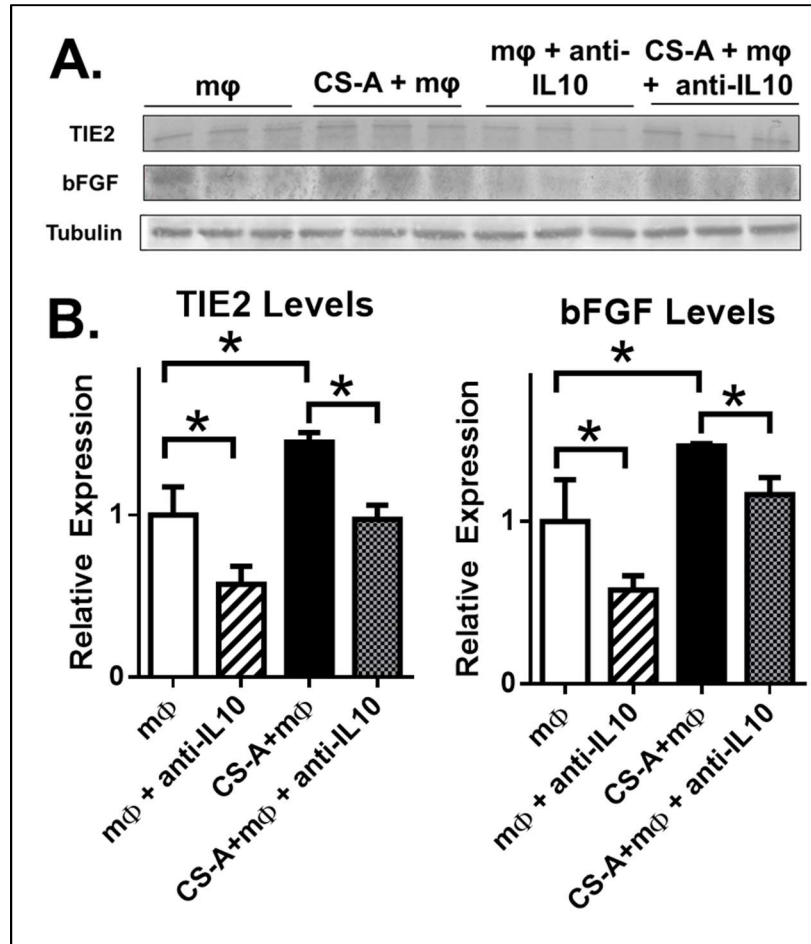


Figure 22. IL-10 neutralization reduces pro-arteriogenic markers in microglia/macrophages collected 3 days after stroke. **A)** Western blotting of TIE2 and bFGF. **B)** Analysis of protein expression. *n*=3 *in vitro* replicates of pooled macrophages from 3 mice per treatment group (3 separate mice per treatment; 12 mice total). * indicates *p*<0.05; 1-way ANOVA with Bonferroni correction.

5.2.3 Neurogenesis and neuroblast recruitment are unaffected by treatment

The endogenous replacement of neurons lost to stroke is a possible mechanism of recovery. To test whether treatment can promote endogenous neurogenesis, we injected mice daily (after treatment) with BrdU which labels newly formed cells. The number of NeuN (neuronal marker) and BrdU colabelled cells were counted. We found that the levels of newly formed neurons across all treatment groups and

controls was extremely low (~0.2 cells per section). There was no difference in neurogenesis between treatment groups (Figure 23). Prior to the endogenous formation of newborn neurons, doublecortin (DCX) + neuroblasts migrate from the subventricular zone to the peri-infarct region over the course of days to weeks [22, 111, 180, 305]. We counted the number of migrating neuroblasts in the peri-infarct region and also measured the intensity of DCX expression in the subventricular zone. We found that there was no significance between treatment groups in DCX levels at the peri-infarct or SVZ (Figure 23). Together, these findings indicate that CS-A encapsulation of NPCs does not promote neuronal regeneration. Cellular therapy in other treatment paradigms, such as transplantation of these same iPSC derived NPCs directed to the peri-infarct, and intranasal delivery of BMSCs, has been shown to promote neurogenesis following treatment after stroke [6, 7, 23, 35, 186]. Since we found no improvements in neurogenesis, this may suggest that targeting the infarct core for transplantation may not be a viable strategy for inducing neurogenesis after stroke.

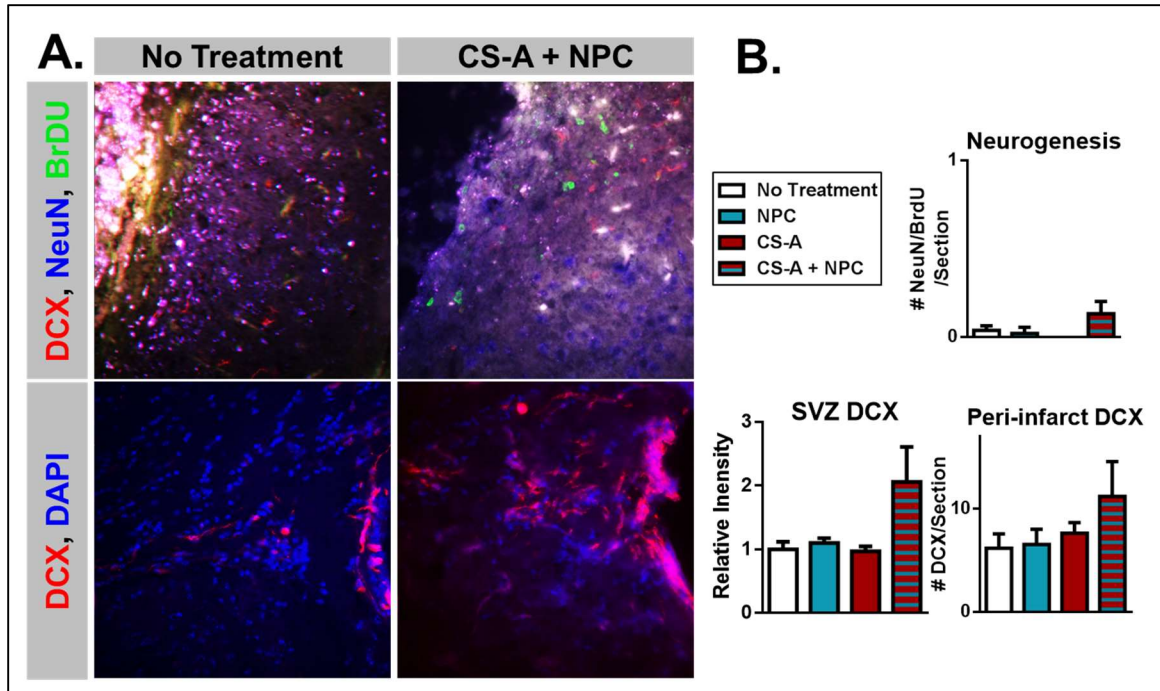


Figure 23. CS-A + NPC treatment directed to the stroke core does not improve neurogenesis after stroke. A) Representative images of NeuN/BrdU and DCX staining at the peri-infarct region (top panel) and SVZ 2 weeks after intracranial transplantation. B) Analysis of neurogenesis, SVZ DCX staining intensity, and number of peri-infarct DCX+ neuroblasts. n=8-12. * indicates $p<0.05$; 1-way ANOVA with Bonferroni correction.

Next, we tested whether treatment with CS-A+NPCs may affect protein expression of neurogenic factors. Using Western blotting, we measured the levels of BDNF and NGF, both of which have been shown to be enriched within CS-A hydrogel *in vitro* [53, 324]. We found that levels of brain derived neurotrophic factor (BDNF) were significantly increased in the CS-A+NPC treatment group compared to all other controls (Figure 24). However, the levels of nerve growth factor (NGF) were not statistically different between groups. BDNF is associated with both neurogenesis and neural plasticity [35, 352]. The neurogenesis results above (Figure 23) indicated that neurogenesis was unaffected in any treatment group.

Therefore, it is unlikely that the increased BDNF levels in the stroke core region played a role in endogenous neurogenesis. Furthermore, given that the axons produced in the stroke core were unable to penetrate the astrocytic barrier, it is unlikely that the enhanced BDNF levels promoted synaptic plasticity in the stroke core. Others have shown that BDNF is also neuroprotective during brain ischemia [352]. It is possible that increased levels of BDNF within the CS-A hydrogel promoted enhanced retention and resistance to cell death following transplantation into the infarct core. However, synaptic plasticity in the stroke core or the peri-infarct region, and the effect of BDNF on transplant cell retention were not tested and are potential areas for future study.

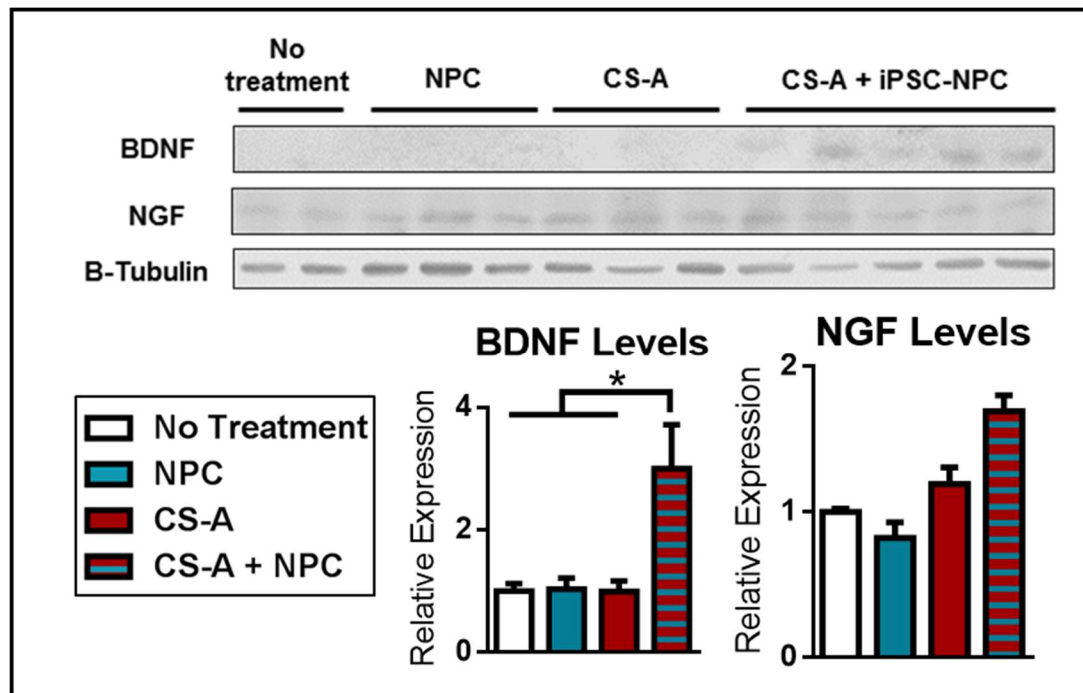


Figure 24. CS-A+NPC treatment increases BDNF expression in the stroke core region 1 week after transplantation. BDNF levels were increased in the CS-A+NPC group compared to all controls. NGF levels were not statistically different between groups. n=4-8. * indicates $p < 0.05$; 1-way ANOVA with Bonferonni correction.

5.2.4 Vascularity and angiogenesis are increased by CS-A+NPC treatment

Vascular regeneration is at the center of recovery processes following cerebral infarction. To assess the potential for angiogenic benefits of CS-A encapsulation of NPCs, we treated mice daily with BrdU to monitor newly formed cells. The number of Glut1+ microvessels co-labelled with BrdU were counted, and the total number of microvessels within the stroke core region were also counted to measure newly formed endothelium and vascular density. We found that CS-A encapsulation of NPCs significantly improves their potential to induce angiogenesis, resulting in a greater number of newly formed endothelium, and a higher density of blood vessels within the stroke core region (Figure 25). We also noted formation of numerous muscular arteries (SMA+, Glut1+ vessels) within the hydrogels in mice treated with CS-A + NPCs (Figure 26).

We probed signaling pathways that are involved in induction of angiogenesis using Western blotting. We found that bFGF and VEGF were significantly elevated in the CS-A+NPC group compared to all controls. These two molecules are well-known for their important roles as mediators of angiogenesis and vascular remodeling in health and disease [252, 353-355]. Furthermore, we also found that p-AKT was also upregulated in CS-A+NPC compared to the stroke and cellular controls. At the cellular level, enhanced AKT signaling reflects growth and proliferation, suggesting that regenerative processes such as angiogenesis are enhanced by treatment with CS-A+NPCs. However, we cannot rule out the expression of p-AKT in cell types other than endothelium, including microglia, astrocytes, or the transplanted cells.

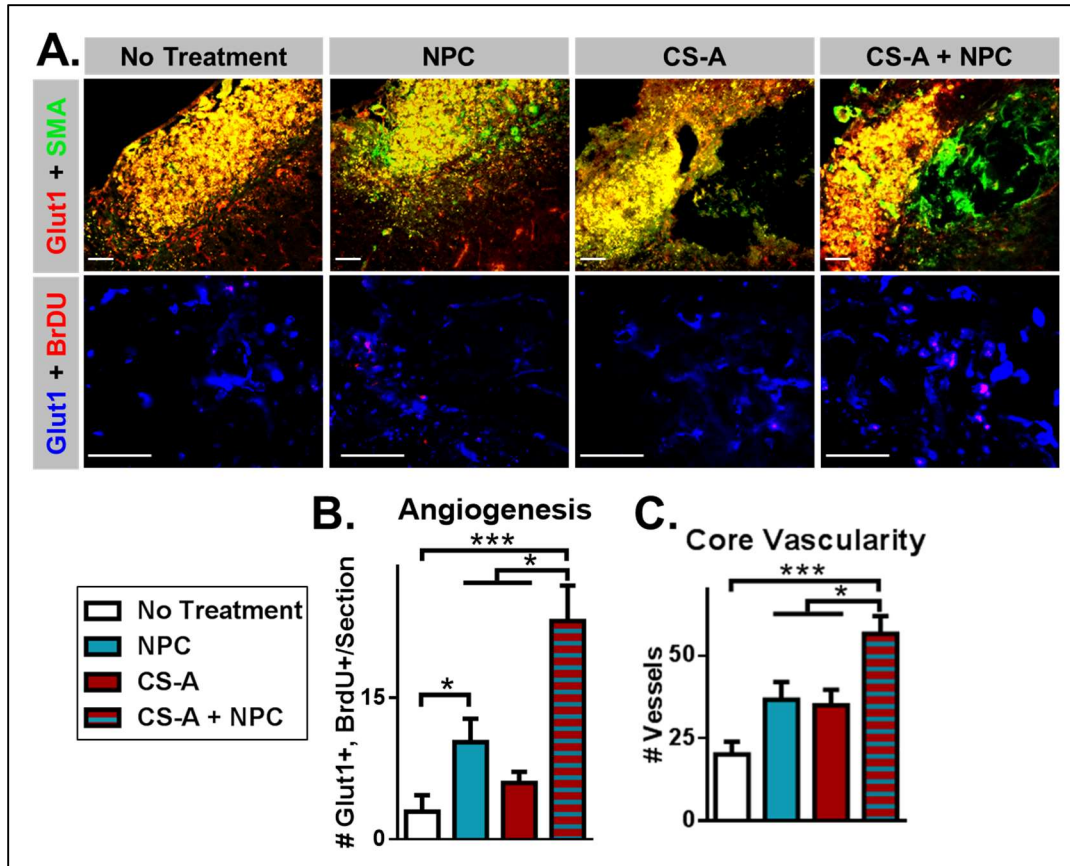


Figure 25. CS-A encapsulation of NPCs improves angiogenesis and stroke core vascularity. A) Glut1 and BrdU costaining. B) Analysis of angiogenesis (#Glut1/BrdU co-labelled endothelium). C) Analysis of vascularity. n=8-12. *, **, and * indicate $p < 0.05$, $p < 0.005$, and $p < 0.001$, respectively; 1-way ANOVA with Bonferonni correction.**

The relative cellular contributions of bFGF within the stroke core are unclear. Numerous cell types can produce and release bFGF, including macrophages/microglia, endothelial cells, vascular mural cells, astrocytes, neurons, and transplanted NPCs. However, given the robust generation of bFGF by stroke core macrophages *in vitro* (Figure 19), we hypothesize that microglia/macrophages are a likely candidate for the main source of bFGF. This hypothesis is also consistent with findings in the literature regarding the role of microglia/macrophages in vascular regeneration [102, 205, 328, 331].

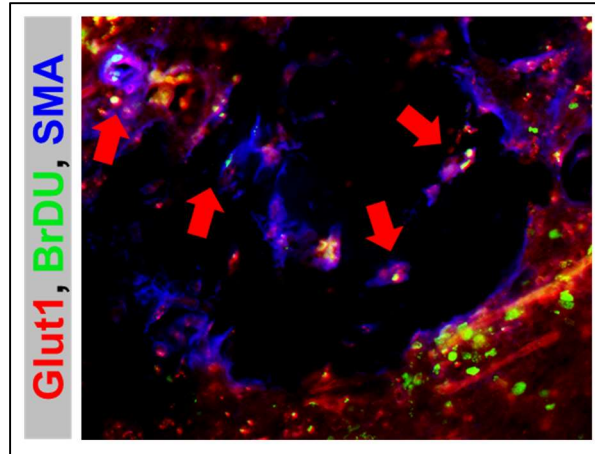


Figure 26. Representative image of a muscular artery (SMA/Glut/BrdU) formation within the hydrogel of mice treated with CS-A + NPC.

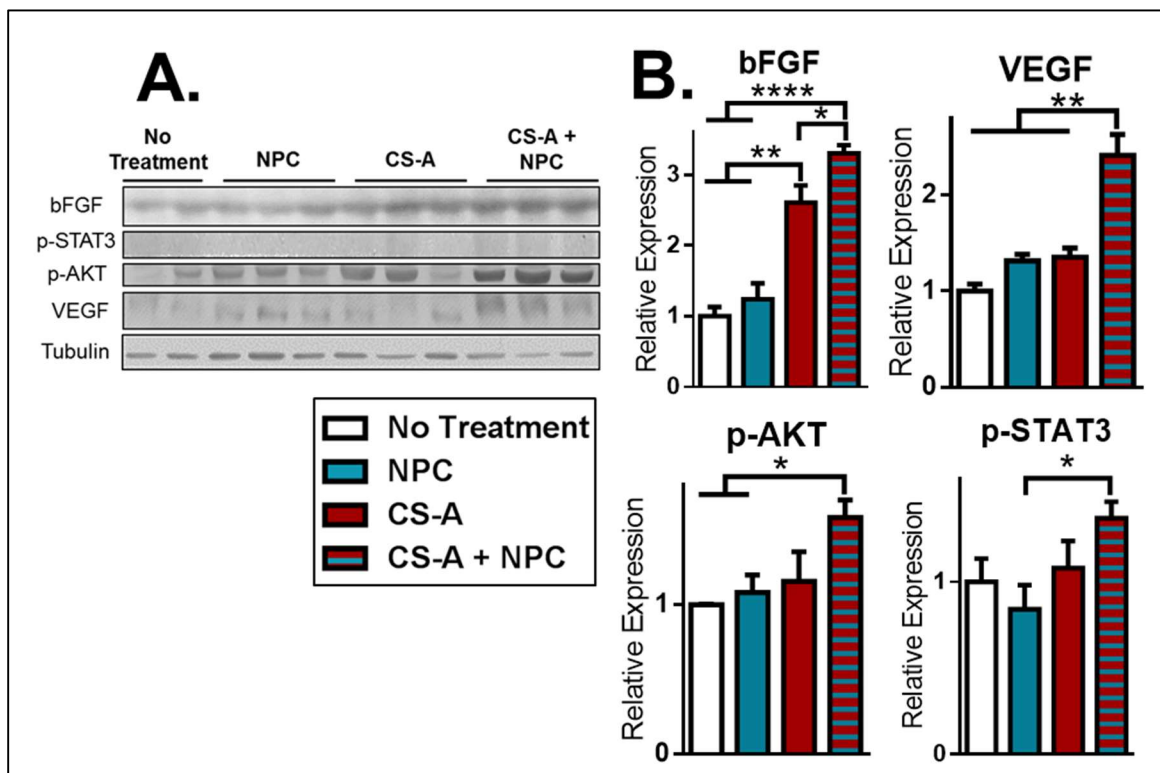


Figure 27. Increased expression of angiogenic proteins after treatment with CS-A+NPC. A) Western blotting of bFGF, p-STAT3, p-AKT, and VEGF. B) Analysis of angiogenic protein expression. *, **, and **** indicates $p < 0.05$, $p < 0.005$, and $p < 0.0001$, respectively; 1-way ANOVA with Bonferonni correction.

Angiogenesis entails the migration and proliferation of endothelial cells. We next sought to test whether the CS-A hydrogel may have an effect on either of these processes. To test for endothelial migration and haptotaxis, we used a microfluidic device developed by our collaborators [338] which allows for the comparison of migration into either a CS-A or hyaluronan hydrogel (Figure 28). Without any type of haptotactic signal (i.e. regular media), immortalized brain endothelial cells (B.end3) migrated equally into the CS-A and hyaluronan gels. However, when a haptotactic gradient was applied using NPC-conditioned media, the endothelial cells preferred to migrate towards the CS-A hydrogel (Figure 28). We also tested whether CS-A may affect proliferation using Western blotting for the cell cycle protein Cyclin D1 (Figure 29). We found there was no difference in Cyclin D1 expression in the CS-A encapsulated versus the non-encapsulated after 3 days *in vitro*.

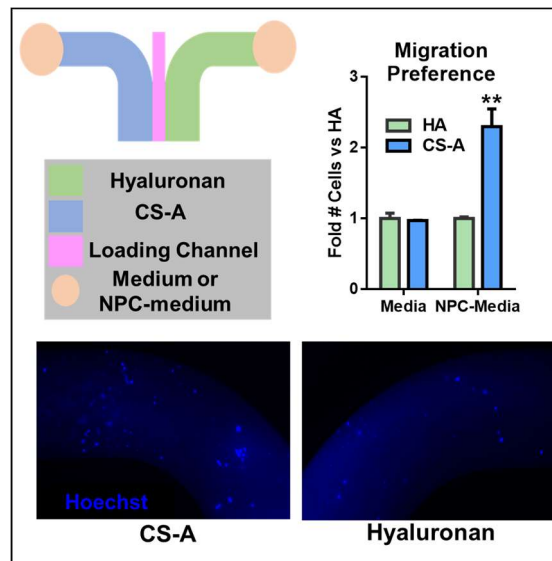


Figure 28. CS-A promotes NPC-mediated endothelial haptotaxis (*Hydrogel haptotaxis assay*). n=3. ** indicates $p < 0.005$; 1-way ANOVA with Bonferonni correction.

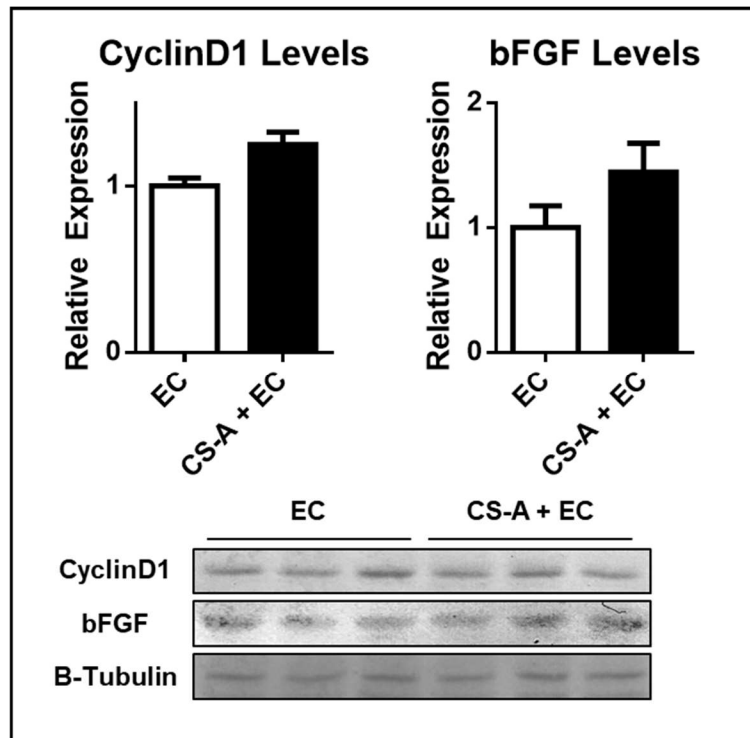


Figure 29. CS-A may not affect endothelial replication *in vitro*. Western blotting analysis indicates CyclinD1, a cell cycle protein and marker for replication, was not different between groups. n=3; two-tailed T-test.

Together, these *in vitro* results suggest that CS-A can promote endothelial migration via released signals from NPCs which were available in the conditioned media. However, CS-A did not appear to affect levels of markers of endothelial replication, suggesting that the major mechanism by which CS-A encapsulation may promote angiogenesis is via recruitment of new endothelial cells.

5.3 Aim 3 Determine the effects of treatment with CS-A encapsulated NPCs on local blood flow restoration and functional recovery after ischemic stroke.

5.3.1 CS-A encapsulation of NPCs augments blood flow to the infarcted cortex

Blood flow to the cerebral cortex is a critical aspect of recovery and regeneration after ischemic stroke. We tested cortical circulation after stroke and treatment using laser Doppler flowmetry to measure local cerebral blood flow (LCBF) in the stroke area (Figure 30). The LCBF was monitored before and weekly after stroke.

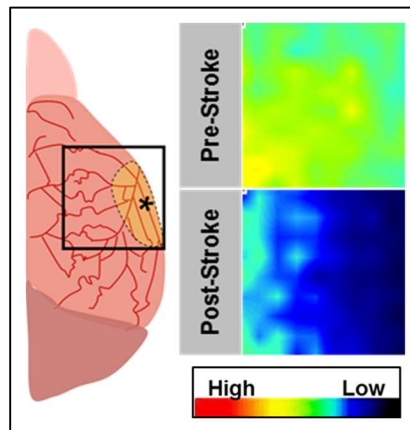


Figure 30. Diagram of cortical areas measured using laser Doppler flowmetry and representative pre-stroke and post-stroke flow heatmaps (*Mouse stroke model, laser Doppler flowmetry, and transplantations*).

We found that blood flow to the infarcted cortex was increased following treatment with CS-A+NPCs at both 1 and 2 weeks after treatment compared to all controls (Figure 31). At 1 week after stroke, we noted that blood flow recovery was also improved by treatment with NPCs, but to a lesser extent than by CS-A encapsulated NPCs. However, the improvement in blood flow from non-encapsulated NPCs was lost by 2 weeks after treatment (Figure 31).

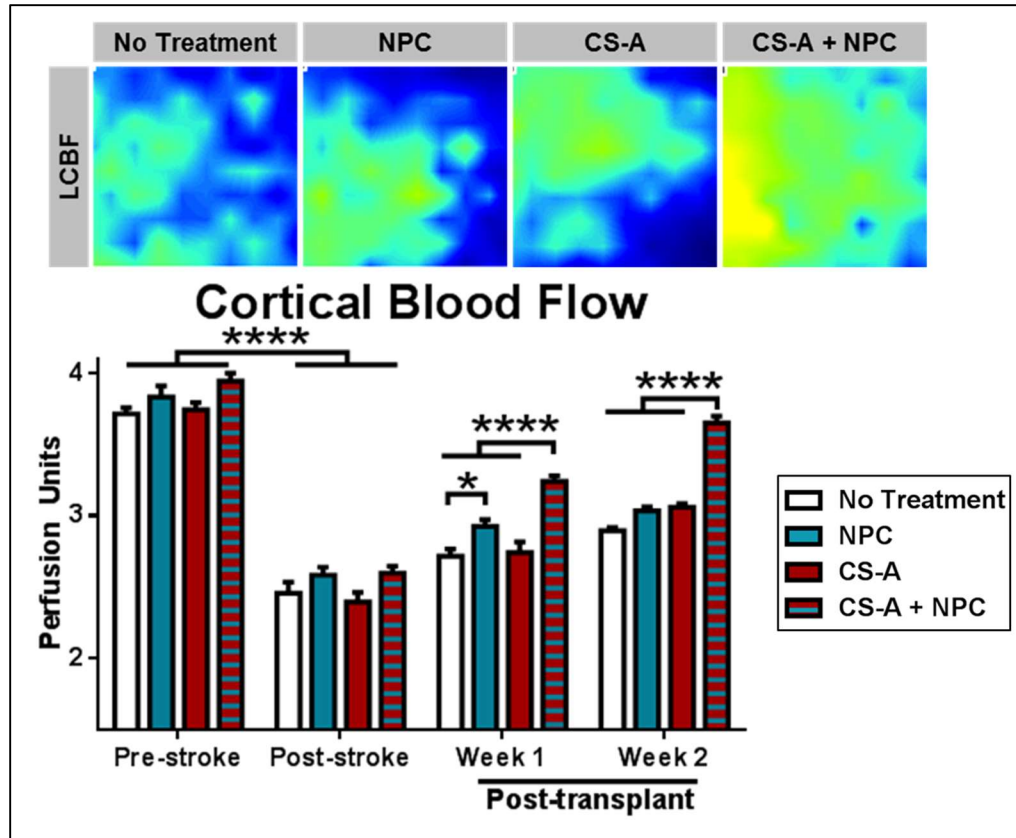


Figure 31. CS-A encapsulation improves cortical blood flow after stroke. The top panel illustrates LCBF heatmaps at 2 weeks after transplantations (Mouse stroke model, laser Doppler flowmetry, and transplantations). n=8-12. * and ** indicates $p < 0.05$ and $p < 0.0001$, respectively; 2-way ANOVA with Bonferroni correction.**

5.3.2 Pial collateral artery diameter and recruitment are increased with CS-A encapsulation of NPCs

We hypothesized that cellular therapy may improve the structural remodeling of large vessels after stroke. To examine pial artery remodeling and collateralization after treatment, we utilized mice with alpha smooth muscle actin tagged with GFP (SMA-GFP). Mice brains were isolated following conclusion of the experiments and imaged using a fluorescent microscope. The number and

widths of pial collateral arteries was collected and analyzed. A recruited collateral was defined as a collateral vessel with at least 25% greater diameter than the average sham collateral vessel diameter, which corresponds to >50% increase in flow rate through the collateral channel. We found that average pial collateral diameter and collateral recruitment were significantly improved by CS-A encapsulation (Figure 32). Collateral number was not significantly different between groups, affirming that collaterogenesis, or the *de novo* formation of anastomoses, is not a prominent phenomenon in our ischemic stroke model and is unaffected by treatment. We verified that the arteriogenesis was due to outward remodeling of large pial arteries using immunohistochemistry (Figure 33). Large arteries undergoing outward remodeling (SMA+/BrdU+ vessels) in the pial layer of the meninges were found in both the peri-infarct region and in the stroke core area.

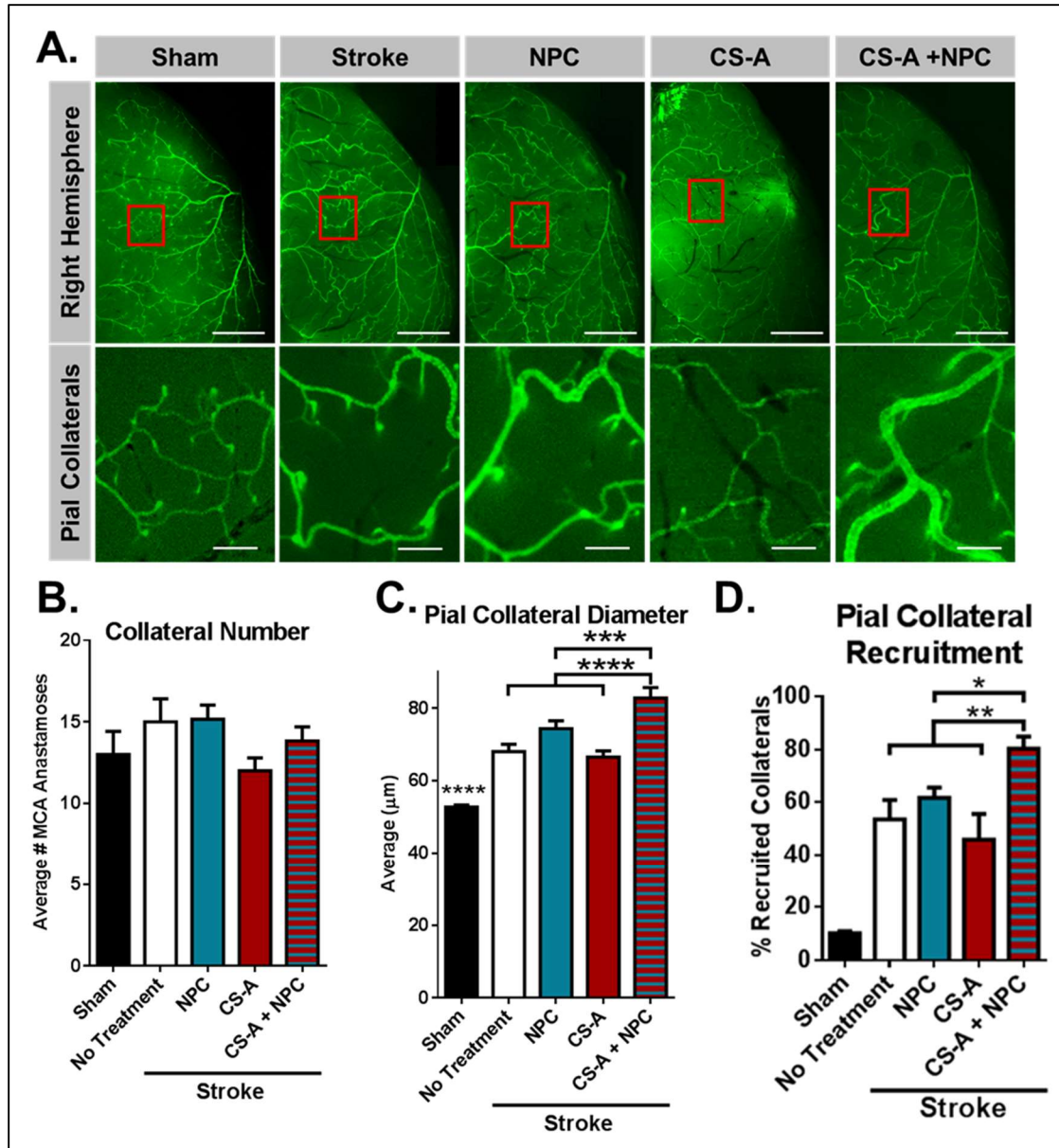


Figure 32. Treatment with CS-A+NPCs improves pial artery collateralization after stroke. A) Representative images of pial collaterals; red box indicates MCA-ACA anastomoses in similar locations between animals. B) Analysis of collateral vessel number. C) Analysis of average collateral vessel width. D) Analysis of pial collateral recruitment. $n=8-12$. * and ** indicates $p<0.05$ and $p<0.005$, respectively; 1-way ANOVA with Bonferroni correction; all groups significantly (****) greater than sham in C) and D).

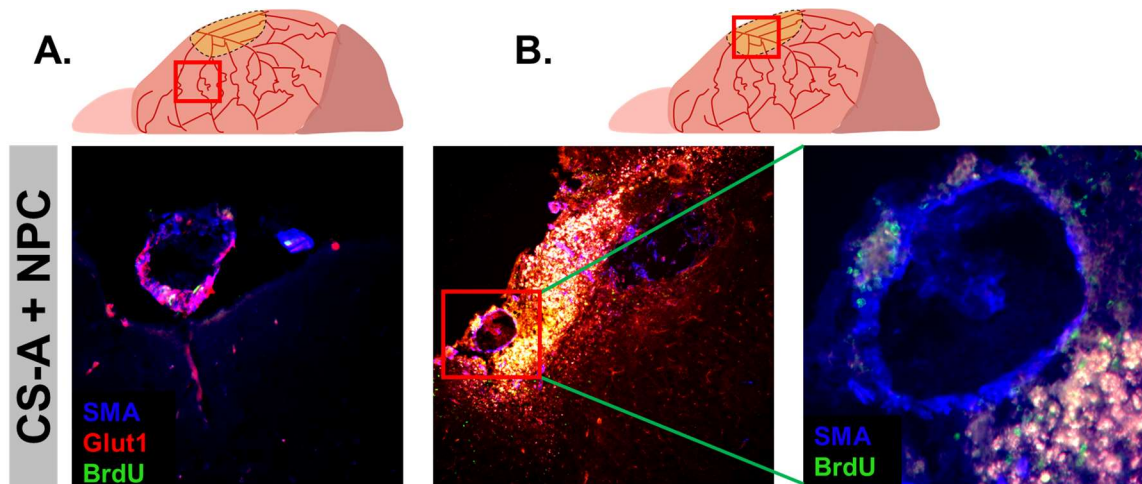


Figure 33. Confirmation of outward remodeling in pial vessels following treatment with CS-A + NPC. A) Representative image of pial artery in the peri-infarct region with numerous SMA/BrdU colabelled cells. B) Representative image of pial artery in the stroke core region with multiple SMA/BrdU colabelled cells.

5.3.3 CS-A encapsulation of NPCs fails to provide additional functional benefits in sensorimotor tests after ischemic stroke

Recovering functional deficits lost to stroke is the primary goal of therapy. Our ischemic stroke model targets the sensorimotor cortex responsible for mouse whisker and forelimb sensation and motor function [177, 186, 215]. We evaluated whisker sensation using the corner test. Mice tend to turn right following stroke due to a lack of sensation of the left whiskers, resulting in an elevated right/left turn. Two weeks after stroke, the CS-A+NPC group showed a reduced rightwards deviation compared to the stroke control, but not the cellular or material controls. Forepaw sensorimotor function was evaluated using the adhesive removal test. Mice treated with CS-A + NPCs showed a significantly improved time to removal 1 week after transplantation compared to the stroke control, but not to the cellular or material control groups.

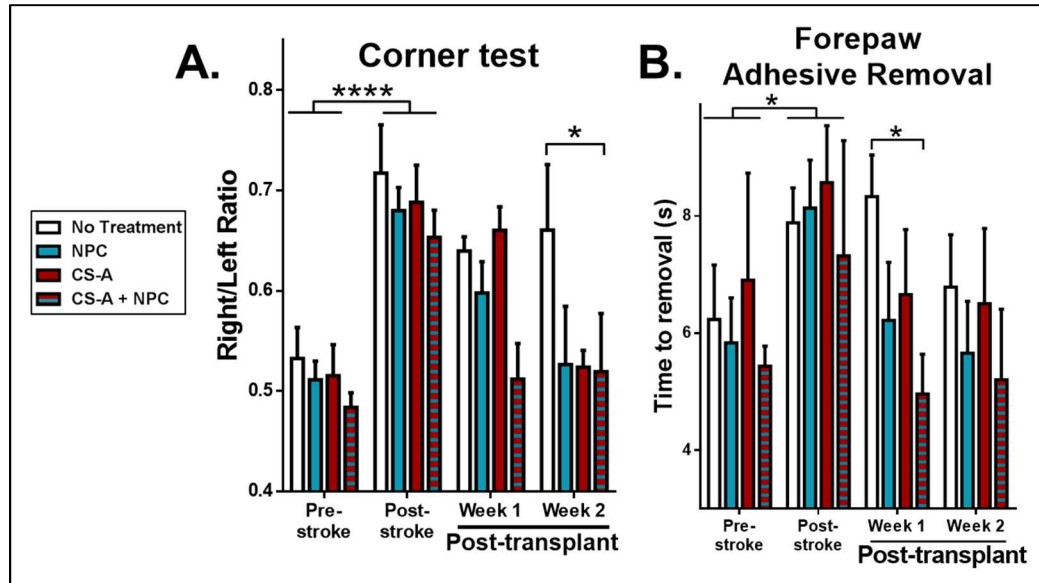


Figure 34. Corner and adhesive removal test performance after treatment. n=8-12. *, **, *, and **** indicates $p<0.05$, $p<0.005$, $p<0.0005$, and $p<0.0001$, respectively; 2-way ANOVA with Bonferroni correction.**

General motor coordination and balance was assessed using the rotarod test, where the time to fall off a rotating wheel is compared. We found that at 1 and 2 weeks after transplantation, mice treated with either NPCs or CS-A encapsulated NPCs showed a greater ability to stay on the rotating rod compared to stroke controls, but not to CS-A acellular hydrogel controls (Figure 35). This suggests that CS-A encapsulation does not improve NPC-mediated functional improves in motor coordination and balance after stroke.

Forepaw motor function was tested using the volitional isometric pull test. These tests required extensive training for the mice, therefore, we opted to eliminate the CS-A acellular control which showed no effect in the previous behavior studies. Two weeks after transplantation, mice treated with CS-A + NPC showed improved pull strength compared to the stroke control, but not the cellular

control. The pull test successful hit rate was significantly increased in the CS-A + NPC treatment compared to the cellular treatment, but not the stroke control.

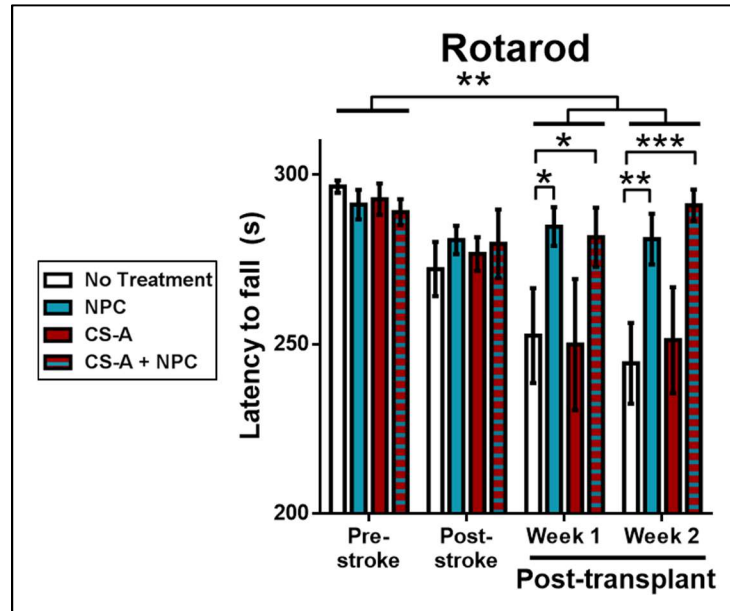


Figure 35. Rotarod test performance after transplantation. n=8-12. *, **, ***, and **** indicates $p < 0.05$, $p < 0.005$, $p < 0.0005$, and $p < 0.0001$, respectively; 2-way ANOVA with Bonferroni correction.

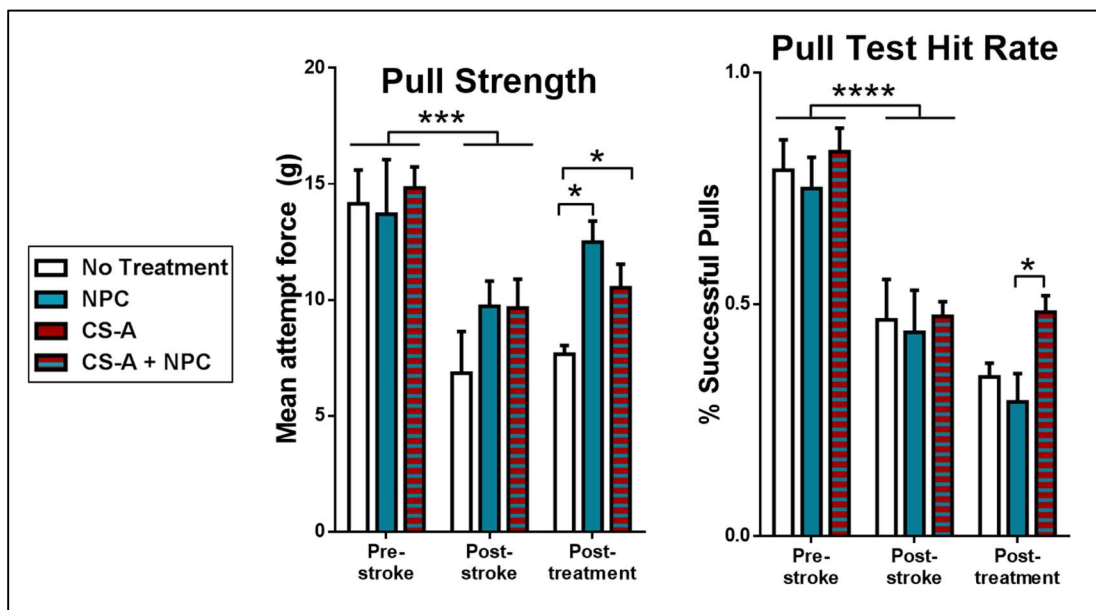


Figure 36. Isovolumetric pull test performance after treatment. n=3-4 *, **, *, and **** indicates $p<0.05$, $p<0.005$, $p<0.0005$, and $p<0.0001$, respectively; 2-way ANOVA with Holm-Sidak correction.**

Post-stroke neuropsychiatric deficits have also been reported in humans and in rodent stroke models. We tested the possibility that treatment may affect these outcomes (Figure 37). The open field test assesses anxiety-like behavior by monitoring the proportion of time the mice spend in the center of the arena; it can also be used to gather sensorimotor data such as distance travelled and average velocity during the test. We found that all treatment groups showed an increased time spent in the center of the arena, suggesting they have reduced anxiety compared to the stroke control; there were no differences between the transplantation groups. Furthermore, there were no differences in average travel distance or velocity between treatment groups. The tail suspension test assesses apathy-like behavior. We found that mice treated with the CS-A + NPC treatment have reduced immobility time compared to the stroke and cellular controls, suggesting they have reduced apathy-like behavior (Figure 37). However, there was no difference between the CS-A acellular hydrogel and the combined CS-A + NPC group. These results suggest that CS-A encapsulation may improve post-stroke apathy-like behavior, however, encapsulation does not affect anxiety-like behavior.

Next, we tested the overall relative performance in the sensorimotor behavior tests by treatment group at 2 weeks following transplantation to ascertain whether or not the group sensorimotor performance profiles as a whole were significantly different from each other. We found that there was no statistically

difference between overall sensorimotor test performance between groups (Figure 38). This suggests that CS-A encapsulation of NPCs, under the treatment paradigms and strategies implemented for this work, are not effective at facilitating sensorimotor recovery after ischemic stroke.

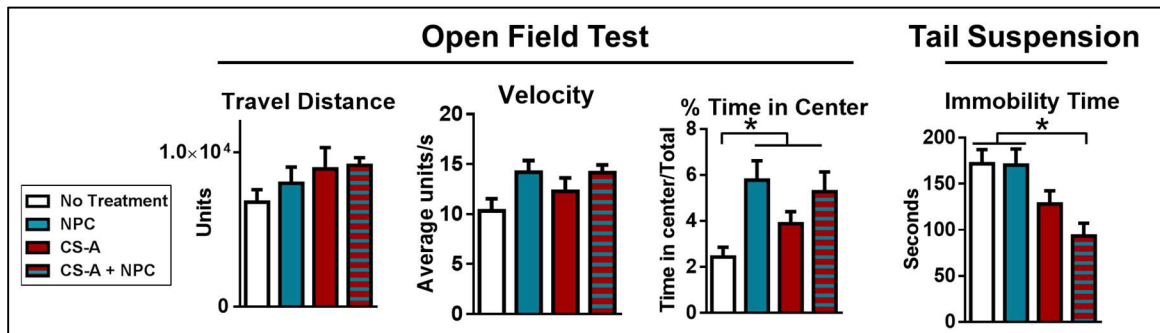


Figure 37. Recovery of post-stroke neuropsychiatric deficits following treatment. n=8-12. * indicates p<0.05; 2-way ANOVA with Bonferroni correction.

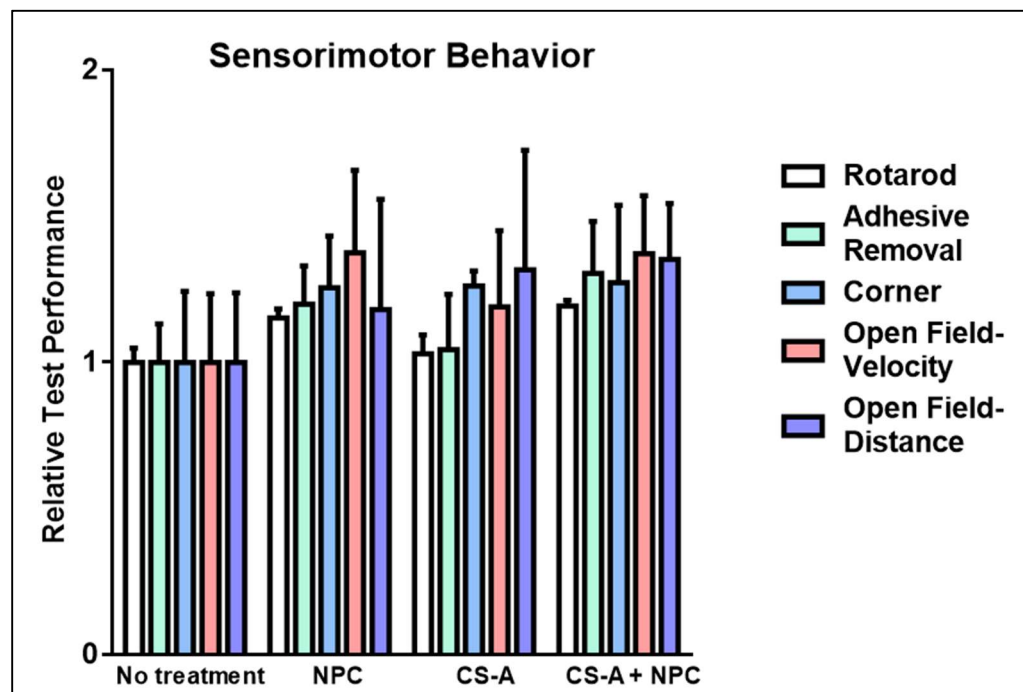


Figure 38. Analysis of group relative sensorimotor test performance 2 weeks after ischemic stroke. Two-way ANOVA with Bonferroni correction. CS-

A+NPC vs NPC $p=0.6722$; CS-A+NPC vs No treatment $p=0.0604$. NPC vs no treatment $p=0.2334$.

5.3.4 Neutralization of bFGF abolishes CS-A + NPC-mediated improvements in vascular regeneration and blood flow recovery

A major benefit of CS-A encapsulation appears to be highly improved vascular regeneration and blood flow recovery. CS-A has a high affinity for bFGF which is known to play a key role in these processes, and in our previous experiments, was found to be increased in the stroke core region (Figure 27). Thus, we sought to determine whether bFGF plays a critical role in CS-A+NPC mediated vascular regeneration and blood flow recovery. To test this possibility, we administered a neutralizing antibody towards bFGF (anti-bFGF) concurrently with CS-A+NPC transplantation (CS-A+NPC+anti-bFGF). This group was compared head to head with the CS-A encapsulated NPC group (Figure 39). We measured and compared angiogenesis, pial artery dynamics, and local cerebral blood flow 2 weeks after treatment using the same methods described above (Figure 25, Figure 31, Figure 32). Furthermore, we also measured whisker function using the corner test, since this was our most sensitive test at 3 weeks after cerebral infarction.

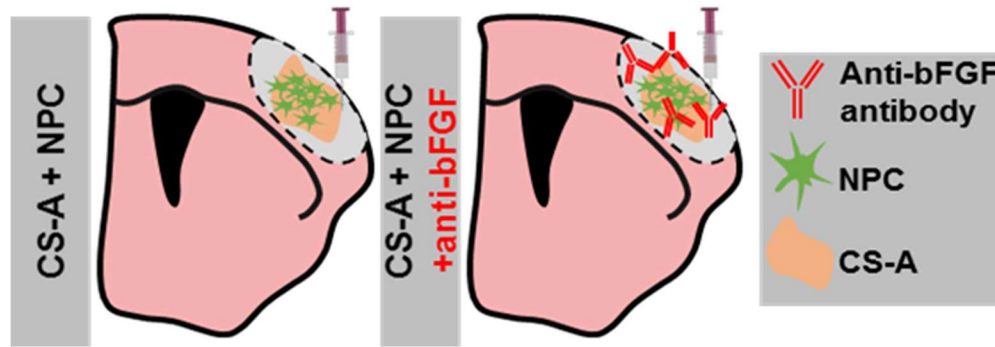


Figure 39. Experimental design for bFGF neutralization animal experiments.

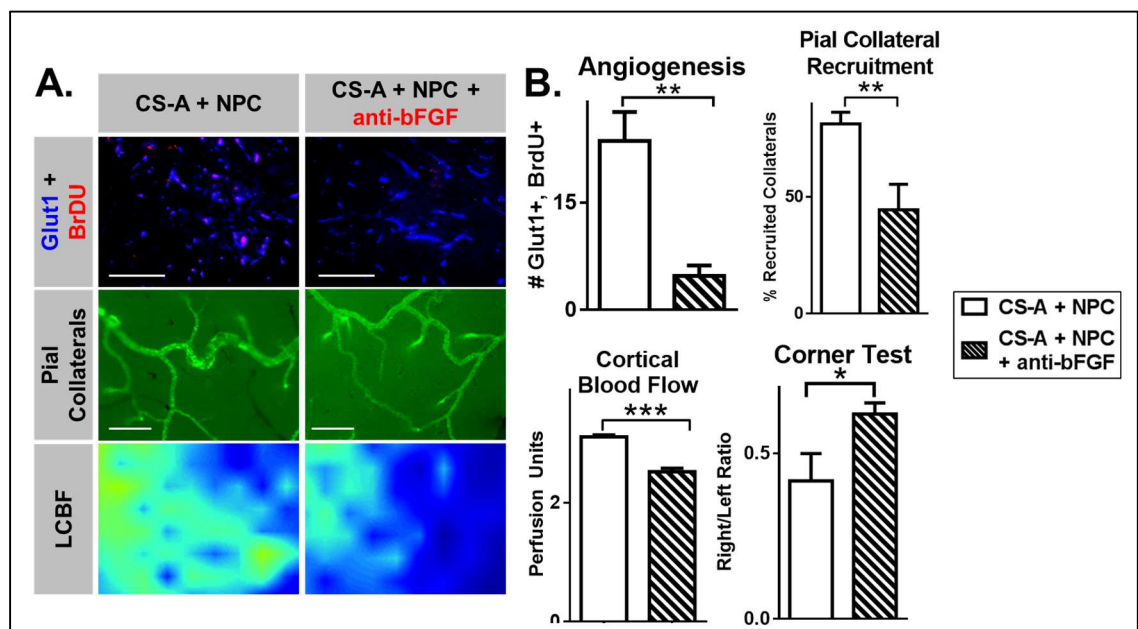


Figure 40. Neutralization of bFGF abolishes vascular regeneration and blood flow in CS-A+NPC treated mice following ischemic stroke. A) Representative images of Glut1/BrdU costaining for angiogenesis, pial collateralization, and local cerebral blood flow in the stroke region 2 weeks after stroke. B) Analysis of angiogenesis, pial collateral recruitment, cortical blood flow, and corner test. $n=4-5$. *, **, and *** indicates $p<0.05$, $**p<0.005$, $***p<0.0005$ respectively; two-tailed T-test.

We found that addition of the bFGF neutralizing antibody into the hydrogel prior to transplantation resulted in significant reduction in the number of Glut1/BrdU colabelled cells in the stroke region (Figure 40). Furthermore, the extent of

collateralization was also reduced as measured by the percentage of recruitment of pial collateral arteries. Correspondingly, the amount of blood flow recovery measured by laser Doppler was reduced (Figure 40). Whisker functional recovery was reduced with addition of the bFGF neutralizing antibody as the CS-A+NPC+anti-bFGF group showed a higher rightwards deviation in turning behavior. Taken together, and with consideration of the vascular repair results detailed in Aim 2, these results suggest that bFGF plays an important role in mediating the angiogenic and arteriogenic regeneration and repair induced by treatment with CS-A encapsulated NPCs.

CONCLUSIONS

6.1 CS-A encapsulation of NPCs increases transplant retention, elicits a pro-regenerative inflammatory response, and augments vascular regeneration and blood flow after ischemic stroke

Growing evidence suggests that the transplantation of neural progenitor cells may be a viable approach to regenerate brain tissue lost to stroke or other brain injuries. Despite their well-documented therapeutic effects in the lab, clinical trials thus far have not been as successful as expected [13, 290, 356]. Work in animals has identified key deficiencies in transplant cell retention, engraftment, differentiation, and ability to generate sufficient regenerative activities for functional recovery as major impediments to clinical translation [13, 104, 262, 290]. The present study investigates the therapeutic effects of encapsulated NPCs in a hydrogel matrix composed of chondroitin-4-sulfate A (CS-A) following transplantation into the ischemic stroke core.

A primary outcome for transplantation studies is the successful survival, retention, and engraftment of transplanted cells. Using immunohistochemical methods and cell tracking of DiR labelled transplanted cells, we found that CS-A encapsulation reduces transplant cell death (Figure 2) and enhances cellular retention (Figure 4) following transplantation into the ischemic brain. We also determined that the CS-A hydrogel is amenable to neuronal differentiation *in vitro* (Figure 6) and *in vivo* (Figure 8) following transplantation. CS-A encapsulated NPCs can form axons/neurites, synapses, and express mature neuronal markers

following the differentiation protocol (Figure 6). Furthermore, following transplantation into the brain after stroke, CS-A appears to reduce glial differentiation of NPCs, which may be preferable to support neuronal replacement (Figure 9). However, in examination of axonal formation after transplantation, we found that transplantation to the stroke core region is not conducive to axonal formation through the inhibitory glial scar (Figure 10). This suggests that despite the increased retention and neural differentiation of transplanted NPCs encapsulated in CS-A, and also despite the reduction in peri-infarct reactive astrocytosis, neuronal replacement may not occur via transplant cell engraftment. It is likely that the inability of the CS-A + NPC treatment to reduce the thickness of the astrocytic scar (Figure 11) played a role in the failure of transplanted NPCs to develop axon and synapses which reached the viable parenchyma in the peri-infarct region. The implications of this finding are further discussed in 6.2: Pitfalls in CS-A + NPC therapy and transplantation directed to the infarct core region.

The immune response plays a major role in the natural history of stroke pathophysiology and the response to transplanted materials [11, 27, 329, 330]. Microglia/macrophages are the major immune cells involved in stroke [103]. It is desirable for the hydrogel to either reduce harmful inflammation, remain immune-inert, or promote a regenerative immune phenotype [41, 45]. The pro-regenerative M2-type macrophage population is associated with neurogenesis, angiogenesis, and stroke recovery, while the M1 response is inhibitory to recovery and associated with infarct progression [103, 331].

The microglial response to the transplanted CS-A encapsulated NPCs was interrogated using immunohistochemical, molecular biological, and cell culture techniques. We found that CS-A + NPC treatment enhanced microglial polarization towards the regenerative M2/alternatively activated phenotype (Figure 12) using immunohistochemical techniques. The immune response was further characterized by analyzing the protein expression of a variety of immune factors (Figure 13, Figure 14, Figure 15, Figure 16, Figure 17). We found that the immunomodulatory interleukin 10 (IL-10) was enhanced in the stroke core following encapsulated cellular therapy (Figure 13). The chemoattractant protein MCP-1, which is important for recruiting vascular associated macrophages to promote angiogenesis and arteriogenesis, was also significantly increased by CS-A + NPC treatment compared to all other treatments (Figure 14). The group expression of immune factors was found to be different between treatment groups, suggesting that the combination of CS-A and the encapsulated NPCs, elicit different immune responses following treatment (Figure 17).

Given the robust enrichment of IL-10 in the stroke core following treatment with CS-A + NPCs (Figure 13), and knowing that the CS-A sulfation moiety can facilitate IL-10 signaling[47, 53], we hypothesized the CS-A gel may act via IL-10 to affect microglia/macrophage phenotype. We first tested the specific response of macrophages to the CS-A hydrogel in a controlled *in vitro* environment (Figure 18). We found that *in vitro* culture of primary stroke core macrophages/microglia in the CS-A hydrogel increased expression of proteins bFGF and IL-10, and markers such as VEGFR2, TIE2, and PPAR γ , which are associated with a regenerative and

reparative macrophage phenotype (Figure 19). Using neutralization studies (Figure 20, Figure 21, Figure 22) *in vitro*, we also found that the immunomodulatory factor interleukin 10 may play a role in promoting a pro-arteriogenic macrophage/microglial phenotype, particularly in macrophages isolated 3 days after cerebral infarction (Figure 22).

The innate capability of the adult brain to create new neurons is inadequate to facilitate meaningful recovery after stroke. Formation of new neurovascular units is paramount to reestablishment of neuronal circuitry lost to infarction [332]. Intracranially transplanted iPSC-NPCs provide trophic support to the surrounding tissue via the production and release of regenerative factors [6, 7, 9]. Neovascularization in the hypoxic stroke region is necessary for the survival and success of both endogenously formed newborn neurons and transplanted iPSC-NPCs and is also prognostic of recovery [176]. The interaction of released growth factors with surrounding ECM is a critical step of trophic support and growth factor mediated regenerative activities [28, 55, 333]. Following ischemic damage, the ECM is extensively degraded and is unable to fully support trophic enrichment offered by transplanted NPCs [37, 41, 57, 334]. CS-A is an ECM component of the endogenous neural stem cell niche and can bind, partition, and orchestrate signaling of BDNF, FGF, IL10, and other released factors important for healing [39, 53]. These factors can promote endogenous neurogenesis and angiogenesis/arteriogenesis to facilitate recovery [5, 6, 9, 22, 36, 335]. We hypothesized that the combination of CS-A and NPCs may synergize to enhance the formation of new neurovascular units.

The ability of CS-A encapsulated NPCs to facilitate neurogenesis was studied using immunohistochemistry. Contrary to our hypothesis, we found that the number of newly formed neurons was extremely low in all treatment groups and was not enhanced by CS-A encapsulation (Figure 23). Furthermore, the migration of neuroblasts from the SVZ to the peri-infarct region was similarly unaffected by CS-A encapsulation of NPCs or any treatment (Figure 23). The implications of these findings are further discussed in 6.2: Pitfalls in CS-A + NPC therapy and transplantation directed to the infarct core region.

The effect of treatment on vascular regeneration was also tested. Our studies indicate that treatment with CS-A + NPCs significantly improves angiogenesis and vascular density within the stroke core region (Figure 25). Numerous arteries were detected within the hydrogel implant in mice treated with CS-A + NPCs (Figure 26). Protein markers of angiogenesis and vascular regeneration were also elevated, including bFGF and VEGF expression within the stroke core region (Figure 27). *In vitro* studies suggested that CS-A can enhance endothelial haptotaxis towards signals released by NPCs (Figure 28), but may not have effects on endothelial replication (Figure 29). Vascular remodeling of large pial arteries was monitored using genetically modified mice expressing alpha smooth muscle actin tagged with GFP (SMA-GFP). We found that treatment with CS-A encapsulated NPCs results in increased collateral artery diameter and augmented collateral recruitment (Figure 32). We verified that the collateralization was due to outward remodeling of the large pial arteries in the stroke core region and also in the peri-infarct region in mice treated with CS-A + NPCs (Figure 33).

In agreement with the vascular regeneration and repair effects following treatment with CS-A + NPCs, we found that blood flow to the infarcted cortex was also improved (Figure 31).

Given the central role of bFGF in angiogenesis and arteriogenesis, the ability of CS-A to bind, partition, and promote signaling of bFGF, and the finding that transplanted CS-A + NPCs can upregulate bFGF in the stroke core, we hypothesized this molecule may important for the vascular regeneration benefits provided by CS-A encapsulation. To test this possibility, we performed a head-to-head comparison of CS-A encapsulated NPCs with or without the addition of a bFGF neutralizing antibody (Figure 39). In agreement with this hypothesis, we found that addition of the anti-bFGF antibody resulted in reduced angiogenesis, collateralization, and blood flow to the infarcted cortex (Figure 40). These findings suggest bFGF plays a central role in mediating the vascular regeneration and reparative effects of CS-A encapsulation.

Improving functional behavioral recovery is the primary goal of designing, testing, and implementing preclinical studies for disease. We tested behavioral recovery using methods specific to our sensorimotor cortex mini-stroke model. Results from the corner test, adhesive removal test, and isovolumetric volitional pull tests indicate that CS-A encapsulation is not superior to non-encapsulation, and rarely and inconsistently superior to the stroke controls (Figure 34). Analysis of the summary behavior findings illustrated no significant different between the stroke control, cellular control, material control, or combined treatment groups (Figure 38). We also assessed post-stroke neuropsychiatric deficits using tests for

anxiety and apathy (Figure 37). These tests were inconclusive. The tail suspension test indicated that CS-A encapsulation may reduce apathy-like behaviour, however, the open field test showed no benefits for anxiety-like behaviour compared to the intermediate controls. The implications of these functional results are discussed in the section 6.2.2: CS-A encapsulation of NPCs failed to improve functional outcomes below.

6.2 Pitfalls in CS-A + NPC therapy and transplantation directed to the infarct core region

6.2.1 Cellular therapy targeted to the infarct core failed to provide neuronal replacement after ischemic stroke

Neuronal replacement can occur via 1) differentiation and integration of transplanted cells into existing neuronal networks, or 2) mobilization of endogenous neural progenitors which following stroke, which migrate from the SVZ towards the peri-infarct region to become newborn neurons. While the CS-A hydrogel can improve retention and permit neuronal differentiation, we were unable to find evidence that axons formed within the stroke core of any treatment group could transverse the glial scar (Figure 10). This suggests that the transplanted cells may not be able to directly participate in the neuronal circuits to repair networks damaged by infarction. However, it is possible that the transplanted cells may be able to promote synaptic plasticity of neighboring endogenous neurons, although this was not tested. Furthermore, no treatments had any effect of endogenous neurogenesis, including formation of newborn peri-

infarct neurons or migration or accumulation of migrating neuroblasts from the SVZ to the peri-infarct region (Figure 23). Together, these findings indicate that transplantation of CS-A+NPCs into the stroke core does not facilitate neuronal replacement by either endogenous or exogenous addition of neurons lost to cerebral infarction.

6.2.2 CS-A encapsulation of NPCs failed to improve functional outcomes

Recovering functional deficits lost to stroke is the primary goal of therapy and the overarching objective for encapsulating NPCs with CS-A. In the sensorimotor behaviour experiments described above, CS-A+NPC was occasionally better than the stroke controls but was consistently not superior to the material or cellular controls. Cumulatively, there was no difference in sensorimotor behaviour recovery between all experimental groups (Figure 38).

There are multiple potential reasons for failure of the CS-A encapsulation of NPCs to yield statistically significant improvements in sensorimotor behavior following treatment. The first is the possibility of a type 2 error, or failure to reject the null hypothesis, which is that CS-A+NPC does not provide additional sensorimotor benefits. The studies described in this experiment may have been underpowered to make conclusive statements regarding potential behavior benefits. Originally, the experiments were powered for determining differences in local cerebral blood flow measurements. The power analysis estimated a minimum of 9 animals per group to find significant differences in blood flow, and approximately 12 were used per timepoint per group to allow for unpredicted

excess uncertainty. This may not have been sufficient to capture differences in behavior, which in this study, had large variation and a lower average effect size. If the behavior experiments were to be repeated, the sensorimotor behavior results produced in this study could be used as preliminary data for an additional power analysis focused on finding potential differences in behavioral outcomes. In the sensorimotor test with the greatest post-stroke deficit levels, the corner test (Figure 34), the average effect size was 26.27% 2 weeks after transplantation. Assuming a power of 0.8 and determining significance at 0.05, an estimated sample size of 41 animals per group is necessary to verify a difference between groups, if there is one to be detected. This estimation is over 3x the number used for many of the experiments in this work. Similarly, the average effect size of the sensorimotor behavior tests cumulatively is 23.30% at 2 weeks after treatment (Figure 38); approximately 53 animals/group are needed to determine if the treatments have differential effects on sensorimotor outcomes. These estimates suggest the behavior tests were underpowered and highlight the likelihood of a type 2 error.

A second possibility for the failure of the sensorimotor tests to detect differences between treatment groups is that there are no differences to detect and we have made the correct inference in failing to reject the null hypothesis. This is also a likely possibility given the failure of the CS-A encapsulation of NPCs, or other treatment groups targeted to the stroke core, to facilitate meaningful neuronal replacement (Figure 10, Figure 23). Despite the other positive findings, functional behavior recovery may indeed be limited by the lack of neuronal replacement observed in our treatment paradigm.

Future efforts may also consider a different stroke model for the study of behavioral recovery. While the mini-stroke model is advantageous for the study of cellular and molecular mechanisms of therapy for stroke, the behavioral phenotypes are less severe than those in other models. For example, the middle cerebral artery occlusion (MCAo) model greatly extends the window for distinguishing behavioral deficits which may allow for better detection of differences in behavior outcomes between treatment groups [217]. However, stroke models with greater infarct sizes also carry the risk of hiding the possible benefits of therapy simply due to extent, severity, and possibly the irreversibility of brain damage. Regardless, the encapsulation of NPCs with CS-A should be tested in at least one other rodent stroke model and various other multiple other animal stroke models before the possibility of clinical translation, as dictated by the Stem Cell Therapy as an Emerging Paradigm for Stroke (STEPS) committee guidelines for preclinical studies [5].

6.3 Opportunities for improvement of CS-A encapsulation of NPCs for the treatment of brain injuries

We provide evidence of enhanced vascular regeneration/repair and augmented cortical blood flow in response to CS-A encapsulation of NPCs, nevertheless, this treatment fails to promote functional behavioral recovery. As it stands, the combination of the CS-A hydrogel scaffolding and neural progenitor cells directed towards the infarct core is not a viable treatment for ischemic stroke. However, additional approaches may be employed to overcome the limitations of the current strategy to fully utilize the beneficial effects of CS-A encapsulated NPCs.

The lack of neuronal replacement is a major impediment for CS-A+NPCs transplanted into the stroke core region. Strategies to augment neuronal replacement may overcome this limitation to promote behavioral recovery. Since the adult brain has limited and saturatable endogenous capabilities to form new neurons after stroke [22, 180, 193, 305], neuronal replacement strategies may focus on addition of neurons exogenously and facilitation of neural integration of transplanted cells. The CS-A hydrogel is a versatile, multifunctional glycosaminoglycan with the capability of binding, enriching, and presenting a number of regenerative molecules, including brain derived neurotrophic factor (BDNF). BDNF plays a major role in axon formation during brain development, in formation of axons in neurons generated endogenously from the SVZ and SGZ, and in axonal generation and synaptic plasticity in iPSC derived neurons [35, 352, 357, 358]. One potential strategy for enhancing neurite/axon outgrowth of transplanted cells is to dope or pretreat the CS-A hydrogel with BDNF or other axonal growth promoting molecules prior to transplantation. We found that BDNF levels were significantly elevated in the stroke core in CS-A+NPC treated mice (Figure 24), however, the levels of BDNF and the timing of BDNF enrichment may not have been sufficient to allow for axonal growth and penetration of the astrocytic barrier surrounding the stroke core. Another potential strategy for encouraging neuronal replacement via successful engraftment of transplanted cells is to stimulate the transplanted cells using optogenetic or chemogenetic methods. Unpublished work from the Wei/Yu lab has shown that stimulation of transplanted

cells can promote neurotrophic factor release and increase their expression of MAP2, TUJ1, Synapsin-1, which are axonal and synaptic markers, respectively.

An alternative strategy to enhancing transplanted cell axonal growth is to reduce the glial barrier, which may permit axonal translation through the stroke core into the healthy tissue to form neuronal connections. We found that axons are indeed produced within the stroke core following transplantation (Figure 10). Outside of the stroke core where the astrocytic scar is not a concern, transplanted NPCs can differentiate into neurons and integrate into the host neuronal networks [17, 20, 56, 285]. This suggests that the glial scar may be the primary limitation to axonal and synaptic formation rather than the inherent potential of transplanted cells to integrate into the existing neural network. Numerous studies have discovered methods to reduce the glial barrier after stroke and other focal lesions such as spinal cord injury [349, 359, 360]. One notable technique that may be applicable to this study is the direct conversion of astrocytes into neuronal cells [361]. Ongoing work in the Wei/Yu lab has shown that viral infection of neuronal transcription factors into astrocytes after stroke can convert them into functional neurons. This strategy is especially attractive for the enhancement of cellular therapy directed to the stroke core since the effect of astrocyte direct conversion is two-fold: 1) the conversion of astrocytes into neurons may reduce the glial impediment to transplanted cells; and 2) additional neurons are formed in the place of what was previously the neuron-void astrocytic scar. One caveat to the approach of reducing the glial barrier is that over-reduction may be harmful. The glial scar, especially at the early stages of stroke, reduces progression of the stroke

core (see 3.3.4: The Inflammatory and Astrocytic Response to Cerebral Infarction). Some research suggests that at later time points, palisading astrocytes may even be necessary for successful axonal regeneration [116].

In summary, the current strategy of transplanted CS-A encapsulated NPCs into the stroke core is insufficient to promote functional recovery, however, there are multiple techniques and strategies which can be coupled with the versatile CS-A hydrogel to potentially overcome these insufficiencies. In particular, methods to enable exogenous neuronal replacement and successful engraftment may synergize with CS-A encapsulated NPC transplantations. The potentially angiogenic and arteriogenic effects of CS-A+NPC therapy are deserving of further study for the treatment of ischemic stroke and other brain disorders.

REFERENCES

1. Writing Group, M., et al., *Executive Summary: Heart Disease and Stroke Statistics--2016 Update: A Report From the American Heart Association*. Circulation, 2016. **133**(4): p. 447-54.
2. Mozaffarian, D., et al., *Executive Summary: Heart Disease and Stroke Statistics-2016 Update: A Report From the American Heart Association*. Circulation, 2016. **133**(4): p. 447.
3. Bliss, T.M., R.H. Andres, and G.K. Steinberg, *Optimizing the success of cell transplantation therapy for stroke*. Neurobiol Dis, 2010. **37**(2): p. 275-83.
4. Bliss, T., et al., *Cell transplantation therapy for stroke*. Stroke, 2007. **38**(2 Suppl): p. 817-26.
5. Stem Cell Therapies as an Emerging Paradigm in Stroke, P., *Stem Cell Therapies as an Emerging Paradigm in Stroke (STEPS): bridging basic and clinical science for cellular and neurogenic factor therapy in treating stroke*. Stroke, 2009. **40**(2): p. 510-5.
6. Chau, M.J., et al., *iPSC Transplantation increases regeneration and functional recovery after ischemic stroke in neonatal rats*. Stem Cells, 2014. **32**(12): p. 3075-87.
7. Qin, J., et al., *Transplantation of Induced Pluripotent Stem Cells Alleviates Cerebral Inflammation and Neural Damage in Hemorrhagic Stroke*. PLoS One, 2015. **10**(6): p. e0129881.
8. Takahashi, K. and S. Yamanaka, *Induction of pluripotent stem cells from mouse embryonic and adult fibroblast cultures by defined factors*. Cell, 2006. **126**(4): p. 663-76.
9. Martino, G. and S. Pluchino, *The therapeutic potential of neural stem cells*. Nat Rev Neurosci, 2006. **7**(5): p. 395-406.
10. Detante, O., et al., *Biotherapies in stroke*. Rev Neurol (Paris), 2014. **170**(12): p. 779-98.
11. Jendelova, P., et al., *Current developments in cell- and biomaterial-based approaches for stroke repair*. Expert Opin Biol Ther, 2016. **16**(1): p. 43-56.
12. Lim, T.C. and M. Spector, *Biomaterials for Enhancing CNS Repair*. Transl Stroke Res, 2017. **8**(1): p. 57-64.

13. Wei, L., et al., *Stem cell transplantation therapy for multifaceted therapeutic benefits after stroke*. Prog Neurobiol, 2017. **157**: p. 49-78.
14. Benninger, F., et al., *Functional integration of embryonic stem cell-derived neurons in hippocampal slice cultures*. J Neurosci, 2003. **23**(18): p. 7075-83.
15. Tornero, D., et al., *Synaptic inputs from stroke-injured brain to grafted human stem cell-derived neurons activated by sensory stimuli*. Brain, 2017.
16. Englund, U., et al., *Grafted neural stem cells develop into functional pyramidal neurons and integrate into host cortical circuitry*. Proc Natl Acad Sci U S A, 2002. **99**(26): p. 17089-94.
17. Espuny-Camacho, I., et al., *Pyramidal neurons derived from human pluripotent stem cells integrate efficiently into mouse brain circuits in vivo*. Neuron, 2013. **77**(3): p. 440-56.
18. Ideguchi, M., et al., *Murine embryonic stem cell-derived pyramidal neurons integrate into the cerebral cortex and appropriately project axons to subcortical targets*. J Neurosci, 2010. **30**(3): p. 894-904.
19. Maroof, A.M., et al., *Directed differentiation and functional maturation of cortical interneurons from human embryonic stem cells*. Cell Stem Cell, 2013. **12**(5): p. 559-72.
20. Tornero, D., et al., *Human induced pluripotent stem cell-derived cortical neurons integrate in stroke-injured cortex and improve functional recovery*. Brain, 2013. **136**(Pt 12): p. 3561-77.
21. Bersano, A., et al., *Clinical studies in stem cells transplantation for stroke: a review*. Curr Vasc Pharmacol, 2010. **8**(1): p. 29-34.
22. Machalinski, B., *Tissue regeneration in stroke: cellular and trophic mechanisms*. Expert Rev Neurother, 2014. **14**(8): p. 959-69.
23. Sun, J., et al., *Intranasal delivery of hypoxia-preconditioned bone marrow-derived mesenchymal stem cells enhanced regenerative effects after intracerebral hemorrhagic stroke in mice*. Exp Neurol, 2015. **272**: p. 78-87.
24. Wei, N., et al., *Delayed intranasal delivery of hypoxic-preconditioned bone marrow mesenchymal stem cells enhanced cell homing and therapeutic benefits after ischemic stroke in mice*. Cell Transplant, 2013. **22**(6): p. 977-91.
25. Gilman, S., *Time course and outcome of recovery from stroke: relevance to stem cell treatment*. Exp Neurol, 2006. **199**(1): p. 37-41.

26. Carmichael, S.T., *Translating the frontiers of brain repair to treatments: starting not to break the rules*. Neurobiol Dis, 2010. **37**(2): p. 237-42.
27. Nih, L.R., S.T. Carmichael, and T. Segura, *Hydrogels for brain repair after stroke: an emerging treatment option*. Curr Opin Biotechnol, 2016. **40**: p. 155-163.
28. Macri, L., D. Silverstein, and R.A. Clark, *Growth factor binding to the pericellular matrix and its importance in tissue engineering*. Adv Drug Deliv Rev, 2007. **59**(13): p. 1366-81.
29. Myles R. McCrary, S.W., Ling Wei, *Ischemic stroke mechanisms, prevention, and treatment: the anesthesiologist's perspective*. J Anesth Perioper Med, 2017. **4**: p. 76-86.
30. Jiang, X., et al., *Blood-brain barrier dysfunction and recovery after ischemic stroke*. Prog Neurobiol, 2018. **163-164**: p. 144-171.
31. Francis, K.R. and L. Wei, *Human embryonic stem cell neural differentiation and enhanced cell survival promoted by hypoxic preconditioning*. Cell Death Dis, 2010. **1**: p. e22.
32. Chau, M., et al., *Transplantation of iPS cell-derived neural progenitors overexpressing SDF-1alpha increases regeneration and functional recovery after ischemic stroke*. Oncotarget, 2017. **8**(57): p. 97537-97553.
33. Moshayedi, P., et al., *Systematic optimization of an engineered hydrogel allows for selective control of human neural stem cell survival and differentiation after transplantation in the stroke brain*. Biomaterials, 2016. **105**: p. 145-155.
34. Nih, L.R., et al., *Injection of Microporous Annealing Particle (MAP) Hydrogels in the Stroke Cavity Reduces Gliosis and Inflammation and Promotes NPC Migration to the Lesion*. Adv Mater, 2017. **29**(32).
35. Cook, D.J., et al., *Hydrogel-delivered brain-derived neurotrophic factor promotes tissue repair and recovery after stroke*. J Cereb Blood Flow Metab, 2017. **37**(3): p. 1030-1045.
36. Boncoraglio, G.B., et al., *Stem cell transplantation for ischemic stroke*. Cochrane Database Syst Rev, 2010(9): p. CD007231.
37. Zhong, J., et al., *Hydrogel matrix to support stem cell survival after brain transplantation in stroke*. Neurorehabil Neural Repair, 2010. **24**(7): p. 636-44.

38. Yu, H., et al., *Combinated transplantation of neural stem cells and collagen type I promote functional recovery after cerebral ischemia in rats*. Anat Rec (Hoboken), 2010. **293**(5): p. 911-7.
39. Martha I. Betancur, H.D.M., Melissa Alvarado-Velez, Phillip V. Holmes, Ravi V. Bellamkonda, and Lohitash Karumbaiah, *Chondroitin Sulfate Glycosaminoglycan Matrices Promote Neural Stem Cell Maintenance and Neuroprotection Post-Traumatic Brain Injury*. ACS Biomaterials Science & Engineering, 2017. **3**(3): p. 420-430.
40. Ballios, B.G., et al., *A hydrogel-based stem cell delivery system to treat retinal degenerative diseases*. Biomaterials, 2010. **31**(9): p. 2555-64.
41. Cohen, L.K. and M.B. Jensen, *Scaffolds for Intracerebral Grafting of Neural Progenitor Cells After Cerebral Infarction: A Systematic Review*. Arch Neurosci, 2015. **2**(4): p. e25364.
42. Lutolf, M.P., P.M. Gilbert, and H.M. Blau, *Designing materials to direct stem-cell fate*. Nature, 2009. **462**(7272): p. 433-41.
43. Miller, K., et al., *Mechanical properties of brain tissue in-vivo: experiment and computer simulation*. J Biomech, 2000. **33**(11): p. 1369-76.
44. Banerjee, A., et al., *The influence of hydrogel modulus on the proliferation and differentiation of encapsulated neural stem cells*. Biomaterials, 2009. **30**(27): p. 4695-9.
45. Moshayedi, P. and S.T. Carmichael, *Hyaluronan, neural stem cells and tissue reconstruction after acute ischemic stroke*. Biomatter, 2013. **3**(1).
46. Seidlits, S.K., et al., *The effects of hyaluronic acid hydrogels with tunable mechanical properties on neural progenitor cell differentiation*. Biomaterials, 2010. **31**(14): p. 3930-40.
47. Karumbaiah, L., et al., *Chondroitin sulfate glycosaminoglycans for CNS homeostasis-implications for material design*. Curr Med Chem, 2014. **21**(37): p. 4257-81.
48. Burdick, J.A. and G. Vunjak-Novakovic, *Engineered microenvironments for controlled stem cell differentiation*. Tissue Eng Part A, 2009. **15**(2): p. 205-19.
49. Nih, L.R., et al., *Dual-function injectable angiogenic biomaterial for the repair of brain tissue following stroke*. Nat Mater, 2018. **17**(7): p. 642-651.
50. Pakulska, M.M., B.G. Ballios, and M.S. Shoichet, *Injectable hydrogels for central nervous system therapy*. Biomed Mater, 2012. **7**(2): p. 024101.

51. Sirko, S., et al., *Chondroitin sulfates are required for fibroblast growth factor-2-dependent proliferation and maintenance in neural stem cells and for epidermal growth factor-dependent migration of their progeny*. Stem Cells, 2010. **28**(4): p. 775-87.
52. Sirko, S., et al., *Chondroitin sulfate glycosaminoglycans control proliferation, radial glia cell differentiation and neurogenesis in neural stem/progenitor cells*. Development, 2007. **134**(15): p. 2727-38.
53. Karumbaiah, L., et al., *Chondroitin Sulfate Glycosaminoglycan Hydrogels Create Endogenous Niches for Neural Stem Cells*. Bioconjug Chem, 2015. **26**(12): p. 2336-49.
54. Mizumoto, S., D. Fongmoon, and K. Sugahara, *Interaction of chondroitin sulfate and dermatan sulfate from various biological sources with heparin-binding growth factors and cytokines*. Glycoconj J, 2013. **30**(6): p. 619-32.
55. Martino, M.M., et al., *Growth factors engineered for super-affinity to the extracellular matrix enhance tissue healing*. Science, 2014. **343**(6173): p. 885-8.
56. Lin, G.Q., et al., *Transplanted human neural precursor cells integrate into the host neural circuit and ameliorate neurological deficits in a mouse model of traumatic brain injury*. Neurosci Lett, 2018. **674**: p. 11-17.
57. Lam, J., et al., *Delivery of iPS-NPCs to the Stroke Cavity within a Hyaluronic Acid Matrix Promotes the Differentiation of Transplanted Cells*. Adv Funct Mater, 2014. **24**(44): p. 7053-7062.
58. Lam, J., et al., *Delivery of iPS-NPCs to the Stroke Cavity within a Hyaluronic Acid Matrix Promotes the Differentiation of Transplanted Cells*. Advanced functional materials, 2014. **24**(44): p. 7053-7062.
59. Schwamm, L.H., et al., *Get With the Guidelines-Stroke is associated with sustained improvement in care for patients hospitalized with acute stroke or transient ischemic attack*. Circulation, 2009. **119**(1): p. 107-15.
60. Meschia, J.F., et al., *Guidelines for the Primary Prevention of Stroke A Statement for Healthcare Professionals From the American Heart Association/American Stroke Association*. Stroke, 2014. **45**(12): p. 3754-3832.
61. Mashour, G.A., et al., *Perioperative care of patients at high risk for stroke during or after non-cardiac, non-neurologic surgery: consensus statement from the Society for Neuroscience in Anesthesiology and Critical Care**. J Neurosurg Anesthesiol, 2014. **26**(4): p. 273-85.

62. Grysiewicz, R.A., K. Thomas, and D.K. Pandey, *Epidemiology of ischemic and hemorrhagic stroke: incidence, prevalence, mortality, and risk factors*. Neurol Clin, 2008. **26**(4): p. 871-95, vii.
63. Bogiatzi, C., et al., *Secular trends in ischemic stroke subtypes and stroke risk factors*. Stroke, 2014. **45**(11): p. 3208-13.
64. Kernan, W.N., et al., *Guidelines for the prevention of stroke in patients with stroke and transient ischemic attack: a guideline for healthcare professionals from the American Heart Association/American Stroke Association*. Stroke, 2014. **45**(7): p. 2160-236.
65. Hankey, G.J., *Potential new risk factors for ischemic stroke what is their potential?* Stroke, 2006. **37**(8): p. 2181-2188.
66. Bejot, Y., B. Daubail, and M. Giroud, *Epidemiology of stroke and transient ischemic attacks: Current knowledge and perspectives*. Rev Neurol (Paris), 2016. **172**(1): p. 59-68.
67. O'Donnell, M.J., et al., *Global and regional effects of potentially modifiable risk factors associated with acute stroke in 32 countries (INTERSTROKE): a case-control study*. Lancet, 2016. **388**(10046): p. 761-75.
68. O'Donnell, M.J., et al., *Risk factors for ischaemic and intracerebral haemorrhagic stroke in 22 countries (the INTERSTROKE study): a case-control study*. Lancet, 2010. **376**(9735): p. 112-23.
69. Patra, J., et al., *Alcohol consumption and the risk of morbidity and mortality for different stroke types--a systematic review and meta-analysis*. BMC Public Health, 2010. **10**: p. 258.
70. Rolfe, D.F. and G.C. Brown, *Cellular energy utilization and molecular origin of standard metabolic rate in mammals*. Physiol Rev, 1997. **77**(3): p. 731-58.
71. George, P.M. and G.K. Steinberg, *Novel Stroke Therapeutics: Unraveling Stroke Pathophysiology and Its Impact on Clinical Treatments*. Neuron, 2015. **87**(2): p. 297-309.
72. Lo, E.H., T. Dalkara, and M.A. Moskowitz, *Mechanisms, challenges and opportunities in stroke*. Nat Rev Neurosci, 2003. **4**(5): p. 399-415.
73. Moskowitz, M.A., E.H. Lo, and C. Iadecola, *The science of stroke: mechanisms in search of treatments*. Neuron, 2010. **67**(2): p. 181-198.
74. Jiang, M.Q., et al., *Long-term survival and regeneration of neuronal and vasculature cells inside the core region after ischemic stroke in adult mice*. Brain Pathol, 2016.

75. Quillinan, N., P.S. Herson, and R.J. Traystman, *Neuropathophysiology of Brain Injury*. Anesthesiol Clin, 2016. **34**(3): p. 453-64.
76. Song, M. and S.P. Yu, *Ionic regulation of cell volume changes and cell death after ischemic stroke*. Transl Stroke Res, 2014. **5**(1): p. 17-27.
77. Ankarcrona, M., et al., *Glutamate-induced neuronal death: a succession of necrosis or apoptosis depending on mitochondrial function*. Neuron, 1995. **15**(4): p. 961-73.
78. Sims, N.R. and H. Muyderman, *Mitochondria, oxidative metabolism and cell death in stroke*. Biochim Biophys Acta, 2010. **1802**(1): p. 80-91.
79. Wang, Y., et al., *Neuronal Gap Junctions Are Required for NMDA Receptor-Mediated Excitotoxicity: Implications in Ischemic Stroke*. Journal of neurophysiology, 2010. **104**(6): p. 3551-3556.
80. Ginsberg, M.D., *Current status of neuroprotection for cerebral ischemia: synoptic overview*. Stroke, 2009. **40**(3 Suppl): p. S111-4.
81. Besancon, E., et al., *Beyond NMDA and AMPA glutamate receptors: emerging mechanisms for ionic imbalance and cell death in stroke*. Trends Pharmacol Sci, 2008. **29**(5): p. 268-75.
82. Dreier, J.P., *The role of spreading depression, spreading depolarization and spreading ischemia in neurological disease*. Nature medicine, 2011. **17**(4): p. 439-447.
83. Takano, T., et al., *Cortical spreading depression causes and coincides with tissue hypoxia*. Nat Neurosci, 2007. **10**(6): p. 754-62.
84. Shin, H.K., et al., *Vasoconstrictive neurovascular coupling during focal ischemic depolarizations*. J Cereb Blood Flow Metab, 2006. **26**(8): p. 1018-30.
85. Strong, A.J., et al., *Peri-infarct depolarizations lead to loss of perfusion in ischaemic gyrencephalic cerebral cortex*. Brain, 2007. **130**(Pt 4): p. 995-1008.
86. Lo, E.H., *A new penumbra: transitioning from injury into repair after stroke*. Nat Med, 2008. **14**(5): p. 497-500.
87. Bolanos, J.P., et al., *Mitochondria and reactive oxygen and nitrogen species in neurological disorders and stroke: Therapeutic implications*. Adv Drug Deliv Rev, 2009. **61**(14): p. 1299-315.

88. Sanderson, T.H., et al., *Molecular mechanisms of ischemia-reperfusion injury in brain: pivotal role of the mitochondrial membrane potential in reactive oxygen species generation*. Mol Neurobiol, 2013. **47**(1): p. 9-23.
89. Brennan, A.M., et al., *NADPH oxidase is the primary source of superoxide induced by NMDA receptor activation*. Nat Neurosci, 2009. **12**(7): p. 857-63.
90. Zhang, Y. and P.A. Rosenberg, *Caspase-1 and poly (ADP-ribose) polymerase inhibitors may protect against peroxynitrite-induced neurotoxicity independent of their enzyme inhibitor activity*. Eur J Neurosci, 2004. **20**(7): p. 1727-36.
91. Chen, X.M., et al., *Targeting reactive nitrogen species: a promising therapeutic strategy for cerebral ischemia-reperfusion injury*. Acta Pharmacol Sin, 2013. **34**(1): p. 67-77.
92. Okamoto, T., et al., *Activation of matrix metalloproteinases by peroxynitrite-induced protein S-glutathiolation via disulfide S-oxide formation*. J Biol Chem, 2001. **276**(31): p. 29596-602.
93. Vosler, P.S., et al., *Mitochondrial targets for stroke: focusing basic science research toward development of clinically translatable therapeutics*. Stroke, 2009. **40**(9): p. 3149-55.
94. Jin, R., et al., *Role of inflammation and its mediators in acute ischemic stroke*. Journal of cardiovascular translational research, 2013. **6**(5): p. 834-851.
95. Wang, Q., X.N. Tang, and M.A. Yenari, *The inflammatory response in stroke*. Journal of neuroimmunology, 2007. **184**(1): p. 53-68.
96. Perera, M.N., et al., *Inflammation following stroke*. Journal of Clinical Neuroscience, 2006. **13**(1): p. 1-8.
97. Nakase, T., et al., *The impact of inflammation on the pathogenesis and prognosis of ischemic stroke*. J Neurol Sci, 2008. **271**(1-2): p. 104-9.
98. Jin, R., G. Yang, and G. Li, *Inflammatory mechanisms in ischemic stroke: role of inflammatory cells*. J Leukoc Biol, 2010. **87**(5): p. 779-89.
99. Weston, R.M., et al., *Inflammatory cell infiltration after endothelin-1-induced cerebral ischemia: histochemical and myeloperoxidase correlation with temporal changes in brain injury*. J Cereb Blood Flow Metab, 2007. **27**(1): p. 100-14.
100. Kriz, J., *Inflammation in ischemic brain injury: timing is important*. Crit Rev Neurobiol, 2006. **18**(1-2): p. 145-57.

101. Pei, J., X. You, and Q. Fu, *Inflammation in the pathogenesis of ischemic stroke*. Front Biosci (Landmark Ed), 2015. **20**: p. 772-83.
102. Hu, X., et al., *Microglial and macrophage polarization-new prospects for brain repair*. Nat Rev Neurol, 2015. **11**(1): p. 56-64.
103. Xiong, X.Y., L. Liu, and Q.W. Yang, *Functions and mechanisms of microglia/macrophages in neuroinflammation and neurogenesis after stroke*. Prog Neurobiol, 2016. **142**: p. 23-44.
104. Savitz, S.I. and C.S. Cox, Jr., *Concise Review: Cell Therapies for Stroke and Traumatic Brain Injury: Targeting Microglia*. Stem Cells, 2016. **34**(3): p. 537-42.
105. Santos Samary, C., et al., *Immunomodulation after ischemic stroke: potential mechanisms and implications for therapy*. Crit Care, 2016. **20**(1): p. 391.
106. Amantea, D., et al., *Post-ischemic brain damage: pathophysiology and role of inflammatory mediators*. FEBS J, 2009. **276**(1): p. 13-26.
107. Hu, X., et al., *Microglia/macrophage polarization dynamics reveal novel mechanism of injury expansion after focal cerebral ischemia*. Stroke, 2012. **43**(11): p. 3063-70.
108. Sofroniew, M.V., *Astrocyte barriers to neurotoxic inflammation*. Nat Rev Neurosci, 2015. **16**(5): p. 249-63.
109. Ding, S., *Dynamic reactive astrocytes after focal ischemia*. Neural Regen Res, 2014. **9**(23): p. 2048-52.
110. Pekny, M., U. Wilhelmsson, and M. Pekna, *The dual role of astrocyte activation and reactive gliosis*. Neurosci Lett, 2014. **565**: p. 30-8.
111. Carmichael, S.T., *The 3 Rs of Stroke Biology: Radial, Relayed, and Regenerative*. Neurotherapeutics, 2016. **13**(2): p. 348-59.
112. Choudhury, G.R. and S. Ding, *Reactive astrocytes and therapeutic potential in focal ischemic stroke*. Neurobiol Dis, 2016. **85**: p. 234-44.
113. Sofroniew, M.V., *Reactive astrocytes in neural repair and protection*. Neuroscientist, 2005. **11**(5): p. 400-7.
114. Pekny, M. and M. Pekna, *Astrocyte reactivity and reactive astrogliosis: costs and benefits*. Physiol Rev, 2014. **94**(4): p. 1077-98.
115. Cregg, J.M., et al., *Functional regeneration beyond the glial scar*. Exp Neurol, 2014. **253**: p. 197-207.

116. Anderson, M.A., et al., *Astrocyte scar formation aids central nervous system axon regeneration*. Nature, 2016. **532**(7598): p. 195-200.
117. Taylor, R.C., S.P. Cullen, and S.J. Martin, *Apoptosis: controlled demolition at the cellular level*. Nat Rev Mol Cell Biol, 2008. **9**(3): p. 231-41.
118. Broughton, B.R., D.C. Reutens, and C.G. Sobey, *Apoptotic mechanisms after cerebral ischemia*. Stroke, 2009. **40**(5): p. e331-9.
119. Cho, Y.S., *Perspectives on the therapeutic modulation of an alternative cell death, programmed necrosis (review)*. Int J Mol Med, 2014. **33**(6): p. 1401-6.
120. Vanden Berghe, T., et al., *Regulated necrosis: the expanding network of non-apoptotic cell death pathways*. Nat Rev Mol Cell Biol, 2014. **15**(2): p. 135-47.
121. Ashkenazi, A. and G. Salvesen, *Regulated cell death: signaling and mechanisms*. Annu Rev Cell Dev Biol, 2014. **30**: p. 337-56.
122. Fuchs, Y. and H. Steller, *Live to die another way: modes of programmed cell death and the signals emanating from dying cells*. Nat Rev Mol Cell Biol, 2015. **16**(6): p. 329-44.
123. Button, R.W., S. Luo, and D.C. Rubinsztein, *Autophagic activity in neuronal cell death*. Neurosci Bull, 2015. **31**(4): p. 382-94.
124. Wei, L., et al., *Necrosis, apoptosis and hybrid death in the cortex and thalamus after barrel cortex ischemia in rats*. Brain research, 2004. **1022**(1): p. 54-61.
125. Degenhardt, K., et al., *Autophagy promotes tumor cell survival and restricts necrosis, inflammation, and tumorigenesis*. Cancer cell, 2006. **10**(1): p. 51-64.
126. Puyal, J., et al., *Neuronal autophagy as a mediator of life and death: contrasting roles in chronic neurodegenerative and acute neural disorders*. Neuroscientist, 2012. **18**(3): p. 224-36.
127. Qin, A.P., H.L. Zhang, and Z.H. Qin, *Mechanisms of lysosomal proteases participating in cerebral ischemia-induced neuronal death*. Neurosci Bull, 2008. **24**(2): p. 117-23.
128. Shi, R., et al., *Excessive autophagy contributes to neuron death in cerebral ischemia*. CNS neuroscience & therapeutics, 2012. **18**(3): p. 250-260.
129. Liu, Y. and B. Levine, *Autosis and autophagic cell death: the dark side of autophagy*. Cell Death Differ, 2015. **22**(3): p. 367-76.

130. Yang, M. and H. Wei, *Anesthetic neurotoxicity: Apoptosis and autophagic cell death mediated by calcium dysregulation*. Neurotoxicol Teratol, 2016.
131. Unal-Cevik, I., et al., *Apoptotic and necrotic death mechanisms are concomitantly activated in the same cell after cerebral ischemia*. Stroke, 2004. **35**(9): p. 2189-94.
132. Yuan, J., *Neuroprotective strategies targeting apoptotic and necrotic cell death for stroke*. Apoptosis, 2009. **14**(4): p. 469-77.
133. Weinlich, R., et al., *Necroptosis in development, inflammation and disease*. Nat Rev Mol Cell Biol, 2016.
134. Rami, A. and D. Kogel, *Apoptosis meets autophagy-like cell death in the ischemic penumbra: Two sides of the same coin?* Autophagy, 2008. **4**(4): p. 422-6.
135. Ünal-Çevik, I., et al., *Apoptotic and necrotic death mechanisms are concomitantly activated in the same cell after cerebral ischemia*. Stroke, 2004. **35**(9): p. 2189-2194.
136. Wei, K., P. Wang, and C.Y. Miao, *A double-edged sword with therapeutic potential: an updated role of autophagy in ischemic cerebral injury*. CNS Neurosci Ther, 2012. **18**(11): p. 879-86.
137. Liu, Y., et al., *Autosis is a Na⁺,K⁺-ATPase-regulated form of cell death triggered by autophagy-inducing peptides, starvation, and hypoxia-ischemia*. Proc Natl Acad Sci U S A, 2013. **110**(51): p. 20364-71.
138. Koike, M., et al., *Inhibition of autophagy prevents hippocampal pyramidal neuron death after hypoxic-ischemic injury*. The American journal of pathology, 2008. **172**(2): p. 454-469.
139. Puyal, J., et al., *Postischemic treatment of neonatal cerebral ischemia should target autophagy*. Ann Neurol, 2009. **66**(3): p. 378-89.
140. Zheng, Y.Q., et al., *RNA interference-mediated downregulation of Beclin1 attenuates cerebral ischemic injury in rats*. Acta Pharmacol Sin, 2009. **30**(7): p. 919-27.
141. Grishchuk, Y., et al., *Beclin 1-independent autophagy contributes to apoptosis in cortical neurons*. Autophagy, 2011. **7**(10): p. 1115-31.
142. Carloni, S., G. Buonocore, and W. Balduini, *Protective role of autophagy in neonatal hypoxia–ischemia induced brain injury*. Neurobiology of disease, 2008. **32**(3): p. 329-339.

143. Wang, J.Y., et al., *Severe global cerebral ischemia-induced programmed necrosis of hippocampal CA1 neurons in rat is prevented by 3-methyladenine: a widely used inhibitor of autophagy*. J Neuropathol Exp Neurol, 2011. **70**(4): p. 314-22.
144. Carloni, S., et al., *Inhibition of rapamycin-induced autophagy causes necrotic cell death associated with Bax/Bad mitochondrial translocation*. Neuroscience, 2012. **203**: p. 160-169.
145. Rami, A., A. Langhagen, and S. Steiger, *Focal cerebral ischemia induces upregulation of Beclin 1 and autophagy-like cell death*. Neurobiology of disease, 2008. **29**(1): p. 132-141.
146. Powers, W.J., et al., *2015 American Heart Association/American Stroke Association Focused Update of the 2013 Guidelines for the Early Management of Patients With Acute Ischemic Stroke Regarding Endovascular Treatment: A Guideline for Healthcare Professionals From the American Heart Association/American Stroke Association*. Stroke, 2015. **46**(10): p. 3020-35.
147. Hacke, W., et al., *Thrombolysis with alteplase 3 to 4.5 hours after acute ischemic stroke*. New England Journal of Medicine, 2008. **359**(13): p. 1317-1329.
148. Powers, W.J., et al., *2018 Guidelines for the Early Management of Patients With Acute Ischemic Stroke: A Guideline for Healthcare Professionals From the American Heart Association/American Stroke Association*. Stroke, 2018. **49**(3): p. e46-e110.
149. Mokin, M., et al., *Indications for thrombectomy in acute ischemic stroke from emergent large vessel occlusion (ELVO): report of the SNIS Standards and Guidelines Committee*. J Neurointerv Surg, 2019. **11**(3): p. 215-220.
150. Liebeskind, D.S., *Collateral circulation*. Stroke, 2003. **34**(9): p. 2279-84.
151. Shuaib, A., et al., *Collateral blood vessels in acute ischaemic stroke: a potential therapeutic target*. Lancet Neurol, 2011. **10**(10): p. 909-21.
152. Campbell, B.C., et al., *Failure of collateral blood flow is associated with infarct growth in ischemic stroke*. J Cereb Blood Flow Metab, 2013. **33**(8): p. 1168-72.
153. Wang, Z., et al., *Dynamic change of collateral flow varying with distribution of regional blood flow in acute ischemic rat cortex*. J Biomed Opt, 2012. **17**(12): p. 125001.
154. Meyer, J.S., *Circulatory changes following occlusion of the middle cerebral artery and their relation to function*. J Neurosurg, 1958. **15**(6): p. 653-73.

155. Lima, F.O., et al., *Prognosis of untreated strokes due to anterior circulation proximal intracranial arterial occlusions detected by use of computed tomography angiography*. JAMA Neurol, 2014. **71**(2): p. 151-7.
156. Seyman, E., et al., *The collateral circulation determines cortical infarct volume in anterior circulation ischemic stroke*. BMC Neurol, 2016. **16**(1): p. 206.
157. Al-Ali, F., et al., *Capillary Index Score in the Interventional Management of Stroke trials I and II*. Stroke, 2014. **45**(7): p. 1999-2003.
158. Liebeskind, D.S., et al., *Collaterals at angiography and outcomes in the Interventional Management of Stroke (IMS) III trial*. Stroke, 2014. **45**(3): p. 759-64.
159. Jung, S., et al., *Factors that determine penumbral tissue loss in acute ischaemic stroke*. Brain, 2013.
160. Marks, M.P., et al., *Effect of collateral blood flow on patients undergoing endovascular therapy for acute ischemic stroke*. Stroke, 2014. **45**(4): p. 1035-9.
161. Cheripelli, B.K., et al., *What is the relationship among penumbra volume, collaterals, and time since onset in the first 6 h after acute ischemic stroke?* Int J Stroke, 2016. **11**(3): p. 338-46.
162. Sakoh, M., et al., *Relationship between residual cerebral blood flow and oxygen metabolism as predictive of ischemic tissue viability: sequential multitracer positron emission tomography scanning of middle cerebral artery occlusion during the critical first 6 hours after stroke in pigs*. J Neurosurg, 2000. **93**(4): p. 647-57.
163. Leng, X., et al., *Impact of collaterals on the efficacy and safety of endovascular treatment in acute ischaemic stroke: a systematic review and meta-analysis*. J Neurol Neurosurg Psychiatry, 2016. **87**(5): p. 537-44.
164. Flores, A., et al., *Poor Collateral Circulation Assessed by Multiphase Computed Tomographic Angiography Predicts Malignant Middle Cerebral Artery Evolution After Reperfusion Therapies*. Stroke, 2015.
165. Hwang, Y.H., et al., *Impact of time-to-reperfusion on outcome in patients with poor collaterals*. AJNR Am J Neuroradiol., 2015. **36**(3): p. 495-500. doi: 10.3174/ajnr.A4151. Epub 2014 Nov 6.
166. Bouts, M.J., et al., *Lesion development and reperfusion benefit in relation to vascular occlusion patterns after embolic stroke in rats*. J Cereb Blood Flow Metab, 2014. **34**(2): p. 332-8.

167. Berkhemer, O.A., et al., *Collateral Status on Baseline Computed Tomographic Angiography and Intra-Arterial Treatment Effect in Patients With Proximal Anterior Circulation Stroke*. Stroke, 2016. **47**(3): p. 768-76.
168. Menon, B.K., et al., *Differential Effect of Baseline Computed Tomographic Angiography Collaterals on Clinical Outcome in Patients Enrolled in the Interventional Management of Stroke III Trial*. Stroke, 2015. **46**(5): p. 1239-44.
169. Jovin, T.G., et al., *Diffusion-weighted imaging or computerized tomography perfusion assessment with clinical mismatch in the triage of wake up and late presenting strokes undergoing neurointervention with Trevo (DAWN) trial methods*. Int J Stroke, 2017. **12**(6): p. 641-652.
170. Beretta, S., et al., *Cerebral collateral therapeutics in acute ischemic stroke: A randomized preclinical trial of four modulation strategies*. J Cereb Blood Flow Metab, 2017: p. 271678x16688705.
171. Anderson, C.S., et al., *Cluster-Randomized, Crossover Trial of Head Positioning in Acute Stroke*. N Engl J Med, 2017. **376**(25): p. 2437-2447.
172. Krishnan, K., et al., *Glyceryl Trinitrate for Acute Intracerebral Hemorrhage: Results From the Efficacy of Nitric Oxide in Stroke (ENOS) Trial, a Subgroup Analysis*. Stroke, 2016. **47**(1): p. 44-52.
173. Ginsberg, M.D., et al., *High-dose albumin treatment for acute ischaemic stroke (ALIAS) Part 2: a randomised, double-blind, phase 3, placebo-controlled trial*. Lancet Neurol, 2013. **12**(11): p. 1049-58.
174. Shuaib, A., et al., *Partial aortic occlusion for cerebral perfusion augmentation: safety and efficacy of NeuroFlo in Acute Ischemic Stroke trial*. Stroke, 2011. **42**(6): p. 1680-90.
175. Munoz-Venturelli, P., et al., *Head Position in Stroke Trial (HeadPoST)--sitting-up vs lying-flat positioning of patients with acute stroke: study protocol for a cluster randomised controlled trial*. Trials, 2015. **16**: p. 256.
176. Liu, J., et al., *Vascular remodeling after ischemic stroke: mechanisms and therapeutic potentials*. Prog Neurobiol, 2014. **115**: p. 138-56.
177. Wei, L., et al., *Collateral growth and angiogenesis around cortical stroke*. Stroke, 2001. **32**(9): p. 2179-84.
178. Arai, K., et al., *Brain angiogenesis in developmental and pathological processes: neurovascular injury and angiogenic recovery after stroke*. FEBS J, 2009. **276**(17): p. 4644-52.

179. Spalding, K.L., et al., *Dynamics of hippocampal neurogenesis in adult humans*. Cell, 2013. **153**(6): p. 1219-1227.
180. Bergmann, O., K.L. Spalding, and J. Frisen, *Adult Neurogenesis in Humans*. Cold Spring Harb Perspect Biol, 2015. **7**(7): p. a018994.
181. Sanai, N., et al., *Unique astrocyte ribbon in adult human brain contains neural stem cells but lacks chain migration*. Nature, 2004. **427**(6976): p. 740-4.
182. Roy, N.S., et al., *In vitro neurogenesis by progenitor cells isolated from the adult human hippocampus*. Nat Med, 2000. **6**(3): p. 271-7.
183. Ernst, A., et al., *Neurogenesis in the striatum of the adult human brain*. Cell, 2014. **156**(5): p. 1072-83.
184. Bergmann, O., et al., *The age of olfactory bulb neurons in humans*. Neuron, 2012. **74**(4): p. 634-9.
185. Zhao, Y., et al., *GSK-3beta Inhibition Induced Neuroprotection, Regeneration, and Functional Recovery After Intracerebral Hemorrhagic Stroke*. Cell Transplant, 2017. **26**(3): p. 395-407.
186. Wei, Z.Z., et al., *Neuroprotective and regenerative roles of intranasal Wnt-3a administration after focal ischemic stroke in mice*. J Cereb Blood Flow Metab, 2018. **38**(3): p. 404-421.
187. Parent, J.M., et al., *Rat forebrain neurogenesis and striatal neuron replacement after focal stroke*. Ann Neurol, 2002. **52**(6): p. 802-13.
188. Sultan, S., et al., *Synaptic Integration of Adult-Born Hippocampal Neurons Is Locally Controlled by Astrocytes*. Neuron, 2015. **88**(5): p. 957-972.
189. Kuge, A., et al., *Temporal profile of neurogenesis in the subventricular zone, dentate gyrus and cerebral cortex following transient focal cerebral ischemia*. Neurol Res, 2009. **31**(9): p. 969-76.
190. Arvidsson, A., et al., *Neuronal replacement from endogenous precursors in the adult brain after stroke*. Nat Med, 2002. **8**(9): p. 963-70.
191. Hollis, E.R., 2nd, et al., *Remodelling of spared proprioceptive circuit involving a small number of neurons supports functional recovery*. Nat Commun, 2015. **6**: p. 6079.
192. Katsimpardi, L., et al., *Vascular and neurogenic rejuvenation of the aging mouse brain by young systemic factors*. Science, 2014. **344**(6184): p. 630-4.

193. Villeda, S.A., et al., *The ageing systemic milieu negatively regulates neurogenesis and cognitive function*. Nature, 2011. **477**(7362): p. 90-4.
194. Miles, D.K. and S.G. Kernie, *Hypoxic-ischemic brain injury activates early hippocampal stem/progenitor cells to replace vulnerable neuroblasts*. Hippocampus, 2008. **18**(8): p. 793-806.
195. Ohab, J.J., et al., *A neurovascular niche for neurogenesis after stroke*. J Neurosci, 2006. **26**(50): p. 13007-16.
196. Yan, Y.P., et al., *Monocyte chemoattractant protein-1 plays a critical role in neuroblast migration after focal cerebral ischemia*. J Cereb Blood Flow Metab, 2007. **27**(6): p. 1213-24.
197. Kawada, H., et al., *Administration of hematopoietic cytokines in the subacute phase after cerebral infarction is effective for functional recovery facilitating proliferation of intrinsic neural stem/progenitor cells and transition of bone marrow-derived neuronal cells*. Circulation, 2006. **113**(5): p. 701-10.
198. Li, Y., et al., *Granulocyte colony-stimulating factor-primed bone marrow: an excellent stem-cell source for transplantation in acute myelocytic leukemia and chronic myelocytic leukemia*. Chin Med J (Engl), 2015. **128**(1): p. 20-4.
199. Kobayashi, T., et al., *Intracerebral infusion of glial cell line-derived neurotrophic factor promotes striatal neurogenesis after stroke in adult rats*. Stroke, 2006. **37**(9): p. 2361-7.
200. Hoehn, B.D., T.D. Palmer, and G.K. Steinberg, *Neurogenesis in rats after focal cerebral ischemia is enhanced by indomethacin*. Stroke, 2005. **36**(12): p. 2718-24.
201. Wang, L., et al., *Treatment of stroke with erythropoietin enhances neurogenesis and angiogenesis and improves neurological function in rats*. Stroke, 2004. **35**(7): p. 1732-7.
202. Gregoire, C.A., et al., *Endogenous neural stem cell responses to stroke and spinal cord injury*. Glia, 2015. **63**(8): p. 1469-82.
203. Liman, T.G. and M. Endres, *New vessels after stroke: postischemic neovascularization and regeneration*. Cerebrovasc Dis, 2012. **33**(5): p. 492-9.
204. Risau, W., *Mechanisms of angiogenesis*. Nature, 1997. **386**(6626): p. 671-4.

205. Prakash, R. and S.T. Carmichael, *Blood-brain barrier breakdown and neovascularization processes after stroke and traumatic brain injury*. Curr Opin Neurol, 2015. **28**(6): p. 556-64.
206. Heil, M., et al., *Arteriogenesis versus angiogenesis: similarities and differences*. J Cell Mol Med, 2006. **10**(1): p. 45-55.
207. Buschmann, I. and W. Schaper, *Arteriogenesis Versus Angiogenesis: Two Mechanisms of Vessel Growth*. News Physiol Sci, 1999. **14**: p. 121-125.
208. Carmeliet, P., *Mechanisms of angiogenesis and arteriogenesis*. Nat Med, 2000. **6**(4): p. 389-95.
209. Cunningham, L.A., K. Candelario, and L. Li, *Roles for HIF-1alpha in neural stem cell function and the regenerative response to stroke*. Behav Brain Res, 2012. **227**(2): p. 410-7.
210. Lin, C.H., et al., *Role of HIF-1alpha-activated Epac1 on HSC-mediated neuroplasticity in stroke model*. Neurobiol Dis, 2013. **58**: p. 76-91.
211. Hayashi, T., et al., *Temporal profile of angiogenesis and expression of related genes in the brain after ischemia*. J Cereb Blood Flow Metab, 2003. **23**(2): p. 166-80.
212. Bovetti, S., et al., *Blood vessels form a scaffold for neuroblast migration in the adult olfactory bulb*. J Neurosci, 2007. **27**(22): p. 5976-80.
213. Lin, C.Y., et al., *Dynamic changes in vascular permeability, cerebral blood volume, vascular density, and size after transient focal cerebral ischemia in rats: evaluation with contrast-enhanced magnetic resonance imaging*. J Cereb Blood Flow Metab, 2008. **28**(8): p. 1491-501.
214. Semenza, G.L., *Vasculogenesis, angiogenesis, and arteriogenesis: mechanisms of blood vessel formation and remodeling*. J Cell Biochem, 2007. **102**(4): p. 840-7.
215. Wei, L., C.M. Rovainen, and T.A. Woolsey, *Ministrokes in rat barrel cortex*. Stroke, 1995. **26**(8): p. 1459-62.
216. Woolsey, T.A., et al., *Neuronal units linked to microvascular modules in cerebral cortex: response elements for imaging the brain*. Cereb Cortex, 1996. **6**(5): p. 647-60.
217. Balkaya, M., et al., *Assessing post-stroke behavior in mouse models of focal ischemia*. J Cereb Blood Flow Metab, 2013. **33**(3): p. 330-8.
218. Zarruk, J.G., et al., *Neurological tests for functional outcome assessment in rodent models of ischaemic stroke*. Rev Neurol, 2011. **53**(10): p. 607-18.

219. Tamura, A., et al., *Focal cerebral ischaemia in the rat: 2. Regional cerebral blood flow determined by [14C]iodoantipyrine autoradiography following middle cerebral artery occlusion*. J Cereb Blood Flow Metab, 1981. **1**(1): p. 61-9.
220. Tamura, A., et al., *Focal cerebral ischaemia in the rat: 1. Description of technique and early neuropathological consequences following middle cerebral artery occlusion*. J Cereb Blood Flow Metab, 1981. **1**(1): p. 53-60.
221. Nagasawa, H. and K. Kogure, *Correlation between cerebral blood flow and histologic changes in a new rat model of middle cerebral artery occlusion*. Stroke, 1989. **20**(8): p. 1037-43.
222. Luo, W., et al., *A modified mini-stroke model with region-directed reperfusion in rat cortex*. J Cereb Blood Flow Metab, 2008. **28**(5): p. 973-83.
223. Watson, B.D., et al., *Induction of reproducible brain infarction by photochemically initiated thrombosis*. Ann Neurol, 1985. **17**(5): p. 497-504.
224. Robinson, M.J., et al., *Reduction of local cerebral blood flow to pathological levels by endothelin-1 applied to the middle cerebral artery in the rat*. Neurosci Lett, 1990. **118**(2): p. 269-72.
225. Robinson, M.J. and J. McCulloch, *Contractile responses to endothelin in feline cortical vessels in situ*. J Cereb Blood Flow Metab, 1990. **10**(2): p. 285-9.
226. Sharkey, J., I.M. Ritchie, and P.A. Kelly, *Perivascular microapplication of endothelin-1: a new model of focal cerebral ischaemia in the rat*. J Cereb Blood Flow Metab, 1993. **13**(5): p. 865-71.
227. Rossant, J., *Stem cells and early lineage development*. Cell, 2008. **132**(4): p. 527-31.
228. Chang, K.H. and M. Li, *Clonal isolation of an intermediate pluripotent stem cell state*. Stem Cells, 2013. **31**(5): p. 918-27.
229. Wu, J. and J.C. Izpisua Belmonte, *Dynamic Pluripotent Stem Cell States and Their Applications*. Cell Stem Cell, 2015. **17**(5): p. 509-25.
230. De Los Angeles, A., et al., *Hallmarks of pluripotency*. Nature, 2015. **525**(7570): p. 469-78.
231. Thomson, J.A., et al., *Embryonic stem cell lines derived from human blastocysts*. Science, 1998. **282**(5391): p. 1145-7.

232. Ware, C.B., et al., *Derivation of naive human embryonic stem cells*. Proc Natl Acad Sci U S A, 2014. **111**(12): p. 4484-9.
233. Theunissen, T.W., et al., *Systematic Identification of Culture Conditions for Induction and Maintenance of Naive Human Pluripotency*. Cell Stem Cell, 2014. **15**(4): p. 524-526.
234. Takashima, Y., et al., *Resetting Transcription Factor Control Circuitry toward Ground-State Pluripotency in Human*. Cell, 2015. **162**(2): p. 452-453.
235. Goldman, S.A. and N.J. Kuypers, *How to make an oligodendrocyte*. Development, 2015. **142**(23): p. 3983-95.
236. Lu, J., et al., *Generation of serotonin neurons from human pluripotent stem cells*. Nat Biotechnol, 2016. **34**(1): p. 89-94.
237. Patani, R., et al., *Retinoid-independent motor neurogenesis from human embryonic stem cells reveals a medial columnar ground state*. Nat Commun, 2011. **2**: p. 214.
238. Bissonnette, C.J., et al., *The controlled generation of functional basal forebrain cholinergic neurons from human embryonic stem cells*. Stem Cells, 2011. **29**(5): p. 802-11.
239. Nilbratt, M., et al., *Neurotrophic factors promote cholinergic differentiation in human embryonic stem cell-derived neurons*. J Cell Mol Med, 2010. **14**(6B): p. 1476-84.
240. Liu, Y., et al., *Medial ganglionic eminence-like cells derived from human embryonic stem cells correct learning and memory deficits*. Nat Biotechnol, 2013. **31**(5): p. 440-7.
241. Ma, L., et al., *Human embryonic stem cell-derived GABA neurons correct locomotion deficits in quinolinic acid-lesioned mice*. Cell Stem Cell, 2012. **10**(4): p. 455-64.
242. Barker, R.A., J. Drouin-Ouellet, and M. Parmar, *Cell-based therapies for Parkinson disease-past insights and future potential*. Nat Rev Neurol, 2015. **11**(9): p. 492-503.
243. Barker, R.A., et al., *The long-term safety and efficacy of bilateral transplantation of human fetal striatal tissue in patients with mild to moderate Huntington's disease*. J Neurol Neurosurg Psychiatry, 2013. **84**(6): p. 657-65.

244. Benraiss, A. and S.A. Goldman, *Cellular therapy and induced neuronal replacement for Huntington's disease*. Neurotherapeutics, 2011. **8**(4): p. 577-90.
245. Liu, H., et al., *Generation of induced pluripotent stem cells from adult rhesus monkey fibroblasts*. Cell Stem Cell, 2008. **3**(6): p. 587-90.
246. Hou, P., et al., *Pluripotent stem cells induced from mouse somatic cells by small-molecule compounds*. Science, 2013. **341**(6146): p. 651-4.
247. Yamanaka, S., *Induced pluripotent stem cells: past, present, and future*. Cell Stem Cell, 2012. **10**(6): p. 678-684.
248. Hussein, S.M., K. Nagy, and A. Nagy, *Human induced pluripotent stem cells: the past, present, and future*. Clin Pharmacol Ther, 2011. **89**(5): p. 741-5.
249. Dolmetsch, R. and D.H. Geschwind, *The human brain in a dish: the promise of iPSC-derived neurons*. Cell, 2011. **145**(6): p. 831-4.
250. Zhao, T., et al., *Immunogenicity of induced pluripotent stem cells*. Nature, 2011. **474**(7350): p. 212-5.
251. Veriter, S., et al., *Human Adipose-Derived Mesenchymal Stem Cells in Cell Therapy: Safety and Feasibility in Different "Hospital Exemption" Clinical Applications*. PLoS One, 2015. **10**(10): p. e0139566.
252. Garcia, K.O., et al., *Therapeutic effects of the transplantation of VEGF overexpressing bone marrow mesenchymal stem cells in the hippocampus of murine model of Alzheimer's disease*. Front Aging Neurosci, 2014. **6**: p. 30.
253. Guimaraes-Camboa, N., et al., *Pericytes of Multiple Organs Do Not Behave as Mesenchymal Stem Cells In Vivo*. Cell Stem Cell, 2017. **20**(3): p. 345-359 e5.
254. Cano, E., V. Gebala, and H. Gerhardt, *Pericytes or Mesenchymal Stem Cells: Is That the Question?* Cell Stem Cell, 2017. **20**(3): p. 296-297.
255. Stein, J.L., et al., *A quantitative framework to evaluate modeling of cortical development by neural stem cells*. Neuron, 2014. **83**(1): p. 69-86.
256. Sandoe, J. and K. Eggan, *Opportunities and challenges of pluripotent stem cell neurodegenerative disease models*. Nat Neurosci, 2013. **16**(7): p. 780-9.

257. Merkle, F.T. and K. Eggan, *Modeling human disease with pluripotent stem cells: from genome association to function*. Cell Stem Cell, 2013. **12**(6): p. 656-68.
258. Luo, Y., et al., *Single-cell transcriptome analyses reveal signals to activate dormant neural stem cells*. Cell, 2015. **161**(5): p. 1175-1186.
259. Wu, J. and E.S. Tzanakakis, *Deconstructing stem cell population heterogeneity: single-cell analysis and modeling approaches*. Biotechnol Adv, 2013. **31**(7): p. 1047-62.
260. Carmichael, S.T. and J.W. Krakauer, *The promise of neuro-recovery after stroke: introduction*. Stroke, 2013. **44**(6 Suppl 1): p. S103.
261. Corbett, D., et al., *Enhancing the Alignment of the Preclinical and Clinical Stroke Recovery Research Pipeline: Consensus-Based Core Recommendations From the Stroke Recovery and Rehabilitation Roundtable Translational Working Group*. Neurorehabil Neural Repair, 2017. **31**(8): p. 699-707.
262. Dobkin, B.H. and S.T. Carmichael, *The Specific Requirements of Neural Repair Trials for Stroke*. Neurorehabil Neural Repair, 2016. **30**(5): p. 470-8.
263. Pollock, K., et al., *A conditionally immortal clonal stem cell line from human cortical neuroepithelium for the treatment of ischemic stroke*. Exp Neurol, 2006. **199**(1): p. 143-55.
264. Bliss, T.M., et al., *Transplantation of hNT neurons into the ischemic cortex: cell survival and effect on sensorimotor behavior*. J Neurosci Res, 2006. **83**(6): p. 1004-14.
265. Hara, K., et al., *Neural progenitor NT2N cell lines from teratocarcinoma for transplantation therapy in stroke*. Prog Neurobiol, 2008. **85**(3): p. 318-34.
266. Drury-Stewart, D., et al., *Highly efficient differentiation of neural precursors from human embryonic stem cells and benefits of transplantation after ischemic stroke in mice*. Stem Cell Res Ther, 2013. **4**(4): p. 93.
267. Aharonowiz, M., et al., *Neuroprotective effect of transplanted human embryonic stem cell-derived neural precursors in an animal model of multiple sclerosis*. PLoS One, 2008. **3**(9): p. e3145.
268. Wei, L., et al., *Transplantation of embryonic stem cells overexpressing Bcl-2 promotes functional recovery after transient cerebral ischemia*. Neurobiol Dis, 2005. **19**(1-2): p. 183-93.
269. Mueller, D., et al., *Transplanted human embryonic germ cell-derived neural stem cells replace neurons and oligodendrocytes in the forebrain of*

- neonatal mice with excitotoxic brain damage*. J Neurosci Res, 2005. **82**(5): p. 592-608.
270. Zhang, P., et al., *Transplanted human embryonic neural stem cells survive, migrate, differentiate and increase endogenous nestin expression in adult rat cortical peri-infarction zone*. Neuropathology, 2009. **29**(4): p. 410-21.
 271. Modo, M., et al., *Transplantation of neural stem cells in a rat model of stroke: assessment of short-term graft survival and acute host immunological response*. Brain Res, 2002. **958**(1): p. 70-82.
 272. Newman, M.B., et al., *Tumorigenicity issues of embryonic carcinoma-derived stem cells: relevance to surgical trials using NT2 and hNT neural cells*. Stem Cells Dev, 2005. **14**(1): p. 29-43.
 273. Kokaia, Z., I.L. Llorente, and S.T. Carmichael, *Customized Brain Cells for Stroke Patients Using Pluripotent Stem Cells*. Stroke, 2018. **49**(5): p. 1091-1098.
 274. Savitz, S.I., et al., *Stem Cell Therapy as an Emerging Paradigm for Stroke (STEPS) II*. Stroke, 2011. **42**(3): p. 825-9.
 275. Maden, M. and N. Holder, *Retinoic acid and development of the central nervous system*. Bioessays, 1992. **14**(7): p. 431-8.
 276. Rohwedel, J., K. Guan, and A.M. Wobus, *Induction of cellular differentiation by retinoic acid in vitro*. Cells Tissues Organs, 1999. **165**(3-4): p. 190-202.
 277. Horschitz, S., et al., *Impact of preconditioning with retinoic acid during early development on morphological and functional characteristics of human induced pluripotent stem cell-derived neurons*. Stem Cell Res, 2015. **15**(1): p. 30-41.
 278. Bain, G., et al., *Embryonic stem cells express neuronal properties in vitro*. Dev Biol, 1995. **168**(2): p. 342-57.
 279. Burns, T.C., C.M. Verfaillie, and W.C. Low, *Stem cells for ischemic brain injury: a critical review*. J Comp Neurol, 2009. **515**(1): p. 125-44.
 280. Buhnemann, C., et al., *Neuronal differentiation of transplanted embryonic stem cell-derived precursors in stroke lesions of adult rats*. Brain, 2006. **129**(Pt 12): p. 3238-48.
 281. Darsalia, V., et al., *Cell number and timing of transplantation determine survival of human neural stem cell grafts in stroke-damaged rat brain*. J Cereb Blood Flow Metab, 2011. **31**(1): p. 235-42.

282. Darsalia, V., T. Kallur, and Z. Kokaia, *Survival, migration and neuronal differentiation of human fetal striatal and cortical neural stem cells grafted in stroke-damaged rat striatum*. Eur J Neurosci, 2007. **26**(3): p. 605-14.
283. Tonnesen, J., et al., *Functional integration of grafted neural stem cell-derived dopaminergic neurons monitored by optogenetics in an in vitro Parkinson model*. PLoS One, 2011. **6**(3): p. e17560.
284. Wernig, M., et al., *Functional integration of embryonic stem cell-derived neurons in vivo*. J Neurosci, 2004. **24**(22): p. 5258-68.
285. Chu, K., et al., *Human neural stem cells can migrate, differentiate, and integrate after intravenous transplantation in adult rats with transient forebrain ischemia*. Neurosci Lett, 2003. **343**(2): p. 129-33.
286. Chau, M., et al., *Regeneration after stroke: Stem cell transplantation and trophic factors*. Brain Circ, 2016. **2**(2): p. 86-94.
287. Calió, M.L., et al., *Transplantation of bone marrow mesenchymal stem cells decreases oxidative stress, apoptosis, and hippocampal damage in brain of a spontaneous stroke model*. Free Radical Biology and Medicine, 2014. **70**: p. 141-154.
288. Dillon-Carter, O., et al., *T155g-immortalized kidney cells produce growth factors and reduce sequelae of cerebral ischemia*. Cell Transplant, 2002. **11**(3): p. 251-9.
289. Johnston, R.E., et al., *Trophic factor secreting kidney cell lines: in vitro characterization and functional effects following transplantation in ischemic rats*. Brain Res, 2001. **900**(2): p. 268-76.
290. Bang, O.Y., *Clinical Trials of Adult Stem Cell Therapy in Patients with Ischemic Stroke*. Journal of Clinical Neurology, 2016. **12**(1): p. 14-20.
291. Iguchi, F., et al., *Trophic support of mouse inner ear by neural stem cell transplantation*. Neuroreport, 2003. **14**(1): p. 77-80.
292. Caplan, A.I. and J.E. Dennis, *Mesenchymal stem cells as trophic mediators*. J Cell Biochem, 2006. **98**(5): p. 1076-84.
293. Haynesworth, S.E., M.A. Baber, and A.I. Caplan, *Cytokine expression by human marrow-derived mesenchymal progenitor cells in vitro: effects of dexamethasone and IL-1 alpha*. J Cell Physiol, 1996. **166**(3): p. 585-92.
294. Bang, O.Y., et al., *Autologous mesenchymal stem cell transplantation in stroke patients*. Annals of neurology, 2005. **57**(6): p. 874-882.

295. Malgieri, A., et al., *Bone marrow and umbilical cord blood human mesenchymal stem cells: state of the art*. Int J Clin Exp Med, 2010. **3**(4): p. 248-69.
296. Chau, M.J., et al., *Delayed and repeated intranasal delivery of bone marrow stromal cells increases regeneration and functional recovery after ischemic stroke in mice*. BMC Neurosci, 2018. **19**(1): p. 20.
297. Tse, W.T., et al., *Suppression of allogeneic T-cell proliferation by human marrow stromal cells: implications in transplantation*. Transplantation, 2003. **75**(3): p. 389-97.
298. Crook, J.M., G. Wallace, and E. Tomaskovic-Crook, *The potential of induced pluripotent stem cells in models of neurological disorders: implications on future therapy*. Expert review of neurotherapeutics, 2015. **15**(3): p. 295-304.
299. Hess, D.C. and C.V. Borlongan, *Cell-based therapy in ischemic stroke*. Expert Rev Neurother, 2008. **8**(8): p. 1193-201.
300. Phillips, A.W., M.V. Johnston, and A. Fatemi, *The potential for cell-based therapy in perinatal brain injuries*. Transl Stroke Res, 2013. **4**(2): p. 137-48.
301. Savitz, S.I., et al., *Stem Cell Therapy as an Emerging Paradigm for Stroke (STEPS) II*. Stroke, 2011. **42**(3): p. 825-9.
302. Chen, X., et al., *Ischemic rat brain extracts induce human marrow stromal cell growth factor production*. Neuropathology, 2002. **22**(4): p. 275-9.
303. Vendrame, M., et al., *Infusion of human umbilical cord blood cells in a rat model of stroke dose-dependently rescues behavioral deficits and reduces infarct volume*. Stroke, 2004. **35**(10): p. 2390-5.
304. Takahashi, K., et al., *Embryonic neural stem cells transplanted in middle cerebral artery occlusion model of rats demonstrated potent therapeutic effects, compared to adult neural stem cells*. Brain Res, 2008. **1234**: p. 172-82.
305. Schmidt, A. and J. Minnerup, *Promoting recovery from ischemic stroke*. Expert Rev Neurother, 2016. **16**(2): p. 173-86.
306. Theus, M.H., et al., *In vitro hypoxic preconditioning of embryonic stem cells as a strategy of promoting cell survival and functional benefits after transplantation into the ischemic rat brain*. Exp Neurol, 2008. **210**(2): p. 656-70.

307. Wei, L., et al., *Transplantation of hypoxia preconditioned bone marrow mesenchymal stem cells enhances angiogenesis and neurogenesis after cerebral ischemia in rats*. Neurobiol Dis, 2012. **46**(3): p. 635-45.
308. Saldin, L.T., et al., *Extracellular matrix hydrogels from decellularized tissues: Structure and function*. Acta Biomater, 2017. **49**: p. 1-15.
309. Ghuman, H., et al., *ECM hydrogel for the treatment of stroke: Characterization of the host cell infiltrate*. Biomaterials, 2016. **91**: p. 166-181.
310. Boisserand, L.S., et al., *Biomaterial Applications in Cell-Based Therapy in Experimental Stroke*. Stem Cells Int, 2016. **2016**: p. 6810562.
311. Ju, R., et al., *The experimental therapy on brain ischemia by improvement of local angiogenesis with tissue engineering in the mouse*. Cell Transplant, 2014. **23 Suppl 1**: p. S83-95.
312. Sanchez-Rojas, L., et al., *Biohybrids of scaffolding hyaluronic acid biomaterials plus adipose stem cells home local neural stem and endothelial cells: Implications for reconstruction of brain lesions after stroke*. J Biomed Mater Res B Appl Biomater, 2018.
313. Bible, E., et al., *Neo-vascularization of the stroke cavity by implantation of human neural stem cells on VEGF-releasing PLGA microparticles*. Biomaterials, 2012. **33**(30): p. 7435-46.
314. Bible, E., et al., *Non-invasive imaging of transplanted human neural stem cells and ECM scaffold remodeling in the stroke-damaged rat brain by (19)F- and diffusion-MRI*. Biomaterials, 2012. **33**(10): p. 2858-71.
315. Purushothaman, A., K. Sugahara, and A. Faissner, *Chondroitin sulfate "wobble motifs" modulate maintenance and differentiation of neural stem cells and their progeny*. J Biol Chem, 2012. **287**(5): p. 2935-42.
316. Rauvala, H., et al., *Inhibition and enhancement of neural regeneration by chondroitin sulfate proteoglycans*. Neural Regen Res, 2017. **12**(5): p. 687-691.
317. Nishimura, K., et al., *Opposing functions of chondroitin sulfate and heparan sulfate during early neuronal polarization*. Neuroscience, 2010. **169**(4): p. 1535-47.
318. Kwok, J.C., P. Warren, and J.W. Fawcett, *Chondroitin sulfate: a key molecule in the brain matrix*. Int J Biochem Cell Biol, 2012. **44**(4): p. 582-6.

319. Maeda, N., *Structural variation of chondroitin sulfate and its roles in the central nervous system*. Cent Nerv Syst Agents Med Chem, 2010. **10**(1): p. 22-31.
320. Le Jan, S., et al., *Functional overlap between chondroitin and heparan sulfate proteoglycans during VEGF-induced sprouting angiogenesis*. Arterioscler Thromb Vasc Biol, 2012. **32**(5): p. 1255-63.
321. Ryan, E., D. Shen, and X. Wang, *Structural studies reveal an important role for the pleiotrophin C-terminus in mediating interactions with chondroitin sulfate*. FEBS J, 2016. **283**(8): p. 1488-503.
322. Liu, Z. and M. Chopp, *Astrocytes, therapeutic targets for neuroprotection and neurorestoration in ischemic stroke*. Prog Neurobiol, 2016. **144**: p. 103-20.
323. Cekanaviciute, E. and M.S. Buckwalter, *Astrocytes: Integrative Regulators of Neuroinflammation in Stroke and Other Neurological Diseases*. Neurotherapeutics, 2016. **13**(4): p. 685-701.
324. Betancur, M.I., et al., *Chondroitin Sulfate Glycosaminoglycan Matrices Promote Neural Stem Cell Maintenance and Neuroprotection Post-Traumatic Brain Injury*. ACS Biomater Sci Eng, 2017. **3**(3): p. 420-430.
325. Smith, S.M., et al., *Heparan and chondroitin sulfate on growth plate perlecan mediate binding and delivery of FGF-2 to FGF receptors*. Matrix Biol, 2007. **26**(3): p. 175-84.
326. Salehi, A., J.H. Zhang, and A. Obenaus, *Response of the cerebral vasculature following traumatic brain injury*. J Cereb Blood Flow Metab, 2017. **37**(7): p. 2320-2339.
327. Lapi, D. and A. Colantuoni, *Remodeling of Cerebral Microcirculation after Ischemia-Reperfusion*. J Vasc Res, 2015. **52**(1): p. 22-31.
328. Nishijima, Y., et al., *Collaterals: Implications in cerebral ischemic diseases and therapeutic interventions*. Brain Res, 2015. **1623**: p. 18-29.
329. Modo, M., et al., *Bioengineering solutions for neural repair and recovery in stroke*. Curr Opin Neurol, 2013. **26**(6): p. 626-31.
330. Murray, P.J. and T.A. Wynn, *Protective and pathogenic functions of macrophage subsets*. Nat Rev Immunol, 2011. **11**(11): p. 723-37.
331. Taylor, R.A. and L.H. Sansing, *Microglial responses after ischemic stroke and intracerebral hemorrhage*. Clin Dev Immunol, 2013. **2013**: p. 746068.

332. Iadecola, C., *The Neurovascular Unit Coming of Age: A Journey through Neurovascular Coupling in Health and Disease*. Neuron, 2017. **96**(1): p. 17-42.
333. Wang, Y., et al., *Bioengineered sequential growth factor delivery stimulates brain tissue regeneration after stroke*. J Control Release, 2013. **172**(1): p. 1-11.
334. Yang, Y. and G.A. Rosenberg, *Matrix metalloproteinases as therapeutic targets for stroke*. Brain Res, 2015. **1623**: p. 30-8.
335. Hao, L., et al., *Stem cell-based therapies for ischemic stroke*. Biomed Res Int, 2014. **2014**: p. 468748.
336. Song, M., et al., *Optogenetic stimulation of glutamatergic neuronal activity in the striatum enhances neurogenesis in the subventricular zone of normal and stroke mice*. Neurobiol Dis, 2017. **98**: p. 9-24.
337. Wei, L., et al., *Angiogenesis and stem cell transplantation as potential treatments of cerebral ischemic stroke*. Pathophysiology, 2005. **12**(1): p. 47-62.
338. Logun, M.T., et al., *Glioma Cell Invasion is Significantly Enhanced in Composite Hydrogel Matrices Composed of Chondroitin 4- and 4,6-Sulfated Glycosaminoglycans*. J Mater Chem B, 2016. **4**(36): p. 6052-6064.
339. Kempermann, G., L. Wiskott, and F.H. Gage, *Functional significance of adult neurogenesis*. Curr Opin Neurobiol, 2004. **14**(2): p. 186-91.
340. Thored, P., et al., *Long-term neuroblast migration along blood vessels in an area with transient angiogenesis and increased vascularization after stroke*. Stroke, 2007. **38**(11): p. 3032-9.
341. Taupin, P. and F.H. Gage, *Adult neurogenesis and neural stem cells of the central nervous system in mammals*. J Neurosci Res, 2002. **69**(6): p. 745-9.
342. Caracciolo, L., et al., *CREB controls cortical circuit plasticity and functional recovery after stroke*. Nat Commun, 2018. **9**(1): p. 2250.
343. Ogle, M.E., et al., *Inhibition of prolyl hydroxylases by dimethyloxaloylglycine after stroke reduces ischemic brain injury and requires hypoxia inducible factor-1alpha*. Neurobiol Dis, 2012. **45**(2): p. 733-42.
344. Lee, J.H., et al., *Therapeutic effects of pharmacologically induced hypothermia against traumatic brain injury in mice*. J Neurotrauma, 2014. **31**(16): p. 1417-30.

345. Wei, Z.Z., et al., *Intranasal delivery of bone marrow mesenchymal stem cells improved neurovascular regeneration and rescued neuropsychiatric deficits after neonatal stroke in rats*. Cell Transplant, 2015. **24**(3): p. 391-402.
346. Zhang, L., et al., *A test for detecting long-term sensorimotor dysfunction in the mouse after focal cerebral ischemia*. J Neurosci Methods, 2002. **117**(2): p. 207-14.
347. Whitaker, V.R., et al., *Whisker stimulation enhances angiogenesis in the barrel cortex following focal ischemia in mice*. J Cereb Blood Flow Metab, 2007. **27**(1): p. 57-68.
348. Becker, A.M., et al., *An automated task for the training and assessment of distal forelimb function in a mouse model of ischemic stroke*. J Neurosci Methods, 2016. **258**: p. 16-23.
349. Sofroniew, M.V., *Astrogliosis*. Cold Spring Harb Perspect Biol, 2014. **7**(2): p. a020420.
350. Ziv, Y., et al., *Synergy between immune cells and adult neural stem/progenitor cells promotes functional recovery from spinal cord injury*. Proc Natl Acad Sci U S A, 2006. **103**(35): p. 13174-9.
351. Ghuman, H., et al., *Long-term retention of ECM hydrogel after implantation into a sub-acute stroke cavity reduces lesion volume*. Acta Biomater, 2017. **63**: p. 50-63.
352. Kurozumi, K., et al., *BDNF gene-modified mesenchymal stem cells promote functional recovery and reduce infarct size in the rat middle cerebral artery occlusion model*. Mol Ther, 2004. **9**(2): p. 189-97.
353. Li, W.-L., et al., *The role of VEGF/VEGFR2 signaling in peripheral stimulation-induced cerebral neurovascular regeneration after ischemic stroke in mice*. Experimental brain research, 2011. **214**(4): p. 503-513.
354. Emerich, D.F., et al., *Injectable VEGF hydrogels produce near complete neurological and anatomical protection following cerebral ischemia in rats*. Cell Transplant, 2010. **19**(9): p. 1063-71.
355. Wang, Y., et al., *VEGF-overexpressing transgenic mice show enhanced post-ischemic neurogenesis and neuromigration*. J Neurosci Res, 2007. **85**(4): p. 740-7.
356. Kalladka, D., et al., *Human neural stem cells in patients with chronic ischaemic stroke (PISCES): a phase 1, first-in-man study*. Lancet, 2016. **388**(10046): p. 787-96.

- 357. Miyamoto, N., et al., *Astrocytes Promote Oligodendrogenesis after White Matter Damage via Brain-Derived Neurotrophic Factor*. J Neurosci, 2015. **35**(41): p. 14002-8.
- 358. Park, J., et al., *Nerve regeneration following spinal cord injury using matrix metalloproteinase-sensitive, hyaluronic acid-based biomimetic hydrogel scaffold containing brain-derived neurotrophic factor*. J Biomed Mater Res A, 2010. **93**(3): p. 1091-9.
- 359. Blackburn, D., et al., *Astrocyte function and role in motor neuron disease: a future therapeutic target?* Glia, 2009. **57**(12): p. 1251-64.
- 360. Sofroniew, M.V., *Molecular dissection of reactive astrogliosis and glial scar formation*. Trends Neurosci, 2009. **32**(12): p. 638-47.
- 361. Yin, J.C., et al., *Chemical Conversion of Human Fetal Astrocytes into Neurons through Modulation of Multiple Signaling Pathways*. Stem Cell Reports, 2019. **12**(3): p. 488-501.